The ET Baseline Detector Layout

ETO Design Task Force:
Fiodor Sorrentino, Jonathan Bratanata, Daniel Brown, Tamara Bud, Henk Jan Bulten, Julia Casanueva, Antonino Chiummo, Giacomo Ciani, Angelo Cruciani, Jerome Degallaix, Ulyana Dupletsa, Andreas Freise, Marco Galimberti, Julien Gargiulo, Archisman Ghosh, Anna Green, Steffen Grohmann, Nathan Holland, Francesco Iacovelli, Joseph Ickmans, Mikhail Korobko, Patricia Lamas, Elena Licciardello, Leonardo Lucchesi, Ghada Mahmoud, Max Majoor, Ettore Majorana, Maria Marsella, Paolo Martella, Romano Meijer, Conor Mow-Lowry, Tommaso Napolitano, John Osborne, Antonio Pasqualetti, Antonio Perreca, Piero Rapagnani, Fulvio Ricci, Paolo Ruggi, Riccardo de Salvo, Valeria Sequino, Francesca Spada, Sebastian Steinlechner, Benoît Tuybens, Marco Vardaro, Wissam Wahbeh, Patrick Werneke

External contributors:
Alessandro Agapito, Biswajit Banerjee, Nicolò Cibrario, Andrea Cozzumbo, Francesco Crescimbeni, Martina De Laurentis, Angèlique Lartaux, Sumin Lee, Matteo Leonardi, Alessio Ludovico De Santis, Michele Mancarella, Benedetta Mestichelli, Niccolò Muttoni, Lavinia Paiella, Fabian Pena Arellano, Simona Procacci, Paola Puppo, Alessio Rocchi, Ippocratis Saltas, Filippo Santoliquido, Manuel Arca Sedda, Pawan Tiwari, Cristiano Ugolini, Aymeric Van De Walle, Michal Was, Li Yufeng, Jean-Pierre Zendri

Date: June 27, 2025

ET – Einstein gravitational wave Telescope – Design Study * A joint European Project
Web: `http://www.einsteintelescope.eu`

Contents

1 Introduction, scope and structure of the document

The investment for Einstein Telescope (ET) construction will be dominated by the cost of underground civil infrastructure. The corresponding costing will be based on engineering studies carried out by specialized companies employed by the teams preparing possible ET sites (referred to as "Local Teams" in the following). In 2024 a preliminary detector layout for both the Triangle and the 2L geometry was generated by the Engineering Department (ED) of the ET Organisation (ETO), based upon an update of the ET optical layout by the Instrument Science Board (ISB) of the ET scientific Collaboration (ETC). Such preliminary detector layouts are indicated as "2024 reference" throughout this document. Early feedback based on engineering expertise associated with the work at the Local Teams indicated that the design philosophy of the 2024 reference layout would lead to substantially higher cost for the civil infrastructure than expected in the conceptual ET plan submitted as part of the ESFRI proposal in 2020. Upon request of the ET Coordinators, ETO agreed to set up a task force, coordinated by the ETO Technical Coordinator reporting to the ETO Directors. The task force sourced personnel and support from the ET Collaboration (ETC), ETO, the civil engineering specialists of the local teams and from CERN, as well as from external projects or institutions as needed.

The ETO task force reviewed and updated the 2024 references adapting, in a short time, the detector layout of ET for both the Triangle and 2L configuration towards an acceptable preliminary costing for the civil infrastructure while maintaining ET's scientific performance. The current document illustrates the result of such design effort, and represents the new ET baseline detector layout in two versions, corresponding to the Triangle and 2L geometries. The document contains all necessary information to describe the detector layout to ETO, the ETC, and the Local Teams. An extended supporting document describes the study logic, the motivation for technical choices, the possible alternative layouts, providing a detailed explanation of the resulting baseline layout including trade-off analysis. The extended supporting document contains all necessary details and technical annexes, including diagrams, technical drawings, plots, and tables.
The task force examined the cost and technical risk corresponding to different options for amending the detector layout; the proposed baseline layouts will allow sufficient flexibility to account for unknowns in technical design details. The current document includes suitable civil engineering criteria to guide a coherent design of detector and infrastructure.

The baseline detector layout is built upon substantial background information, which includes the preliminary detector layouts from ETO ED, and many other documents as indicated in the references.
This document provides all basic requirements to the technical and civil infrastructure hosting the ET detector. To such purpose, the detector layout represents a simplified design of the ET detector, including the elements which drive the main space/volume requirements to the hosting infrastructure. A simplified decomposition of the ET detector into subsystems, highlighting the main interfaces among them and allowing to track the flow of requirements to the main design parameters, is illustrated in Section 2.
The baseline ET design is primarily driven by the optical layout of the interferometer, and is build upon it. The baseline optical layouts for Triangle and 2L geometry, as well as the main differences with 2024 reference design, are described in Section 3. The optical layout provides the location and spatial orientation of main nodes, where the key optical elements (mirrors and optical assemblies) interact with the laser field, and the connection between nodes identified by laser beams.
In order to generate a model for the space requirements from the detector's hosting infrastructure, the optical layout is combined with a model for the supporting hardware. Two main elements are identified in the basic system decomposition, namely:

- integrated towers hosting the nodes in the optical layout, and including seismic isolation systems, possible cryogenic payloads, vacuum chambers, and other additional hardware;
- vacuum beampipes connecting the integrated towers.

The structure and classification of integrated towers, depending on the conceptual design of seismic isolation system, payload hosting the suspended optics, vacuum vessel, and cryogenic system in cases LFI test masses, are described in Section 4.

The baseline detector layout, which is a 3D model including the main elements of the whole detector, and representing the volume requirements to hosting civil infrastructure, is generated by combination of the optical layout, the model for integrated towers, a model for connecting vacuum beampipes, and a simplified model for the essential technical infrastructure. Such model is illustrated in Section 5.

Section 6 describes the relevant interfaces between detector and infrastructure; such interfaces provide:

- guidelines and constraints to detector design for a feasible and cost effective infrastructure;
- essential criteria to identify, within the detector layout, the main cost drivers for the hosting civil infrastructure;
- criteria to predict the impact of detector layout configuration on the cost of the hosting civil infrastructure;
- the most relevant engineering requirements on the infrastructure for the sake of instrument performance, operability, and lifetime.

A conceptual design to make the detector layout compatible with a cost effective infrastructure requires some trade-off between cost and technical risk. The baseline layout presented in the present document implies specific choices on the optical configuration and on the conceptual design of the relevant detector elements. A technical risk analysis on critical configuration items, supported by a TRL analysis on concerned technologies, is presented in Section 7. The section includes a simplified analysis of system flexibility versus configuration options.
The baseline detector layout must be compatible with the ET scientific performance requirements. Section 8 provides reference models for the ET sensitivity, and an assessment of the corresponding science case. The model allows to generate scientific requirements on the main design parameters assumed in the detector layout.

The present baseline detector layout represents a cost-effective design for ET, based on a suitable compromise between infrastructure cost, technical risk and flexibility. Further minor cost mitigation may be achieved at the cost of substantially higher technical risk or reduced flexibility, while substantial cost mitigation would imply a descoping of the ET scientific performance.

The current document presents a synthetic description of the essential features to understand the baseline detector layout. An extended supporting document, containing technical annexes, provides additional details and explains the logic behind underlying technical choices. The extended supporting document includes the analysis of alternative configurations, both from the point of view of technical risk and flexibility, and for the inferfaces with civil infrastructure.

1.1 Definitions

For this document we find it important to define the following terms:

- **Requirement**: Is a required property of an element or a part of a subsystem (*e.g.* distance between 2 optical elements);
- **Tolerance**: Is the deviation that can be accepted for the element or subsystem to still fulfill its performance when constructed (*e.g.* deviation of the realised distance of the two optical elements compared to the design/nominal distance);
- **Flexibility Demand**: This is a flexibility that is requested to be kept in the design at the current stage of the design process (*e.g.* we want to keep the possibility in the vacuum system / cavern design to be able to shift an optical element by *e.g.* 1 m sideways off the optical axis);
- **Flexibility Envelope**: This is a range of possible values that is given to the engineering team for optimisation (i.e. the optical design is based on a distance between two optical elements of e.g. 20 m (requirement) ± 0.1 m (tolerance), but the optical design can be tuned to cope also if the distance is in the range from e.g. 15-25 m).

It should be noted that flexibility demand and flexibility envelope are relevant only during the design phase. If their dynamic nature is exploited, this will require an update of the optics specifications (e.g. a radius of curvature of an optical element needs to be changed to make it compatible with the new distance between two optical elements).

2 Task Force system decomposition

Requirements and specifications are typically assigned following a functional and physical partition of the high-level system and its associated subsystems [1], [2], [3]. Applied to the scope of the Task Force work, a system decomposition (otherwise known as a Product Breakdown Structure - PBS) and corresponding traceable requirements and specifications framework has been set-up, following conventional Systems Engineering standards. The implementation is constrained by the timeline and context of the Task Force work, aimed to capture the information rationalizing detector and technical infrastructure system functionality as well as underground excavation volumes into integrated and distributed subsystems - rather than expert disciplines. The requirements and specifications are contained in two sets of traceable output tables, one each for the Triangle and 2L configuration - see also the technical support annexes in Section 9.2.

Systems are uniquely identified by a numerical code - the System ID - following the syntax *SYS_001*. System name abbreviations are derived from a combination of ET legacy names, functional and position (physical) descriptions. Tabular representations of the system decompositions are contained within technical annexes **TAB.1** (Triangle) and **TAB.7** (2L).

The high-level system decomposition is described in Section 2.1. Lower-level subsystems that follow the high-level system branches are described in Section 2.2. The requirements and specifications framework is described in Section 2.4, including the traceable output table structure.

2.1 High-level system decomposition - Lv. 1 and 2

At the principal level, the Einstein Telescope can be modeled as a single system with in- and output interfaces to and from the surrounding environment - the 'site'. Within the context of the Task Force work, interfaces are defined regardless of site location. Instead, the gravitational wave signal is seen as the primary external interface. With this comes the important boundary condition that any baseline design should respect ET's science case - as written in Section 8. The highest-level performance requirement - ET's sensitivity curve - should then match this science case description, and consequently its subsystems should also adhere to these boundary conditions.

At the second decomposition level, the principal system functions and performance requirements are subdivided over four high-level systems: the two instruments - High-Frequency Interferometer (HFI) and Low-Frequency Interferometer (LFI), the Subsurface Civil Infrastructure (SCI) and Technical Infrastructure (TI). Some high-level ET functions might include: detection of GW signals following LFI and HFI's design sensitivity, SCI providing underground space for the detectors or the TI supplying the interferometers with cryogenics. A simple decomposition tree representing the first two decomposition levels of ET is shown in Figure 1.

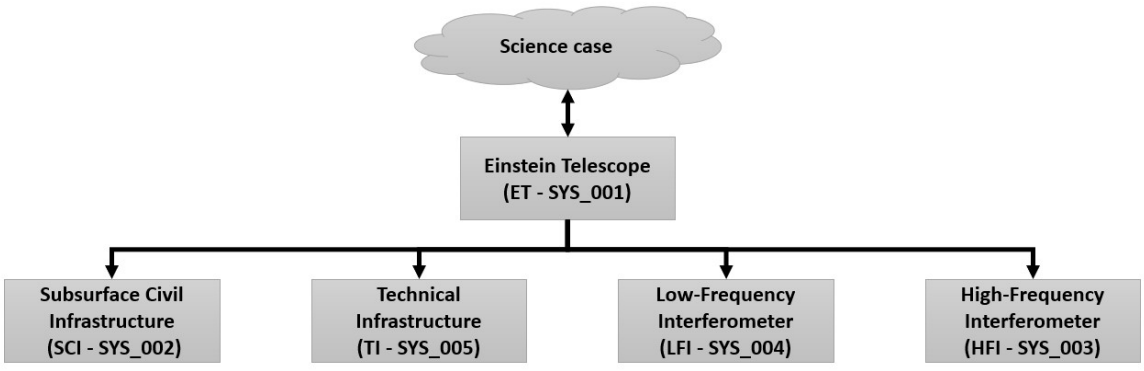

Figure 1: High-level system decomposition of ET as considered within the scope of the Task Force work, also illustrated the connection between the high-level system and Science Case.

Corresponding to the system decomposition, a simple architectural layout can be drafted representing the high-level subsystems with some of their principal functional interactions. Subsystems that have been identified but not worked out within the scope of the Task Force work have not been assigned a System ID in figure 2.

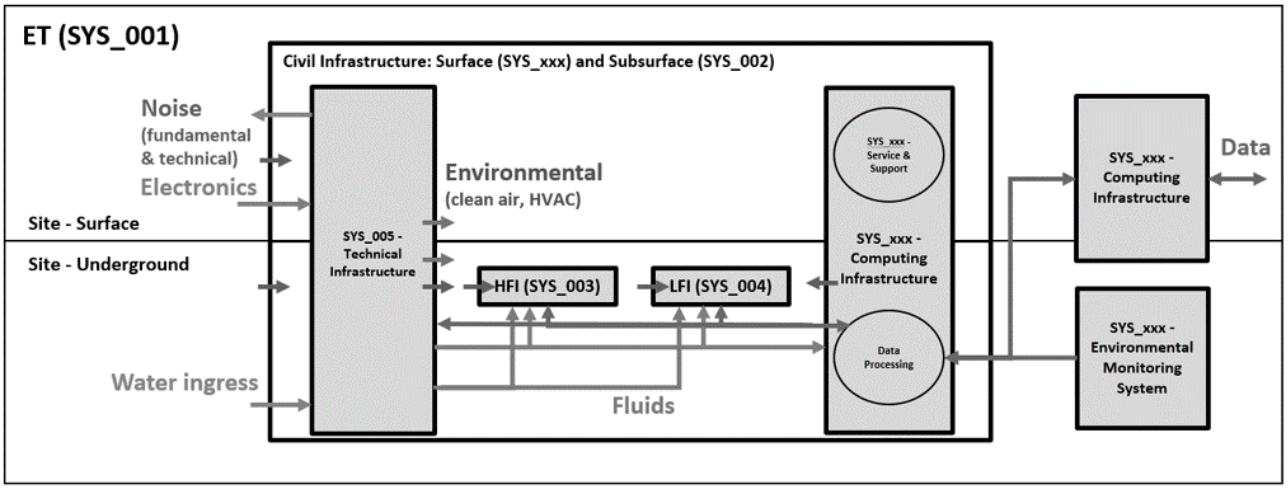

Figure 2: High-level system architecture of ET for decomposition levels 1 and 2. Principal interactions are non-exhaustive.

2.2 Integrated system nodes - Lv. 3

Following the functional partitioning of high-level integrated systems into the four branches (HFI, LFI, SCI and TI), level 3 is derived with an increased emphasis on physical systems. Within the Task Force context, these integrated systems are also referenced as 'nodes'. The decomposition into level 3 subsystems corresponds 1:1 to the Detector layout architectures generated within the Task Force work - a cropped out example of which is the 2L End Station X architecture given in figure 3.

In total, approximately 250 nodes are considered per interferometer pair. As part of the the two instrument branches (HFI and LFI), considered as nodes are for example: the integrated towers (Section 4), a selection of prominent vacuum beampipe segments and HF & LF cryopump subsystems. The Technical Infrastructure decomposition branch (see also Section 5) considers as nodes: cleanrooms, noisy rooms and cryogenic supply infrastructure. Under Civil functional volumes (see also 6) are considered both underground caverns and tunnels.

A schematic decomposition tree, expanded from figure 1, is derived for levels 1-3 in figure 4 below. Included is a selection of node examples taken from the four high-level decomposition branches along with their corresponding System ID, to exemplify the variety of subsystems considered. The examples correspond 1:1 in naming to the nodes depicted in the architecture of figure 3, such that the reader may familiarize themselves with the connection between system decomposition and architectural layout. Please refer to the technical drawings representing the 2L and Triangle Detector layouts (**TD.2**) and System Decomposition output tables (**TAB.1** and **TAB.7**) for a complete overview of integrated system nodes as considered within the Task Force work - where all nodes are listed following the same rationale as the example set.

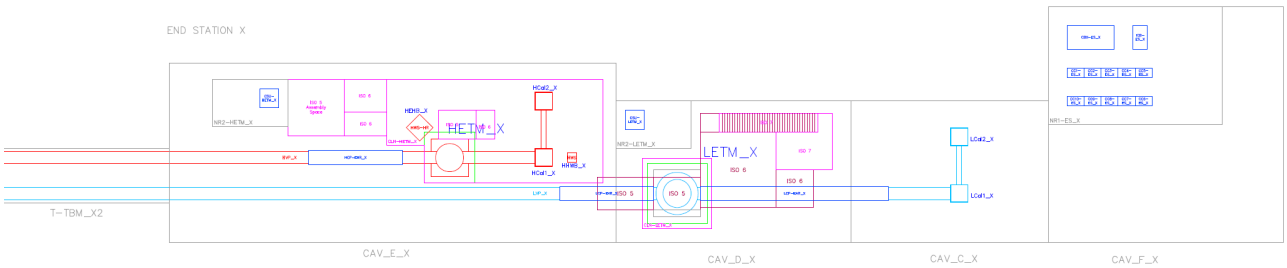

Figure 3: Cropped-out overview of the system nodes considered for an End-Station in the 2L configuration.

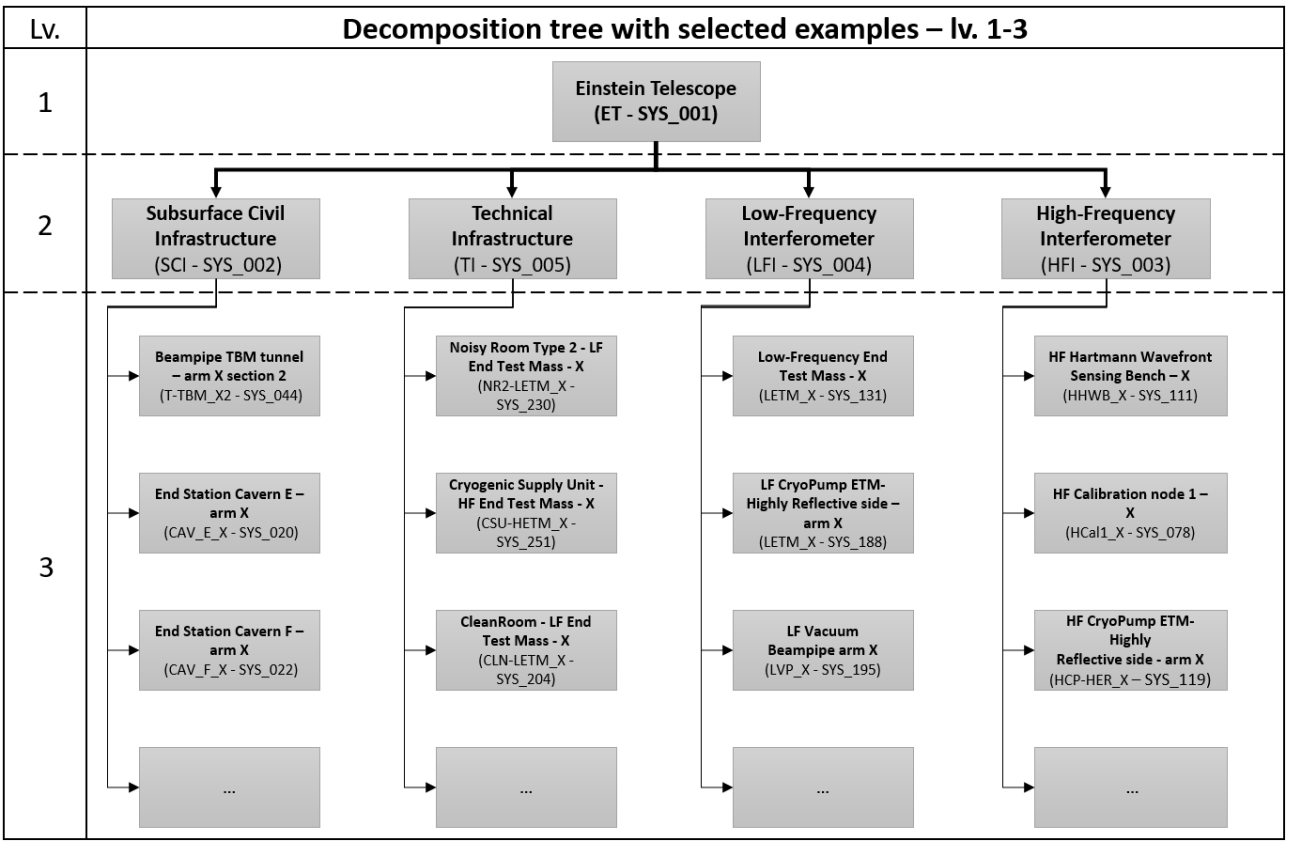

Figure 4: High-level system decomposition with selected examples for decomposition levels 1-3.

2.3 System decompositions for two configurations

Adhering to the Task Force mandate, a system decomposition is made for each geometry: one for the Triangle configuration and one for the 2L. To ensure uniqueness between the configurations and allow for traceability for each set of Output Tables, the following measures are taken:

1. Each configuration is assigned its own range of Unique System IDs: the 2L configuration is constrained between SYS_001 and SYS_299, whereas the Triangle configuration uses any available System ID above SYS_300.

2. The 2L decomposition is made for *one* L observatory: considering one Interferometer pair (HF and LF) and associated Civil and Technical infrastructure (SCI and TI). Output tables are also constructed for *one* L observatory.

3. The Triangle decomposition is made for the *whole* observatory: all three vertices are included in the system decomposition - tripling the number of systems when compared to 2L. This is done to retain consistency with the output Optical and Detector layouts. Output tables are, however, constructed for *one* interferometer pair only - Cornerpoint A - to avoid duplication in the specification lines. This is replicated for the TI and SCI related subsystems unless stated otherwise.

4. Different - but similar - naming conventions are used for 2L and Triangle configurations to more accurately point to a system's position and dependencies. This difference is highlighted in figure 5. Suffix naming considers either the cornerpoint (CornerStation (CS), EndStation_X/Y (ES_X/Y) for 2L, Cornerstation A/B/C for Triangle) or which arm direction a node is placed in (X/Y for 2L, AB/AC, BA/BC, CA, CB for Triangle).

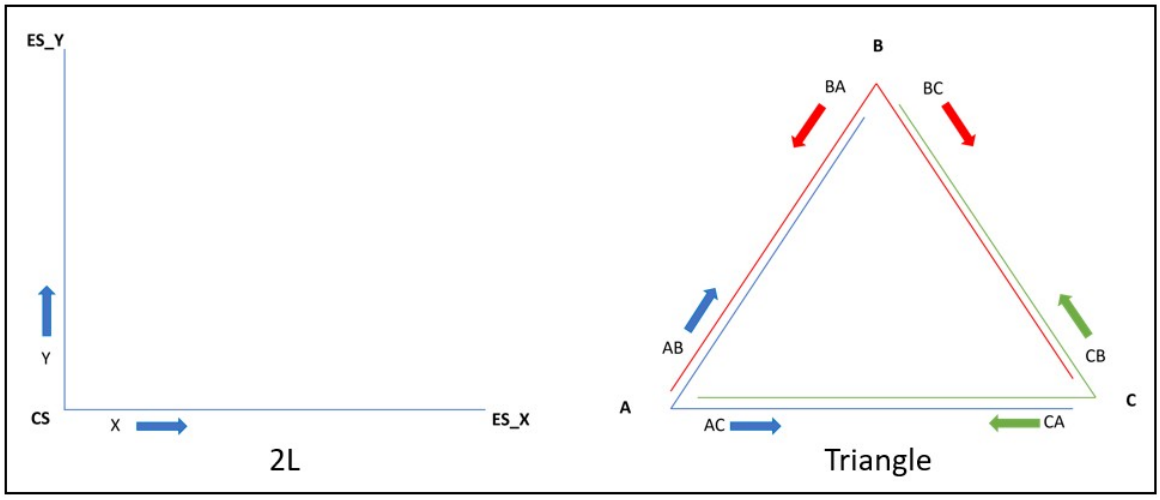

Figure 5: Schematic of naming conventions for both the 2L and Triangle configuration

2.4 Requirements and Specifications framework

The third decomposition level is the lowest considered within the scope of the Task Force work - the scope of which was presented in the previous sections. Given the scale and complexity of ET, the decomposition could certainly be extended beyond this point. For example, some level 4 integrated subsystems in only a single tower - such as the previously mentioned LBS node - might include a dedicated Seismic Isolation system, complex Optical payload and Vacuum Vessel - each with their own complex components - among others.

Representing this properly in a system decomposition would extend the scope beyond what would be possible in the Task Force framework. Therefore, level 4 subsystems are represented by requirements (REQ) and specifications (SPC) lines attached to the level 3 subsystems. These lines represent the boundary conditions considered for their associated subsystems, corresponding to the node's categorization.

The REQ and SPC lines are stored in traceable output table sets. Tables 1-6 correspond to the Triangle configuration, tables 7-12 are reserved for the 2L. They contain, in ascending order, the outcomes of the exercises: System Decomposition (**TAB.1**/**TAB.7**), Tower Integration and Categorization (**TAB.2**/**TAB.8**), Optical Layout (**TAB.3**/**TAB.9**), Detector Layout (**TAB.4**/**TAB.10**), Civil functional volumes (**TAB.5**/**TAB.11**) and Sensitivity & Noise budget (**TAB.6**/**TAB.12**). A schematic of the established information traceability between the output tables contained within one set (TAB1-6: Triangle configuration) is shown in Figure 6, but would be equivalent in the 2L configuration (TAB7-12). An overview of the distribution of System ID's and REQ/SPC line ranges is shown as well in figure 7

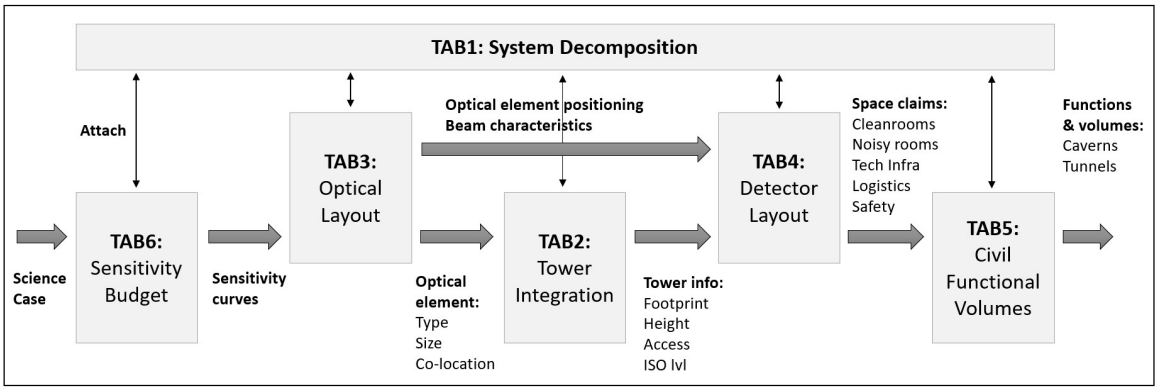

Figure 6: Schematic of information traceability within one set of Output Tables (applied to TAB1-6)

Triangle Requirement (REQ) and Specification (SPC) range allocation:

Output Table #	Requirements Range	Specifications range	Systems range
TAB1: Triangle System Decomposition	N/A	N/A	> SYS_299
TAB2: Triangle Tower Integration	REQ_1000 – REQ_1999	SPC_1000 – SPC_1999	N/A
TAB3: Triangle Optical Layout	REQ_2000 – REQ_2999	SPC_2000 – SPC_2999	N/A
TAB4: Triangle Detector Layout	REQ_3000 – REQ_3999	SPC_3000 – SPC_3999	N/A
TAB5: Triangle Infrastructure Layout	REQ_4000 – REQ_4999	SPC_4000 – SPC_4999	N/A
TAB6: Triangle Science case & Noise Budget	REQ_0001 – REQ_0999	SPC_0001 – SPC_0999	N/A

2L Requirement (REQ) and Specification (SPC) range allocation:

Output Table #	Requirements Range	Specifications range	Systems range
TAB7: 2L System Decomposition	N/A	N/A	SYS_001-SYS_299
TAB8: 2L Tower Integration	REQ_6000 – REQ_6999	SPC_6000 – SPC_6999	N/A
TAB9: 2L Optical layout	REQ_7000 – REQ_7999	SPC_7000 – SPC_7999	N/A
TAB10: 2L Detector Layout	REQ_8000 – REQ_8999	SPC_8000 – SPC_8999	N/A
TAB11: 2L Infrastructure Layout	REQ_9000 – REQ_9999	SPC_9000 – SPC_9999	N/A
TAB12: 2L Science case & Noise Budget	REQ_5000 – REQ_5999	SPC_5000 – SPC_5999	N/A

Figure 7: Overview of distribution of System ID's and Requirement/Specification (REQ/SPC) ranges for the twelve Task Force Output Tables.

3 Optical layout

The Einstein Telescope (ET) is conceptualized in two primary observatory configurations: a Triangle layout and a 2L (dual L-shaped detector) layout, both illustrated in Figure 8. A fundamental aspect shared by both designs is the implementation of a 'xylophone' detector concept. This involves each core detector unit comprising two co-located interferometers: one optimized for low frequencies (ET-LF) and another for high frequencies (ET-HF). When applying this xylophone principle, the triangular configuration will feature an ET-LF and an ET-HF interferometer (the xylophone pair) situated at each of its three vertices. For descriptive simplicity, we refer to the design of a single corner, as this same design will be replicated identically in the other two. This arrangement thereby results in a total of six interferometers for the complete triangular observatory. In contrast, the 2L configuration is envisioned as two independent L-shaped detectors. Analogous to the triangular setup, for descriptive purposes, we can refer to the design of a single L-shaped detector, as the second L-shaped detector will be an identical replication. Each of these L-shaped structures will, in turn, house one ET-LF and one ET-HF interferometer. Consequently, the 2L configuration will comprise a total of four interferometers.
In this chapter, we report on the modifications to the ET optical layout for both the triangular and 2L configurations, as published in 2024 [4, 5].

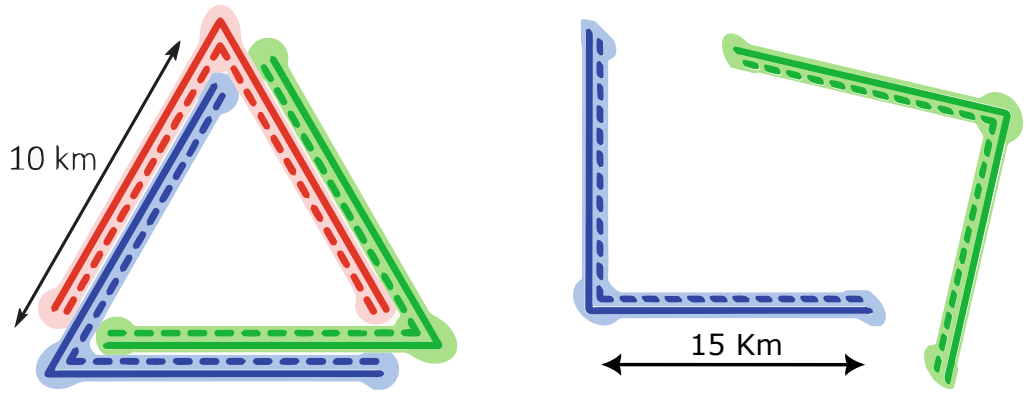

Figure 8: Conceptual layouts for the Einstein Telescope (ET). (a) The Triangle layout, where each of the three vertices hosts a pair of interferometers: one high-frequency (ET-HF, solid lines) and one low-frequency (ET-LF, dashed lines), resulting in a total of six interferometers. (b) The 2L layout, consisting of two independent L-shaped detectors. Each L-shaped detector houses one ET-HF (solid lines) and one ET-LF (dashed lines) interferometer, leading to a total of four interferometers.

The term *optical layout* refers to the placement of all mirrors and the paths of laser beams. It also includes the length and position requirements for both core and auxiliary optical systems that together define the optical configuration of the detector. The *detector layout* represents an evolution of the optical layout, incorporating not only the optics but also the volume allocations for vacuum systems, support structures, cleanrooms, and auxiliary optical benches. The *infrastructure layout* further evolves the detector layout by integrating additional aspects such as tunnel, cavern, and shaft configurations, as well as systems for cooling, ventilation, logistics, and electrical distribution.
The majority of infrastructure-related considerations are consistent with those of the 2024 ET Baseline designs. The baseline optical layout design already considered a number of infrastructure constraints, including the minimum separation between the caverns hosting the beam splitters for mechanical stability, a minimum beampipe diameter to reduce excavation volumes, and a sufficient distance between the input mirrors of the high-frequency (HF) and low-frequency (LF) arm cavities. The latter is essential to ensure adequate space for the LF input mirror cryostats without interference from the HF components. Moreover, the initial assumption was to place both interferometers HF and LF, on two distinct, parallel horizontal planes. In this work, however, we relax this constraint by allowing the filter cavities to lie on a plane different from that of the main interferometer to which they belong.

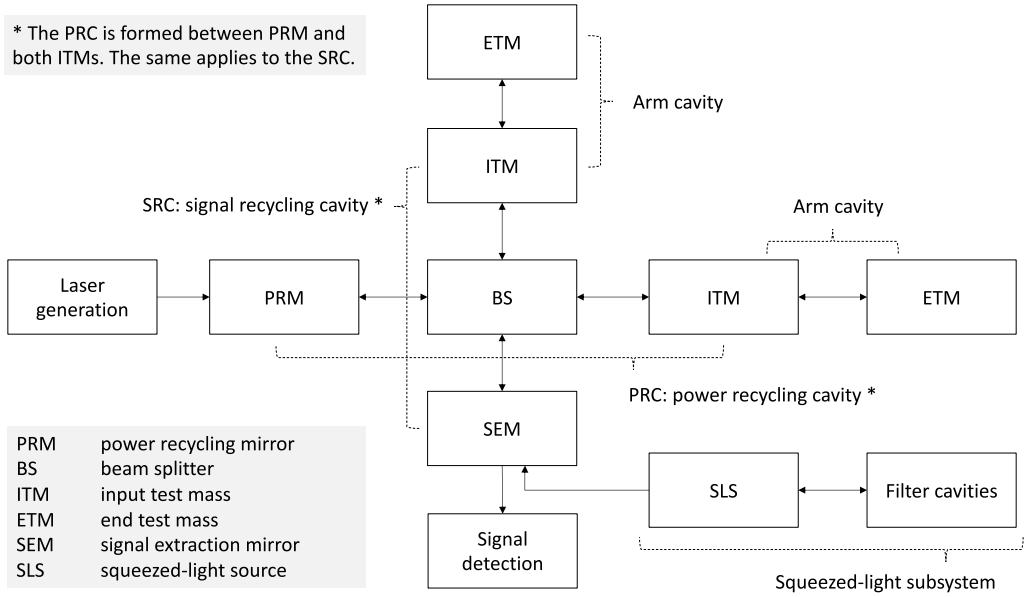

Figure 9: A simplified block diagram of the core components that make up the optical layout.

The design presented herein aims to be more cost-effective than the 2024 ET Baseline while maintaining comparable overall performance. This is achieved, however, by accepting certain forms of increased technical risk. Consequently, a detailed analysis of the impact of these design modifications on the total project cost is a crucial next step. Below is a list of modifications introduced with respect to the baseline layout, valid for both the Triangle and 2L:

- LF filter cavities placed in the X arm, with periscope coupling;
- HF filter cavity relocated to the Y arm with periscope coupling;
- 2-mirror filter cavity design adopted, allowing reduced beampipe diameter;
- Shortened length of the LF input mode cleaner (IMC);
- HF IMCs merged into a single tunnel;
- Beam routing for the Balanced Homodyne Detection (BHD) system passing through the beam splitter;
- Additional reconfiguration of components, primarily by assuming that multiple major optics can be hosted in the same vessel ("tower merging");
- Re-assessment of auxiliary sensing systems, their requirements, and the implementation of these requirements, resulting in smaller, more accessible optical bench footprints.

3.1 Core Optical Layout

The Einstein Telescope (ET) detectors, ET-LF and ET-HF, are *dual-recycled Fabry-Perot Michelson interferometers* (FPMI) with a complex optical layout comprising many subsystems and a large number of optical

elements with strong interdependencies. A simplified overview of the core components of the optical system is illustrated in Figure 9.
There is a hierarchy in the optical layout: at the heart of the detectors, where the interaction with gravitational waves takes place, are the *arm cavities*, which are 10 km and 15 km long for the triangular and 2L configurations, respectively. The laser beams from both arms can be traced back to the central Beam Splitter (BS). Moving further upstream, two optical paths emerge: one leading toward the injection and input laser through the Power Recycling Cavity (PRC), and the other toward the detection system, where gravitational-wave signals are detected, through the Signal Extraction Cavity (SEC).
The overall optical layout has been developed by adhering to a set of optical constraints aimed at maximizing detector performance in terms of sensitivity and controllability. For ET-LF, we prioritize minimizing the number of optics, in order to minimize the number of suspensions and reduce suspension and related control noises. For ET-HF, the circulating power in the interferometer is relatively high (up to 3 MW in the arms) and the optics are subject to thermal deformation. A key constraint is maintaining a sufficiently large beam size on optical surfaces in order to reduce power density, thereby mitigating thermal noise contributions. Additionally, an appropriate accumulation of the Gouy phase ($\sim 20°$) is required to ensure the stability of all optical cavities. Minimization of optical losses, essential for preserving the sensitivity curve, has also guided the layout. To this end, the angles of incidence have been optimized to compensate astigmatism, and a collimated beam has been implemented at the beam splitter for the ET-HF detectors in both 2L and triangular configurations. This requirement has been relaxed for ET-LF, where the lower circulating power (up to 18 kW in the arms) allows for a less stringent collimation condition. More details are provided in [4] and [6].
To satisfy these design constraints, the optical layout begins at the arm cavities and extends toward the recycling mirrors. The beam first encounters a large, flat steering mirror, which redirects it toward a separate cavern housing the beam splitter and the recycling cavity optics. This mirror also enables the recombination of the two arm beams at the appropriate angle of 90° for ET-HF and 60° for ET-LF within the triangular configuration. For the 2L configuration, this angle is 90° for both ET-HF and ET-LF. At the input test mass (ITM) level, a focusing element is included. This may take the form of a curved compensation plate (CP) or a curved anti-reflective (AR) surface on the ITM, serving to focus the beam toward the beam splitter.

Figure 10 illustrates the general arrangement of the core optics. For ET-HF (both triangular and 2L configurations), the beam from the input test mass (ITM) initially propagates to the flat mirror ZX(Y)3. The path is then folded into a Z-shape by this mirror and the subsequent flat mirror ZX(Y)2 before reaching the curved mirror ZX(Y)1. Within this overall path, a two-element telescope is formed by the curved anti-reflective (AR) surface of the ITM (or an associated compensation plate) and ZX(Y)1. This telescope is designed to reduce the beam size and ensure its collimation at the BS (refer to Tables 1 and 3 for component path lengths). A second Z-shaped telescope system is implemented in the recycling cavity paths (PRC and SEC) for Gouy phase management and achieving target beam sizes on the PRM and SEM. For the ET-LF interferometers, which have a more relaxed collimation requirement at the BS, the beam from the ITM also first propagates to the mirror ZX(Y)2. The subsequent path to the BS is also arranged in a Z-shape. The optical elements forming this Z-shaped path and the telescope are the curved ITM-AR surface (or CP) and the curved mirrors ZX(Y)2 and ZX(Y)1, which collectively manage the beam parameters (component path lengths are detailed in Tables 2 and 4). This telescope is employed in both triangular and 2L designs. It should be noted that in the optical modelling for this design, the beam splitter (BS) was treated as a thin optic, neglecting its physical thickness. The resulting beam path deviations are considered minor and are not anticipated to necessitate significant changes to the layout, beyond potential fine-tuning of mirror radii of curvature.
A comprehensive list of optical parameters for all major components, including e.g., the radii of curvature for the optics and spot sizes, is provided in section C of Technical Annexes **TAB.3** and **TAB.9** for the triangular and 2L configurations.

3.1.1 Baseline Triangle layout

The baseline Triangle layout design follows the general design constraints and process outlined in Section 2 of its design document [4]. The triangular configuration inherently faces stricter infrastructural constraints, which limits flexibility for extensive design variations compared to other potential layouts. One significant

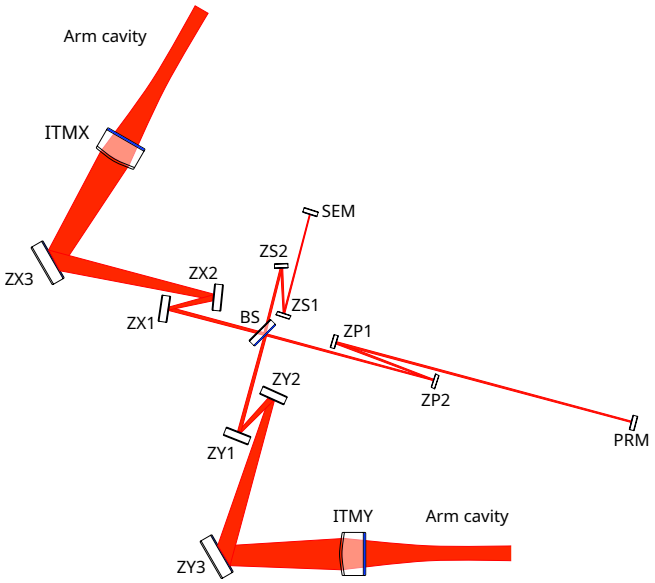

(a) Triangle ET-HF.

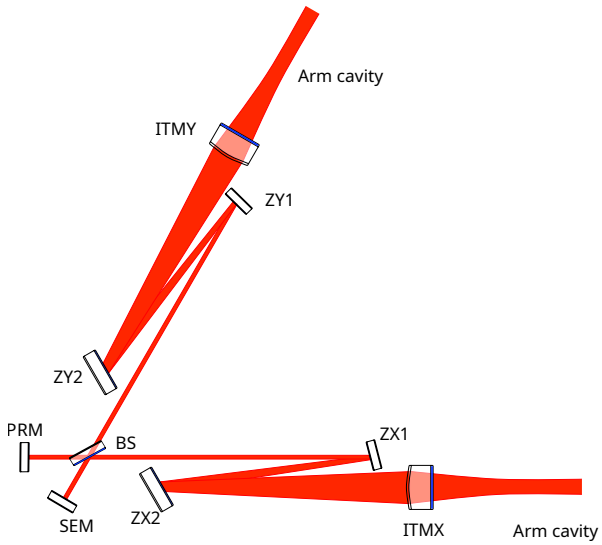

(b) Triangle ET-LF.

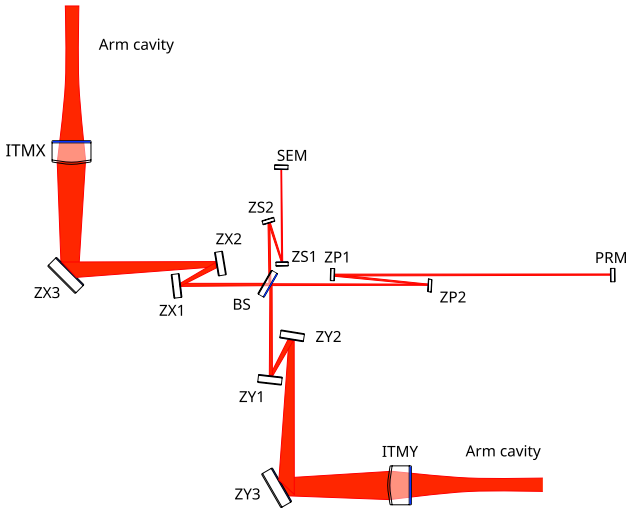

(c) 2L ET-HF.

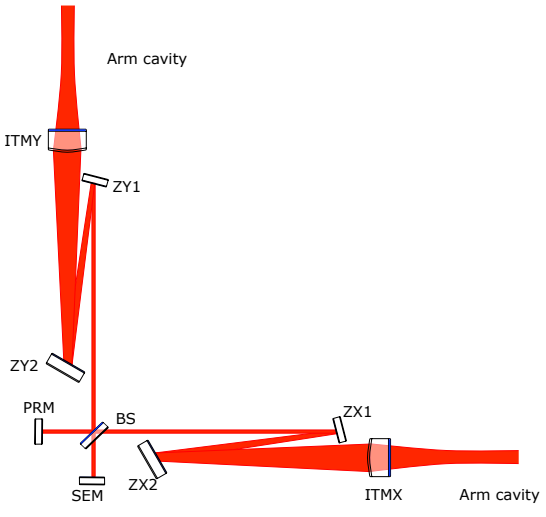

(d) 2L ET-LF.

Figure 10: Overview of the ET optical layouts. (a) Triangle ET-HF, (b) Triangle ET-LF, (c) 2L ET-HF, and (d) 2L ET-LF. These designs illustrate the core optical paths and component arrangements for each interferometer type and geometrical configuration.

example of such constraints is the impact of the LF tank cryostat footprint. Given the co-location of LF and HF interferometers at each vertex, the substantial size of the LF cryostat can constrain the available space for HF components and potentially influence the design of local tunnel sections, limiting overall layout flexibility in this regard.
From an optical design perspective, another key distinction of this configuration lies in the angle of incidence (AoI) at the beam splitters. To optimize central area usage, mitigate some of these spatial constraints, and achieve cost reductions, the core optics surrounding the HF-BS in the triangular configuration have been repositioned. This results in a more compact layout and allows for the co-location of multiple optical components, often within shared vacuum chambers. Specifically for the Triangle, this redesign led to a 10 m reduction in the total length of the signal extraction cavity. Independently of this, its power recycling cavity was also shortened by 40 m as part of a broader cost-reduction strategy.
Table 1 reports the lengths of the arm and recycling cavities in ET-HF for the triangular configuration, along with the corresponding variations with respect to the 2024 design.
Table 2 summarizes the lengths of the arm and recycling cavities in ET-LF for the triangular configuration, which remain unchanged compared to the 2024 design.

3.1.2 Baseline 2L layout

The 2L configuration presents an alternative baseline design. While also adhering to the fundamental design principles (as outlined for the general ET concept, e.g., in [4]), it benefits from fewer infrastructure constraints than the Triangle layout. This characteristic allows for a wider range of designs compatible with the ET requirements to be initially considered.
Notably, the specific arrangement proposed in [5] for the 2L layout was identified as uniquely preventing the long tunnel diameters from being constrained by the LF tank cryostat footprint, a challenge highlighted earlier for the Triangle configuration. This is a crucial technical feature that significantly enhances the detector's practicality in the 2L case. Indeed, this 2L configuration offers a robust solution against potential changes in the LF-ITM tank shape and size (which are not yet finalized) and provides substantial flexibility for future adjustments. Furthermore, the separation between the two caverns hosting the HF and LF vertices is more conservative in this 2L design, affording greater robustness for civil construction.
Consistent with the optimization goals mentioned for the Triangle layout (see Section 3.1.1), the 2L design, as described in [5], also incorporates a strategic repositioning of core optics around its HF beam splitter(s). This approach similarly aims to optimize central area usage and reduce costs, leading to a more compact central station and facilitating co-location of components. This redesign led to a 12 m reduction in the total length of the signal extraction cavity. Independently of this, the power recycling cavity was shortened by 15 m as part of a cost-reduction strategy.

Table 3 reports the lengths of the arm and recycling cavities in ET-HF for the 2L configuration, along with the corresponding variations with respect to the 2024 design.
Table 4 summarizes the lengths of the arm and recycling cavities in ET-LF for the 2L configuration, which remain unchanged compared to the 2024 design.

Distance names	**Lengths** [m]	**Variations**
Arms (identical for both arms)		
ETM to ITM:	10000	Not changed
Recycling cavities (Common path)		
TM's thickness	0.3	Not changed
ITM-AR to ZX(Y)3:	10	Not changed
ZX(Y)3 to ZX(Y)2:	45	Not changed
ZX(Y)2 to ZX(Y)1:	10	Not changed
ZX(Y)1 to BS:	26.05	Not changed
Distance name	**old → new [m]**	**Variation**
Signal Extraction Cavity path		
BS to ZS2:	22 → 20	2 m reduction
ZS2 to ZS1:	15 → 15	Not changed
ZS1 to SEM:	23 → 15	8 m reduction
Total length:	151.35 → 141.35	10 m reduction
Power Recycling Cavity path		
BS to ZP2:	45 → 45	Not changed
ZP2 to ZP1:	30 → 30	Not changed
ZP1 to PRM:	100 → 60	40 m reduction
Total length:	266.35 → 226.35	40 m reduction

Table 1: **Triangle** ET-HF: Arm and Recycling Cavities Lengths

Distance name	**Lengths** [m]	**Variation**
Arms (identical for both arms)		
ETM to ITM:	10070	Not changed
Recycling cavities (Common path)		
TM's thickness	0.57	Not changed
ITM-AR to ZX(Y)2:	54	Not changed
ZX(Y)2 to ZX(Y)1:	45	Not changed
ZX(Y)1 to BS:	56	Not changed
Signal Extraction Cavity path		
BS to SEM:	10	Not changed
Total length:	165.57	Not changed
Power Recycling Cavity path		
BS to PRM:	10	Not changed
Total length:	165.57	Not changed

Table 2: **Triangle** ET-LF: Arm and Recycling Cavities Lengths

Distance names	**Lengths** [m]	**Variations**
Arms (identical for both arms)		
ETM to ITM:	15000	Not changed
Recycling cavities (Common path)		
TM's thickness	0.3	Not changed
ITM-AR to ZX(Y)3:	10	Not changed
ZX(Y)3 to ZX(Y)2:	62	Not changed
ZX(Y)2 to ZX(Y)1:	10	Not changed
ZX(Y)1 to BS:	25.3	Not changed
Distance names	**old → new [m]**	**Variations**
Signal Extraction Cavity path		
BS to ZS2:	25 → 20	5 m reduction
ZS2 to ZS1:	15 → 15	Not changed
ZS1 to SEM:	22 → 15	7 m reduction
Total length:	169.6 → 157.6	12 m reduction
Power Recycling Cavity path		
BS to ZP2:	45 → 45	Not changed
ZP2 to ZP1:	30 → 30	Not changed
ZP1 to PRM:	75 → 60	15 m reduction
Total length:	257.6 → 242.6	15 m reduction

Table 3: **2L** ET-HF: Arm and Recycling Cavities Lengths

Distance names	**Lengths** [m]	**Variations**
Arms (identical for both arms)		
ETM to ITM:	15050	Not changed
Recycling cavities (Common path)		
TM's thickness	0.57	Not changed
ITM-AR to ZX(Y)2:	57	Not changed
ZX(Y)2 to ZX(Y)1:	45	Not changed
ZX(Y)1 to BS:	58	Not changed
Signal Extraction Cavity path		
BS to SEM:	8	Not changed
Total length:	168.57	Not changed
Power Recycling Cavity path		
BS to PRM:	8	Not changed
Total length:	168.57	Not changed

Table 4: **2L** ET-LF: Arm and Recycling Cavities Lengths

3.2 Squeezed Light

The squeezing subsystem for both the HF and LF interferometers in the Einstein Telescope has been redesigned compared to the 2024 baseline. This redesign aims at reducing infrastructure costs while preserving the detector's sensitivity performance that is detailed in [5, 7]. To achieve this, the new optical configuration introduces higher technical risks, reduces system flexibility and tunability, and foregoes the possibility of future upgrades requiring more than one squeezing source.

Before detailing the modifications, the 2024 baseline configuration is summarized below.

- ET-LF employed frequency-dependent squeezing using two parallel 5 km-long filter cavities.
- ET-HF used a single 1 km-long filter cavity.
- A beam-to-pipe diameter ratio of at least 5 was maintained to ensure clipping losses were negligible. This resulted in cavity beampipes with a 1 m internal diameter, including at least 20 cm of space for baffling.
- The two LF FCs were housed in a dedicated tunnel, and the single HF FC in another one. The tunnels were located in the same horizontal plane as the corresponding interferometer.
- The horizontal center-to-center spacing between the two ET-LF FCs was 4.5 m, driven by beam-pipe size and passage clearance in between; the tunnel diameter was 6.5 m.
- Filter cavities were implemented as linear three-mirror coupled cavities, allowing finesse tuning to adapt to changes in the interferometer configuration and/or performance. This required three separate suspension towers hosted in separate caverns, whit the middle one a few hundered meters from the input mirror.
- The squeezing laboratories were located in front of the filter cavities and connected to the respective interferometers via a vacuum beampipe delivering squeezed light to the HF-SQI and LF-SQI benches. The length of this beampipe was kept relatively short (few tens of meters).

Following the finalization of the optical and detector layout documents, the ET squeezing working group began investigating alternative configurations for the filter cavity layout, with the aim of providing flexibility options to be exploited to reduce infrastructure costs. For each configuration, potential risks and optical performance concerns were identified and qualitatively analyzed. The results of this study are summarized in [8], and formed the basis for the design decisions made by the ETO Task Force.

The current baseline places the HF and LF filter cavities inside the interferometer arm tunnels, thus eliminating the need for expensive dedicated tunnels. After analyzing several configurations, the one considered least risky, while still providing the opportunity for substantial cost savings, was selected. The main modifications to the squeezing subsystem are detailed below. The most relevant squeezing subsystem parameter changes between the 2024 configuration and the baseline presented in this document are summarized in Table 5. A list of the considered but discarded configurations is presented both in [8] and in the extended support document [6].

	2024 Reference	**2025 Triangle**	**2025 2L**
Position of FCs	Separate tunnel	ITF Arms Tunnel	ITF Arms Tunnel
Number of FC Mirrors	3	2	2
Diameter of FC Beampipes	1 m (LF and HF)	62 cm LF, 40 cm HF	62 cm LF, 40 cm HF
FC Center-to-Center Distance	4.5 m (LF)	3.4 m (LF)	3.4 m (LF)
Length of Periscope	–	2.0 m (HF), 4.0 m (LF)	2.0 m (HF, LF)
Position of Periscope (HF)	–	Near SQZ Lab	Near SQZ Lab
Position of Periscope (LF)	–	Near the Vertex	Near SQZ Lab
SQZ Lab to Interferometer Distance	∼50 m	∼550 m	∼120 m
# of Suspended Benches (SQZ Lab)	8 HF, 12 LF	6 HF, 11 LF	6 HF, 10 LF
Dimension of Suspended Benches	1.5 × 1.5 m	1.5 × 1.5 m	1.5 × 1.5 m

Table 5: Summary of main modifications to the SQZ subsystem

First of all, the filter cavities' optical configuration is simplified with the aim of reducing the beam spot on the mirrors and consequently the diameter of the vacuum beampipes. The lengths of the HF and LF filter cavities remain unchanged, but they are converted from three-mirror coupled cavities to standard two-mirror Fabry–Pérot cavities. This change brings multiple benefits: it reduces the beam diameter on the mirrors, allowing for smaller beampipe and mirror diameters; it increases the effective optical length of the cavity, which now coincides with the full physical length (e.g. 5 km for the LF filter cavities); it removes the need for an additional tower along each filter cavity, together with the associated caverns and supporting civil infrastructure; and it simplifies the control scheme, which reduces system complexity and associated risks. However, this simplification also reduces the design's flexibility, as it limits the options for tuning the filter cavity linewidth to direct mirror replacement or thermal tuning of the input mirror reflectivity via the etalon effect. This early downselection limits adaptability and may constrain future optimization, increasing performance risks.

A further reduction in beampipe diameter is achieved by a more accurate evaluation of the impact of beam clipping, with associated reduction of the safety margins, thus requiring a smaller clear aperture of the baffle.

The LF FCs are placed together in one of the arm tunnels, while the HF FC is placed in the other. In the triangular configuration, all FCs have their axis laying on a plane that is 4.0 m above the LF interferometer plane and 2.0 m above the HF one. In the 2L configuration, all FCs have their axis in a plane that is 2.0 m above the plane containing both interferometers. A cross section of the arm tunnels of all the described configurations can be found in Figure 17 and in Figure 18. Thanks also to the reduction in the diameter of the beampipes, the center-to-center horizontal separation of the LF FCs is reduced from 4.5 m to 3.4 mm.

The HF and LF squeezing laboratories are located directly in front of the respective FCs, at the same elevation (thus above the interferometer arm beampipes, one laboratory per arm). Their configuration is similar to that shown in [4], with a few modifications:

- The two benches (one in air and one suspended) for the second squeezing sources have been removed; their space is instead reserved for future flexibility. This reduces the system's capacity for future upgrades.
- Mode-matching telescopes are no longer placed on a single bench but are shared between two benches. This is motivated by a more mature study of the telescopes, rather than by cost reduction.
- An additional bench has been added to ease beam reshaping from the squeezing lab to the interferometer via a shared telescope across two optical benches. Also this is motivated by a more mature design of mode matching telescopes.

The vacuum vessels in the squeezing laboratories are arranged to maximize length along the beam axis and minimize width in the transverse direction. This enables the construction of the squeezing clean rooms within the main caverns at the start of the arm tunnels. The laboratory dimensions accommodate all benches, allow the opening of two opposing doors per bench, and support the integration of beam-shaping telescopes implemented using Z-shaped layouts shared across multiple benches.

When locating the squeezing laboratories above the interferometer arms, interference with other critical components need to be avoided.The labs must be placed:

- in the triangular configuration, after both the ITM cryostat of the local interferometer and the ETM cryostat of the far interferometer (approximately 550 m from the vertex).
- in the 2L configuration, after the ITM cryostat (approximately 120 m from the vertex),

The squeezed light beam is lowered to the interferometer level using a periscope. To minimize the risk of polarization rotation, the periscope should be comprised of two 45-degrees mirrors that change the height of the beam without changing direction of propagation of the output beam compared to the input one. The steering of the beam on the horizontal plane is achieved through an additional dedicated mirror. The height of the periscope (from input to output plane) is 4 m in the triangular configuration and 2 m in the 2L configuration. These periscopes are about 10 times taller than what has been implemented so far in gravitational wave detectors; this choice thus introduces additional technical risks associated with stability and controllability issues that are not fully studied and understood yet. Misalignment of the beam and polarization axis with respect with the mirrors normal would induce polarization mixing; thus, residual angular motion of the periscope mirrors must remain be carefully controlled to satisfy scattering and loss requirements (see [6]). The periscope is located near

the vertex (triangular configuration) or near the squeezing lab (2L configuration), allowing personnel to walk in the arm tunnel without interfering with the beampipe connecting the squeezing lab to the interferometer.

The squeezed light is routed from the laboratory to the detector through a beampipe passing through the main cavern and injected into the HF-SQI or LF-SEM vessel. Between the squeezing lab and the SEM vessels, the beam propagates approximately 550 m (Triangle) or 120 m (2L). To preserve beam quality, the beam diameter is set at approximately 4 cm (Triangle) or 1 cm (2L), within a 35 cm (Triangle) or 25 cm (2L) diameter beampipe. At the OFI, the beam is reduced to 3 mm and injected through the second polarizer. A shared telescope between the SEM and SQI benches compresses the beam to the required diameter.

3.3 Input and Output Optics

The Input and Output Optics system (IOO) deals with the injection of the laser beam into the symmetric port of the interferometer on one side, and with the detection of the laser beam coming out from the interferometer at the antisymmetric port on the other.

The Input Optics include the functional systems: to provide radio-frequency phase modulations (RF sidebands) of the main beam to allow interferometer sensing and control, to provide spatial, intensity and frequency filtering of the main beam (via Input Mode Cleaner, IMC cavities), provide frequency reference for the main laser beam (via Input Mode Cleaner and Reference cavities), to provide polarization filtering of the main beam, to adapt the shape of the main beam to the interferometer eigenmode (via a mode matching telescope, MMT), and to provide access to the back-reflected beam from the symmetric port of the interferometer via a Faraday Isolator, which also serves the purpose of mitigating back-reflection issues from the interferometer to the other optical resonators of the system.
In current GW detectors, frequency noise suppression relies on a combination of a suspended IMC cavity, a rigid Reference Cavity to manage low Fourier-frequency noise during lock acquisition of kilometer-scale arm cavities, and feedback from the common-arm degree of freedom of the Interferometer [9, 10]. However, the ET arms are a factor of few longer than the present interferometers, and the much lower cavity pole of the arm cavities renders the common-arm reference impractical, necessitating a rethinking of the frequency stabilization strategy [11]. The IMC for ET must therefore replace the common arm degree of freedom as a reference over a bandwidth much extended towards low Fourier-frequencies.
the LF interferometer has less stringent frequency noise requirements [12], which could be met by using a single IMC. While in 2024 only a first upper estimate of the length was provided, during the Task Force we have calculated that a 120 m long IMC (round-trip length would be 240 m) is appropriate. The choice of this length was driven both by the frequency noise requirements and by the ISC requirement to have small enough free spectral range (FSR) in order not to limit too much the granularity choice of the RF sidebands.
For the HF interferometer, the requirements for frequency noise are much more demanding [12, 11] and a double IMC configuration is foreseen to fulfill the requirements. The two IMCs will be long: $IMC_1 = 100\ m$ and $IMC_2 = 300\ m$ (the relative round-trip lengths will then be 200 m and 600 m, respectively).
The baseline geometry for the IMCs is triangular cavity, although other configurations are currently being studied, particularly a bow-tie geometry which may offer performance advantages where astigmatism is a limiting factor (see [6]). The apex angle of each cavity shall be large enough that backscattering to the reverse sense of circulation is disfavored. This implies the use of vacuum beampipes as large as the ones used for the arms. The orientation of the IMCs axis with respect to the interferometer is not fixed as long as the input and output ports of the IMC lie on the axis between the PSL laser and the PRM mirror. Furthermore, in order to reduce excavated volume and the number and footprint of vacuum vessels, some optimization has been performed on the layout by the Task Force, especially for the two ET-HF IMCs. First of all, both IMCs for the HF interferometer have been placed in the same tunnel. To do so, the separation between the cavity axes has been reduced by removing the intermediate vacuum vessel between the two. This vacuum vessel hosted conditioning optics for output of IMC1 and input of IMC2, and the related optical components were reshuffled and merged with input benches for IMC1 and IMC2.
The pre-stabilized laser (PSL) is not strictly in the IOO scope, but it is clearly strongly entangled with the requirements and the layout of IOO. The PSL room positioning assumes that the final laser is emitted towards one of the long sides of the room for the 2L configuration (and towards the short side of the room for the

Triangle), with free orientation. To reduce overall footprint, some of the optics for the mode matching telescope to the IMC are now hosted on the optical bench launching the laser beam to the IMC.

The Output Optics include the output mode matching telescope to adapt the beam coming out of the antisymmetric port of the interferometer to a size that is manageable on an optical bench, provide spatial and frequency filtering of the main output beam via an output mode cleaner (OMC) cavity which selects only the beam carrying the GW signal, provide an injection point for the squeezed vacuum into the antisymmetric port of the interferometer via a Faraday Isolator which serves also the purpose of mitigate backreflection issues to the interferometer.
Furthermore, the Output Optics include all the necessary components to realize the **Balanced Homodyne Detection** scheme for GW signal readout [13]. A local oscillator (LO) beam to serve as a reference is generated via a pick-off at the symmetric port of the interferometer (LF) or inside the PRC (HF) and routed to the detection bench to interfere with the main beam coming out from the anti-symmetric port.
In ET-HF the pick-off was a straightforward decision due to the presence of two pairs of folded telescopes inside the recycling cavities, so a pick-off similar to that planned for current GW detectors, and path introducing minimal additional infrastructure was chosen. For LF, no equivalent pick-off is available, so a long beampipe was needed in the 2024 optical layout to deliver the LO from the symmetric port to the detection bench. However, this severely limited access to the LF main vessels/clean rooms (especially LF SEM, which was only accessible from inside a triangle of beampipes). Furthermore, the long beampipe implied a larger cavern. The optimization operated by the Task Force thus eliminated the beampipe, instead routing of the LO through the same beampipes as the main beam via the BS vessel. This allowed to reduce the central cavern space, and to improve operability of the vessels in the central area. The cost to pay is that additional optical elements are needed inside the BS vessel to steer the LO to the detection bench, i.e. vessels housing major LF optics must be compatible with suspending multiple optical elements (note this was already true for the SEM vessel, as it is used for routing of the SQZ beam).
The most downstream vessel at the antisymmetric port (OMC) hosts also the wavefront sensors and detection photodiodes, the latter arranged in a setup realizing the balanced homodyne detection. Presenting a design for these photodiodes is well beyond the scope of the present document, only some generic requirements can be listed here: they should be in an ultra-high vacuum compatible housing, feature a very high quantum efficiency, be able to withstand the designed power of the Local Oscillator at the antisymmetric port without thermal effects and non linearities, be shot noise limited and as similar as possible to each other, in order to minimize the corrections for the balanced detection, have a frequency response as smooth as possible over the whole detection bandwidth.

Differences between 2L and Triangle IOO versions are described in the following.
Most of the functions in the two configurations are absolved with exactly the same blocks and distances. There could be slightly less demanding requirements in terms of frequency noise for the Triangle configuration, due to the shorter arm length which in turns makes for a larger FSR. This could mean that the common arm degree of freedom could be used to a larger extent in the Triangle configuration as compared with the 2L configuration. However, this is hugely dependent on the control strategy which is far from being mature at this stage, so we assume the same implementation of the Input Optics both for Triangle and 2L configurations.
No relevant differences are evident for the Output Optics in the two configurations.

3.4 Auxiliary Optics

The auxiliary optics are a broad collection of many small optical subsystems that are used to sense and control key parameters of the interferometers. They enable the detector to operate at its maximum sensitivity, controlled at the target working point. These subsystems are located on optical benches close to the vessels containing the main optics. Typically, they require more frequent access than the main vessels, but still (with some exceptions) need to be suspended and under vacuum. The required systems and their position in relation to the main optics are identical for the 10 km triangular and 15 km L shaped configurations. However, since these benches typically include some steering and shaping optics to divide the beam and prepare it for the various sensors, there is some freedom in the orientation and the shape of the specified footprints.

The auxiliary optics are grouped into several categories:

- **Global Sensing** - A set of photodiodes used to extract information about the longitudinal and angular degrees of freedom in the core optical layout. These are used together with local sensors co-located with the main vessels, which provide initial feedback to isolate and control the motion of the optics before the global controls signals are available.
- **Auxiliary Laser System** - An additional laser source and set of photodiodes used to control the length of the arm cavities while each interferometer is in the process of being 'locked' to its target working point, as part of the 'lock acquisition strategy'.
- **Wavefront Sensing and Control** - A set of sensors and actuators used to sense and correct the curvature of the optics, and other optical deformations, which are often thermally driven. For this reason, the system includes significantly more elements for ET-HF than for ET-LF. The sub-assemblies include:
  - **Hartmann Wavefront Sensors** (HWS) - to detect the radius of curvature of the test masses and presence of point absorbers in ET-HF.
  - **Mode Converter Telescopes** (MCTs) - to detect the shape of the laser beam resonant in each part of the dual-recycled optical configuration, and mismatches in this shape between various parts of the optical configuration
  - **Phase Cameras** (PCs) - to directly measure the shape of the optical field at key locations
  - actuators to correct the shape of the ITMs (CO2 lasers) and beamsplitter (CO2 or matrix mask) in ET-HF, each with their own dedicated optical systems. These must be in-air to accommodate the laser sources.
  - co-located actuators such as ring heaters or CHRoCCs on major optics
- **Calibration** - Located behind the end mirrors of the arms, these systems are used to calibrate the detector response, e.g. using photon or Newtonian caibrators

We have conducted a review of all of these systems as specified in the 2024 documentation. In collaboration with the detector layout and tower integration teams, we made the following adjustments:

- we now provide the individual footprint for each subsystem at a location, rather than the total area needed at a node. For example, we now provide individual footprints and positioning constraints for the CAL, ALS, ISC and TCS systems co-located on transmission from the end test masses. This provides flexibility to the detector layout and tower integration teams, as a coarse estimate of how these may be grouped into vessels, rather than implying that a single, very large vessel, is the only solution.
- we identified and removed some duplicated systems in the output path.
- we moved some MCTs in ET-HF's recycling cavities to locations that are likely better for meeting their performance goals. This also resulted in a more consistent sizing of auxiliary benches in this part of the interferometer.
- some subsystems were previously implemented with larger footprints than was stated and justified in the main text, so could simply be revised down.
- some subsystems were implemented as vacuum vessels rather than in-air systems, this was corrected.

This has allowed the overall configuration to be slightly compacted, and reduced the need for some extremely large vessels (e.g. 2.5x2.5m optical benches) which would have been challenging to work in.

3.5 Flexibility Considerations

As outlined in section 1.1, we have considered several specific categories of flexibility in these designs, both those provided as an *envelope* to the detector layout and local teams that can be exploited to suit the local geography, and those we '*demand*' as a flexibility within the infrastructure, to allow for future design adjustments and upgrades. This work is limited to considering the primary drivers of the detector layout, i.e. aspects that are anticipated to have an impact on the overall footprint of the facility.

3.5.1 Flexibility Envelope of the Optical Layout

We broadly define four categories, following a 'traffic light' - style rating:

- **Free** (green): unconstrained.
  A parameter that can be freely chosen to optimize the design for cost, geography, accessibility, and other factors.
  For example: the orientation of the IMCs with respect to the main interferometer.

- **Minor redesign** (yellow): likely possible.
  Changing this parameter will have some moderate impact on the local optical layout with limited impact on the global configuration.
  For example: distance between vessels in the input path from PSL to PRM.

- **Major redesign** (orange): some limited flexibility.
  Changing this parameter is likely to have significant knock-on impacts for the global optical layout that will need careful study, depending on the magnitude of the requested change.
  For example: lengths within the recycling cavities.

- **None** (red): completely constrained.
  A parameter that can *not* be altered by teams other than optical layout. The value of the parameter may be altered as a result of an optical layout redesign, but may not be considered independently.
  For example: angles of ZMs in the recycling cavities.

It is essential that *any* exploitation of the flexibility envelope, including alterations within the tolerance values where stated, is done in consultation with the optical layout team. This is both to ensure that the alteration is compatible with the performance requirements of the optical design, and so that continued studies to evaluate and further complete the optical design (e.g. control scheme design) are based on consistent numbers.

The flexibility envelope categorisations are directly integrated into section B of **TAB.3** and **TAB.9**.

3.5.2 Flexibility Demands of the Optical Layout

Defining the flexibility demands of the Einstein Telescope optical layout is highly essential, and highly challenging. By constructing the observatory underground, we immediately constrain ourselves to a limited volume. This immediately means that any design revisions that necessitate increasing the volume very disruptive, time consuming, and expensive. The goal of the flexibility demands activity has therefore focused on considering the motivations for various types of flexibility. Two main perspectives are considered: (1) providing options to adjust the existing optical design to mitigate a risk associated with that design choice, and (2) providing volume allocations that could be exploited by future upgrades.

Some initial thoughts which inform this work are collected in Section [3.6] of the Supporting Document [6]. Towards (1), we reviewed the experience of current detector facilities. Category (2) is extremely nebulous. [6] includes some examples of both high likelihood options, and options that are considered very far from the baseline concept of ET, at various degrees of readiness.

For the purposes of this study, we have restricted ourselves to consider flexibilities that could be considered adaptations to the baseline concept. This immediately excludes several highly relevant design options, which instead represent *complete facility redesigns* as they would require significantly different components or infrastructure (e.g. change in wavelength, changes in which parts of the system are cryogenic, changes in tunneling). We consider this as an appropriate cut-off for exploring the flexibility demands that might reasonably

be incorporated into the constructed facility. However, it is essential that these alternative options continue to be explored, as they have the potential to address several key open questions for the optical layout - see each Section 4 of [5] and [4] - and may prove essential for ET to achieve its performance targets over the facility lifetime.

A list of flexibility demands is provided in section D of **TAB.3** and **TAB.9**, categorised by their primary motivation, the physical scale of the flexibility requested, and (in collaboration with detector layout and civil engineering colleagues) the likely impact on the overall facility.

3.6 The Optical Layout Technical Annexes

3.6.1 Output Tables

TAB.3 and **TAB.9** collect the full extent of the optical information currently used in developing these detector designs. We have grouped this into four categories which fulfill different purposes:

TAB.3/9A: **general**
This lists global/general geometric requirements and assumptions used throughout the design process, which cannot be assigned to a single optic or group of co-located optics (as in TAB.3/9B and C).

TAB.3/9B: **layout**
This provides positions, footprints and orientations of optics and optical sub-assemblies, fulfilling the equivalent role to the outputs Tables provided with the 2024 optical layout documents.

TAB.3/9C: **optic specs**
This collects additional parameters assigned to particular optics or groups of optics (sometimes referred to as 'optical sub-assemblies') There are many optical parameters to define beyond those that directly describe the layout of the interferometers. Here, we do not provide an exhaustive list of all parameters, as many will depend on studies beyond the scope of the Task Force. However first estimates for several parameters have been derived either as a direct outcome of the optical layout (e.g. curvatures of optics in the core interferometers), or at the request of detector layout or other teams (e.g. diameters and masses of large optics).

TAB.3/9D: **flexibility demands**
This summarises the flexibility demands of the optical layout, as described in section 3.5. It is identical for the Triangle and 2L.

A detailed guide to these Tables, and the calculations and thought processes behind the values, are provided in the supporting document [6].

3.6.2 Drawings

A conceptual overview of the core optical layout and the major optics of each interferometer configuration are provided in Figure 10. This, in combination with the output Tables, contains the complete current information of the optical layouts.

The full optical layout of both ET configurations is then captured in the technical drawings collected in **TD.1**, which are intended as a first interface between the optical layout and wider detector layout.

Two drawing types are provided:

- **scale drawing**: a full scale drawing of each configuration, showing both HF and LF. This shows the position of all of the vessels and beampipes intended to house the optics and laser beams in each detector facility. (Thus, the Triangle drawing shows a total of 6 interferometers in a single facility, while the drawing for the L configuration shows a single pair of interferometers, for a total of four interferometers distributed across two facilities/locations.)

- **vector drawing**: a compacted version, which truncates the large-scale lengths to create a more legible drawing. This additionally depicts the beam paths of the major beams in the core of the interferometer, i.e. the main science beam (shown between the PRM and SEM), the BHD LO beam (shown from it's pick off point also to the SEM), and the SQZ beam (shown from the end of the SQZ lab to the point it enters the vessels also occupied by the main beam). It gives a first indication of vessels that will contain multiple optics (for example, because a beam path includes a sharp angle as it reflects off and optic), and beampipes that must accommodate multiple beams (for example, the main, BHD and SQZ beams, or the main beam as it zig-zags between recycling telescope optics).

4 Integrated towers - Summary of tower categorization

Many level 4 subsystems within ET's High-Frequency (HF) and Low-Frequency (LF) interferometers are clustered in large towers - called 'nodes'. Together with some distributed systems, the tower nodes ensure that higher-level interferometer functions are met - such as lock acquisition, optical cavity stability and - in the end - ET's design sensitivity. ET's many tower nodes also influence the dimensions of the Subsurface Civil Infrastructure, and are supplied with - among other things - power, cryogenics and control signals by the Technical Infrastructure. Within this context, special attention is given to a baseline categorization of tower types, and how they are integrated to respect the boundary conditions given by external subsystems.

4.1 Tower nodes within the Task Force System Decomposition

Nodes refer to integrated subsystems at level 3 of the System Decomposition - see also Section 2 and figure 11. Approximately half of ET's nodes are integrated towers, where single or co-located optical elements and/or auxiliary optical subassemblies are contained - either in-vacuum and suspended or in-air and non-suspended. The remaining nodes are allocated to Technical and Civil Infrastructure subsystems, some of which interface with the integrated towers directly. Previously, the concepts of nodes and classified towers were introduced in the 2024 ET Detector Layouts [7] [14] - following in turn from a preliminary exercise on Suspension system classification [15]. Within the Task Force context, the scope of the exercise is extended by:

- Expanding the range of existing Residual Motion categories by one level, now spanning from CAT1-CAT6. On top of this, providing a preliminary estimate of *quantified* Residual Motion levels for a select number of nodes.
- Increasing maturity in integration with Optical and Detector layout for the identification of external constraints on tower nodes - such as optical bench space requirements and detector layout constraints on tower accessibility.
- Performing an improved recategorization of the Triangle configuration and extending this to also consider a dedicated categorization for the 2L configuration.
- Including Auxiliary optical benches into the categorization scope, both In-vacuum/Suspended and In-air/Non-suspended, that were previously left unconsidered.

Figure 11 represents the context of the Integrated tower nodes in the high-level Low-Frequency Interferometer architecture.

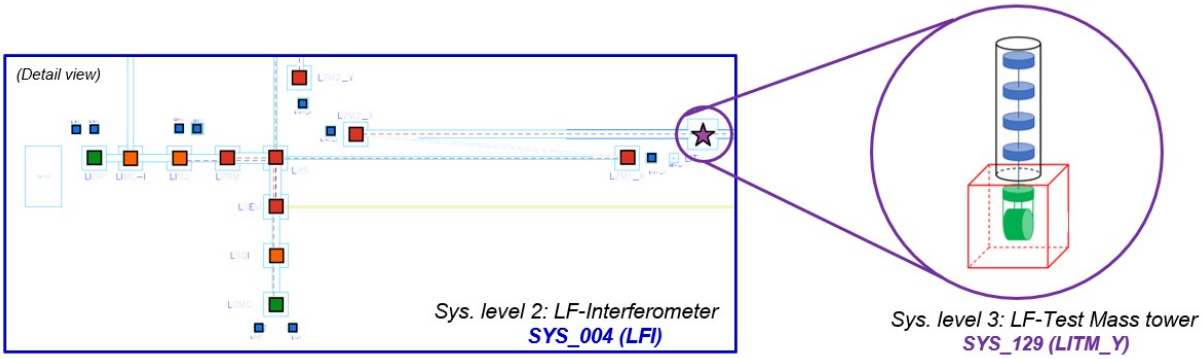

Figure 11: Schematic of integrated tower nodes as a Level 3 subsystem, visualized using the conventional 'heatmap' representation of the Level 2 LF interferometer.

4.2 Categorizing integrated tower subsystems

In a previous exercise, preliminary categorization work was done for the Suspension subsystems of core optics of the Triangle configuration [15]. Within the scope of the Task Force, this concept is revisited and extended - as detailed in 4.2.1. We consider as integrated tower node any subsystem where an optical payload is to be suspended in-vacuum - including both core and auxiliary optic locations. Boundary conditions for the towers are given on the one hand by optical payload needs and on the other by detector layout constraints. Non-suspended in-air auxiliary systems are also listed as node subsystems, but no particular Suspension or Tower vessel designs are prescribed within the Task Force work. The resulting tower categorization is contained in output tables **TAB.2** and **TAB.8**.

4.2.1 Boundary conditions considered for categorization

In the categorization of different tower types for both Triangle and 2L configurations, boundary conditions are taken as inputs from the Optical and Detector layouts such that future tower design efforts might be better constrained. From the Optical layouts, we consider:

- The type of optic and number of optics to be suspended within the node. Single-optic, co-location of optical elements or auxiliary optical subassemblies are considered. These result from the design of beam path propagation through the optical layout as well as functional allocation to auxiliary optical subsystems - as detailed in Supporting Annex output tables **TAB.3** and **TAB.9**.
- In the case of auxiliary optical subassemblies: the requested bench space per functional subsystem.
- The vacuum environment of the optic: this can be assigned to the main science beam or auxiliary systems. Optical subassemblies that need to be (partially) in-air and thus have no vacuum requirement are also listed. Required in-vessel ISO levels are estimated in the node specification lines.
- An estimate for the residual motion category and level required for suspending the optic such that the interferometer adheres to ET's sensitivity curves, which is derived per node in collaboration with Suspension experts. Suspension systems are grouped along Residual Motion categories 1-6 (CAT1-CAT6: from least to most stringent).
- Any special features requested by High-level Interferometer design - such as the Cryogenic operation of the LF-Test mass optical elements.

From the detector layouts, **TAB.4** and **TAB.10**, considered are:

- Any constraints on maximum allowed footprint following the optical layout or other aspects of the detector layout - such as cleanroom placement and beampipe routing.
- Any constraints on accessibility (bottom vs lateral access) following the proximity of surrounding nodes.

Along with these external interfaces, preliminary specifications for the Suspension and Vacuum vessel subsystems are generated as outputs to describe the Suspension quantified residual motion design level, Suspension system architecture (e.g. Top- or Bottom-loaded bench, Multi-optic or Single-optic), estimated Suspension system height, Vacuum vessel ISO level, vessel footprint and height and proposed access type. These considerations are detailed in the Supporting Document under Section 4: Integrated Towers. These outputs are then used to in part describe the excavation volumes by Civil Infrastructure.

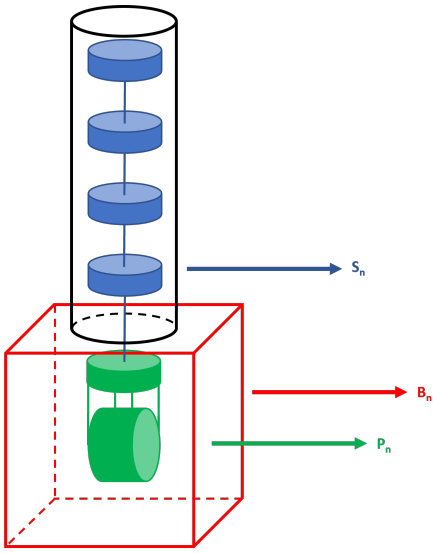

Figure 12: Schematic of tower subsystems considered for the scope of the Task Force work. Following the example of a Single-Optic type optical payload (P_x), with corresponding Suspension (S_X) and vessel base (B_x) architectures. Adapted from [7]. A unique tower type category would be the product of any unique combination of Payload, Suspension system and Vessel.

4.2.2 Tower categorization strategy

The space claims of ET's integrated towers impact the required cavern and tunnel excavation volume. Tower height, largely determined by the vertical space required for feasible Seismic Isolation systems, impacts cavern excavation height. Tower footprint, especially the footprint of the many auxiliary vessels, in turn drives the floor area in caverns. Summarized below are the items expected to have a large impact on excavation volumes and the explored mitigation. Small/medium impact items are listed in the Supporting document (Section 4). Section 6.2 of this document discusses the cost %-change expected from some large impact items considered for the Optical Layout and Tower Integration exercises done within the Task Force work.

Large impact on excavation volume expected

- *Reduction of footprint of Auxiliary benches.* Auxiliary benches are many (Approx. 80 out of 128) and were previously poorly defined. Efforts within the Task Force work are aimed to group auxiliary subassemblies previously allocated to separate benches (thus eliminating vessels) and to increase the maturity of optical bench space requirements.

- *General reduction in height of HF interferometer towers.* With a previously conservative estimate in HF non-Test Mass tower height, it is believed that with the comparatively lower residual motion requirements for the HF interferometer, many of the HF tower nodes can be reduced in height significantly.

- *Improvement of layout flexibility resulting from tower access.* While bottom access does offer some degree of layout flexibility, lateral tower access would reasonably give more flexibility with less impact on cavern construction. It is therefore proposed to default to lateral access, unless otherwise required following the boundary conditions of the node.

- *Reduction of the height of the Low-Frequency Test Mass nodes.* The height of the LF test mass towers drives the minimum height of LF cornerpoint caverns. By reducing this, bringing it closer to the height of the shorter adjacent LF core optic tower nodes, cavern space becomes better optimized.

- *Increased compatibility with co-located optics.* Major gains in the reduction of excavation volume are achieved through optical layout adjustments. An increased emphasis is put on bench- and multi-optic

rather than single-optic architectures. A new tower type hosting co-located Periscope optics is introduced to enable a bi-planar optical layout design.

A note on design flexibility: Within the scope of the Task Force work, some high-level conceptual design considerations for node Suspension, Cryostat and Vacuum vessel subsystems were explored - as detailed in the Supporting document. However, no single integrated tower conceptual design is proposed for any of the tower node categories. Rather, the categorization remains largely agnostic to subsystem design and will list all boundary condition flexibilities wherever available. This way, detailed design flexibility remains open as much as possible for future design efforts, while for the purpose of the Task Force work, increased maturity in high-level system design and tower categorization following node boundary conditions can still be achieved.

4.3 Tower categorization outcomes - executive summary

Below, a short summary of the categorization outcomes is given - along with the expected impact on excavation volumes as introduced in the previous section. For a detailed overview of the node type allocation, please refer to the External Document sections 4.1 and 4.2, as well as the Technical Annex Output Tables **TAB.2** and **TAB.8** for a per-node overview.

- Total: 128 nodes for a 2L interferometer pair (HF+LF) *+1 additional SQZ system steering node for Triangle (total 129).*
- Recorded 25 as in-air, non-suspended benches. No vessel and suspension architecture design assigned for now. Space claim 1:1 represents OPT need in Detector layout. No impact other than increasing the maturity of overall categorization.
- Recorded 56 as CAT1 top-loaded bench nodes *(57 in Triangle*), almost exclusively for Auxiliary optical subassemblies. All CAT1 benches are compatible with OPT area demand and captured in either 'small' (2.25m2 - 1.5mx1.5m or equivalent) and 'medium' (3.24 m2 - 1.8mx1.8m or equivalent) variants. Short towers (3.5m) are foreseen for these nodes. Efforts were aimed to group auxiliary subassemblies previously allocated to separate benches and to increase the maturity of optical bench space requirements. This has allowed the reduction of the total amount of auxiliary nodes as well as footprint reserved per node. Large impact expected on cavern footprint.
- Recorded 18 as CAT2 top-loaded bench nodes, applies to non-Test Mass core optics of the HF interferometer. Some retain Single Optic (SO) architecture as design flexibility. All would fall within the 'medium' bench footprint, assumed short tower height equivalent to CAT1 benches - allowing for a flexible submodular design. Large impact on excavation volume of HF cornerpoint caverns expected due to this height reduction.
- In general: tower node categorization is expected to be largely equivalent between 2L and Triangle configurations. Any difference is listed in the extended document and Technical Annex output tables **TAB.2** and **TAB.8**.

Summarizing the above: the majority (99 out of 128) nodes are captured in only a few node types, with a large expected impact on excavation volume.

For the remaining 29 nodes:

- Recorded 2x HF Steering optics ($HZM5_{X/Y}$) following the original CAT2 SO architecture [15] due to large optic size and mass. Low impact on excavation volume expected due to proximity of taller towers.
- Recorded 4x HF Test Mass optics ($HITM_{X/Y}$ and $HETM_{X/Y}$) as unique category (CAT3) SO architecture, in part due to expected constraints from Triangle configuration. Medium excavation volume impact.
- Recorded 6x SQZ subsystem nodes (Filter Cavity IM/EMs for both HF and LF) as CAT4 bench nodes of subvariant 'small', flexibility for SO architecture retained. Conservative estimate due to uncertainty in Residual Motion requirements. Impact on excavation volume expected to be small.

- Recorded 4x LF non-Test Mass nodes (LSQI, LINJ, LIMC-I, LIMC-E) as CAT4 bench nodes of subvariant 'medium' due to co-location of multiple optical elements. Low impact expected.
- Recorded 7x (LF non-TM core optics) as CAT5 bench nodes 'medium' due to co-location of optics. Some retain SO flexibility. Low impact.
- Recorded 4x LF Test Mass nodes as CAT6 SO. No amendments within Task Force work in comparison to pre-existing classification, detailed design efforts to be studied in a separate and ongoing LF-TM exercise. Following the progress in the parallel activity, SUS height feasibility is expected to be reduced from 17m to 12m. This preliminary result is adopted in the Task Force baseline, expected to have a large impact on excavation volume of LF cornerpoint caverns.
- Introduced and recorded 2x unique Periscope benches as CAT1 Periscope Bench (medium footprint) following the OPT layout efforts to propagate the SQZ system filter cavities in the main arm tunnel, requiring a 'periscope' to bridge the height difference between the two planes. Maximum flexibility is maintained for the classification of these benches due to large design uncertainty. Introduction has a large positive effect on reduction of excavation volume due to the omission of dedicated Filter Cavity tunnels.
- The reserved vertical space claim of the suspension system was reduced for all category towers when compared to the 2024 reference, an overview is given in Table 6.
- The optical benches are now categorized as either 'small' (1.5m $\times$ 1.5m or equivalent) or 'medium' (1.8m $\times$ 1.8m), where a previously considered 'grand' variant (2.5m $\times$ 2.5m) has been omitted for accessibility reasons. The footprint for these nodes was therefore directly reduced.

5 Detector layout

The detector layout matures the optical layout to a simplified three-dimensional instrument layout, using position-inputs from the optical layout 3 and volumetric-inputs (tower base footprints and tower heights) from integrated tower categorization 4, further complemented by volume envelopes for vacuum beampipes, scaffolding, cleanrooms, noisy rooms for cryogenic infrastructure and logistics. The aim of this section is to describe the minimum dimensions required for the detector layout to be used in the infrastructure layout studies for e.g. cost calculations and feasibility studies.

5.1 Common features, definition of flexibility envelope

The detector layouts for 2L and triangular configurations have a majority of similar features, primarily focusing on volume envelopes.

5.1.1 Scaffolding

Scaffolding will be placed around each main optic tower vessel, preferably on all sides, to accommodate a platform for accessing the upper part of the tower, housing the suspension system and other components. It is to be used for only personnel and to place relatively low weight equipment on, not to be used for (temporary) storing of heavy components. The strategy for scaffolding is coupled with the integrated tower categorization, separated into two categories:

- permanent scaffolding; only applied for tower suspension categories *CAT6*, *CAT5*, *CAT4* and *CAT3*.
- temporary scaffolding; applied for tower suspension categories *CAT2* (primarily HFI) , which are either relatively low main optics vessels.

The permanent scaffolding follows the similar height as the tower it is connected to. The footprint is parametric to the footprint of the vessel, with an offset of 0.7 m on all sides. This offset derives from the requirement that 0.7 m clearance must be present at all times in case of an emergency. As result, all vessels with a 4.0x4.0 m base footprint (suspension *CAT3* or higher) has a permanent scaffolding with a 5.4x5.4 m footprint with a height similar as the total height of the vessel.

Additional features to permanent scaffolding is the possibility to connect them to adjacent vessels, creating a multi-story scaffolding for a group of tower vessels. As boundary condition, this additional feature applies to tower vessels within 8.0 m center-to-center proximity. The permanent scaffolding will likely be a custom structure of which the design features will be determined at a later stage in the project.

For the temporary scaffolding, it is assumed that industry standard components can be used, simplifying disassembling and storing the scaffolding. Another benefit of this is that a single set of scaffolding can be used for multiple tower vessels, and it does not necessarily obstruct logistical paths.

5.1.2 Hoisting clearances

Where the scaffolding increases the tower footprint, some clearance above tower vessels must be reserved for hoisting and installation operations. It is expected that every cavern has an overhead crane installed. Based on preliminary tower base designs, the assumed heaviest load to lift is approximately 20 tons. The Occupational and Health Safety Administration (OSHA) defines a safety factor between 2 and 3 for the crane capacity and maximum load. Applying a factor 2.5, the expected crane capacity to be used in the underground infrastructure is 50 tons. Assuming average dimensions, the clearance for the crane (the bridge, hoist and hook) is 1.5 m.

In addition to the crane clearance, additional clearance for the hoisting operations is required. This is primarily dependent on the height of the virola's (the rings that combined create the upper vacuum-part of the tower vessel containing the suspension system) which is expected to be 2.0 m. OSHA Standard 1910.179(b)(6)(i) states that a minimum 3 inch (approximately 0.08 m) overhead clearance is required between the crane and obstructions, resulting in a minimum required clearance of 2.16 m. Combined with the crane clearance and

rounded up, a clearance of 4.0 m must be provided above the tower vessels to the top of the overhead crane. This number is subject to change when updated designs will be made.

5.1.3 Cleanrooms

In order to protect the optical substrates and suspension fibres from particle contamination, alike existing gravitational wave detectors Virgo, LIGO and KAGRA, contamination control must be taken to the next level. A document on preliminary cleanroom consideration [16] outlines the rationale for contamination control, the clean kinematics of material from cleaning process to installation, ISO level requirements during operation and cleanroom footprints, which is summarized below and further elaborated in the Supporting Document.

The analysis of the cleanrooms is limited only to areas surrounding the tower vessels, as its function is to protect optical elements from dust, particularly when the tower vessel is opened. The ISO levels stated for cleanrooms are referring to Operational Mode scenario, where personnel is working inside the cleanroom. Although each access cleanroom is tailored in terms of orientation and the vessels access requirements, the following general statements can be made:

- Tower vessels containing main optics (non-auxiliary) require an ISO 5 cleanroom access.
- Tower vessels containing auxiliary optics and other systems require an ISO 7 cleanroom access.
- For this analysis, it is assumed that the ambient environment in the caverns containing tower vessels is ISO 9.
- To pass from ISO 7 environments to lower ISO levels (meaning more stringent requirements), it is mandatory that personnel and material passes through the ISO stages in between. It is assumed that it is possible to pass from the ISO 9 ambience directly to the ISO 7 cleanroom without having to pass an intermediate stage.
- The cleanroom attached to the tower vessel servicing the clean access is an ISO 6 environment, however when a tower is opened, a specialized ISO 5 area is established using curtains and additional filtration. It is assumed that this is sufficient, based on experience at Virgo.
- ISO 5 access cleanrooms provide a footprint of 4.0x3.0 m for two technicians and either a bench-payload or a large single-optic payload.
- Space in between adjacent ISO 5 access areas are connected via an ISO 6 area.
- All tower vessels except the LF-TM nodes (and HZM5 in 2L configuration) have lateral access cleanrooms as baseline solution, in perpendicular orientation to the beam-axis. For the beamsplitter vessels, this will be at 45 degrees lateral with respect to the beam axis. The LF-TM nodes (and HZM5 for 2L configuration) have bottom access cleanrooms as baseline solution. The HZM5 nodes have lateral access in the Triangle configuration due to the LF beampipe being underneath the HZM5 vessel. For HIMC-I1 and HIMC-I2 nodes, these are still open points, as all four sides are occupied limiting lateral access and the payload being a top-loaded bench disfavouring bottom-access.

The vacuum vessels, main interferometer and auxiliary vessels, are to be placed in an ISO 7 cleanroom. To limit the amount of cleanrooms and thus the amount of process-cycles, tower vessels within 10 m center-to-center proximity (including the auxiliary vessels) are grouped in a large ISO 7 cleanroom. The smaller ISO 5 and ISO 6 cleanrooms are placed inside the larger ISO 7 cleanroom (box-in-a-box).

As LFI contains much taller vessels than HFI, different solutions are foreseen for the ISO 7 cleanrooms. LFI follows an approach similar to KAGRA as the varying heights allow for a more flexible cleanroom, where HFI follows an approach similar to LIGO. As result of this, all HFI vessels with exception of ZM5s and TMs are placed in a single large ISO 7 cleanroom. The ISO 5 and ISO 6 access cleanrooms can be realized using modular tent designs encapsulating the entire tower vessel, using a temporary solution. Another possibility is to make this a permanent cleanroom, however this could potentially obstruct logistical paths therefore increasing the span of the larger ISO 7 cleanroom.

On the contrary, for LFI the ISO 5 and ISO 6 lateral cleanrooms are considered to be permanently installed. As aforementioned, the LF-TM tower vessels will be accessed via bottom access cleanrooms. Similarly to the lateral access cleanrooms, the bottom access cleanroom is a large 8.0x8.0 m ISO 6 environment with a specialized ISO 5 area directly underneath the tower which is established using curtains and additional filtration upon opening the vessel. In addition, an ISO 5 payload assembly room is considered for maintenance on the LF-TM payload. Since this type of payload is considered the most critical one for ET, a specialized room adjacent to the bottom access cleanroom is foreseen.

For the towers with lateral access, which are considered to be hosting bench-loaded payloads, specialized assembly cleanrooms are located in LF corner station, HF corner station and one at each end station. These assembly rooms must be an ISO 5 room with enough footprint to provide two largest benches with at minimum four personnel to work on those payloads. Subsequently, the ISO stages in between the assembly room and the cavern space must be provided for the material and personnel.

The scaffolding, hoisting clearances and cleanrooms make up the tower volume envelopes. These volumes are visualized in Figure 13.

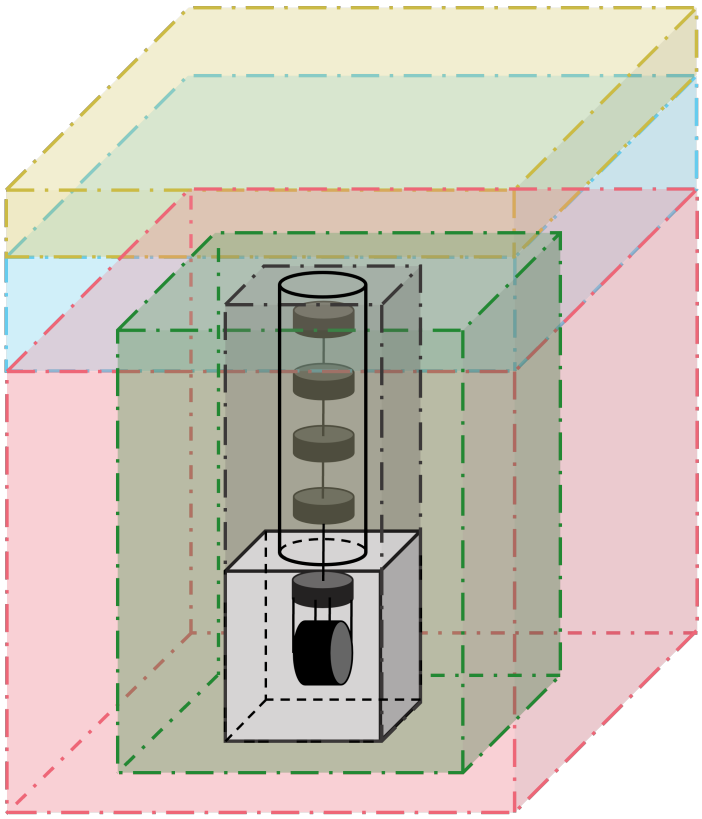

Figure 13: Tower volume envelopes, where the tower envelope is grey, the scaffolding envelope green, the ISO 7 cleanroom pink, the hoisting clearance cyan and the crane clearance yellow.

5.1.4 Vacuum Beampipes

Vacuum beampipes in the detector layouts are considered vacuum pipes containing the main beam, SQZ-beam and BHD-beam. Although ghost beams also run through sections of vacuum beampipes, these are out of scope for this analysis.

As of 2024, described in [17], the diameter of the vacuum beampipes for the arm cavities (Ø1.0 m) are frozen. The diameter of the FC beampipes are provided in Table 5. For the other vacuum beampipes, a similar approach as in [7] is used to provide initial values, which are to be verified at a later stage in the project. In [17], the aperture radius profile is given as a function of the distance traversed and clipping losses:

$$r(z, L_{\mathrm{c}}) = \frac{\omega(z)}{\sqrt{2}} \sqrt{\ln\left(\frac{1}{L_{\mathrm{c}}}\right)} + r_{\mathrm{offset}} + h_{\mathrm{baffle}} \tag{1}$$

Wherein: *ω(z)* denotes the laser beamradius, L_c the clipping losses, and r_{offset} is added to included a eventual offset of the laser with respect to the cavity longitudinal axis. The height of the baffles is to be added to the radius to arrive at a minimum required inner diameter for the vacuum beampipe. A baffle-height of 8 cm is considered for all vacuum beampipe segments.

As the optical layout differs per configuration with different lengths and spotsizes, the diameters per segments of vacuum beampipes differs accordingly, specified in there respective sections later in this document. In both configurations, certain vacuum beampipe segments containing multiple beams occur. For these sections, the inner diameter is specified by calculating the minimum aperture radii of the two outer beams using 1 and adding the center-to-center distance of the two beams to this combination.

As additional features to the vacuum beampipes, several cryo-pump sections are considered, however all sections except those indicated adjacent to the TMs are out of scope for this analysis. Gate valves attached to the vacuum beampipes are out of scope as well.

Cryogenic pumping sections adjacent to the TMs remain undifferentiated from what is described in [7].

5.1.5 Noisy rooms

As part of the technical infrastructure, noisy equipments are considered for systems such as vacuum or cryogenics. These noisy equipment are to be placed in noise isolating rooms to be reserved in the subsurface infrastructure. Although for the majority of the technical infrastructure information is still immature, for the cryogenic infrastructure information is provided in [18], where the major instruments for the cryogenic system are described and approximate locations in the underground infrastructure are indicated.

Each vertex (or end station) has a warm helium storage and compressor station at the surface close to the entrance to the subsurface infrastructure. The warm helium is transported to a coldbox which is placed underground relatively close to the LFI corner station (plural for triangular configuration) and close to the end-stations in case of 2L configuration. The coldbox is placed in a noisy room together with an interconnection box and several control cabinets depending on the amount of receivers. Some additional space for other noisy equipment is reserved in this noisy room as well. From these noisy rooms at the corner/end stations, the cold helium is transferred to a cryogenic supply unit for each TM-tower. Although the CSU is expected to be relatively low noise, a noisy pump is required for the performance of the cryogenic system during run-time, therefore the CSU's are to be placed either near or inside noisy rooms, at maximum 20 m distance from the end-users;

Each LF-CSU can provide the cooling of the cryostat shields and its adjacent cryopumps. Each HF-CSU services the HF cryopump located near the HF-TM. To summarize; 3 large noisy rooms are required for the received helium from the surface and several smaller noisy rooms (8 per 2L configuration and 24 for Triangle configuration).

The general HVAC system servicing the main caverns requires HVAC plants, distributed over the subsurface, surface and inter-surface infrastructures. It should have the capacity to facilitate air changes per hour up to ISO 9 specifications. It is not possible to provide information estimating the required HVAC plant footprints accommodating the ambient HVAC for the subsurface infrastructure, although it is assumed that certain elements of the HVAC system require a noise-isolating room.

The cleanrooms indicated require specialized HVAC systems for the servicing of the required ISO environments. The footprints for specialized HVAC systems per ISO level volume can be extrapolated from the Virgo site,

scaled to the volumes of ET. In total, the required footprints for specialized HVAC to be allocated in the sub-surface civil infrastructure are:

ISO class	**ISO m^3**	**HVAC m^2**
ISO 5	12 000	819
ISO 6	4 000	130
ISO 7	47 000	133

The distribution and locations of these specialized HVAC plants are to be determined in future studies, although it is assumed that certain elements of the specialized HVAC systems require a noise-isolating room.

It is foreseen that electronic racks with noisy electronics are to be placed in a noise-isolating room, primarily for DAQ and accompanying hardware systems. Other electronic racks are expected, however not required to be in a noisy room. For the seismic-isolation systems, two electronic racks per main tower vessel are required for controlling of the suspension systems at the Virgo site. For the vacuum system, ten racks for twelve in-vacuum vessels for the vacuum-system, where one rack can service either one main optic vessel or two auxiliary optic vessels. It is expected that the same quantities can be applied for ET.

5.1.6 Logistics envelope

The subsequent step in defining the required volumes in the caverns and tunnels is to reserve a volume envelope for logistics; the movement of large components from the entrance of the underground infrastructure to its defined location in the detector. For this analysis, a scenario where the detector construction is completed and a component of the detector needs to be replaced is envisioned. The frequency of occurrence is assumed to be low, however the severity of disassembling parts of the detector to allow for transportation is very high, therefore this extreme scenario is assumed. The modes of transportation are either a solution on the ground (main cavern floor or tunnel floor) or the use of overhead cranes there were a path is obstructed. The use of overhead cranes requires longer time and increases safety risks for personnel and equipment, thus ground transportation is preferred. If ground transportation requires increasing the cavern span significantly, transportation using overhead cranes is preferred, although taking into account that hoisting over sensitive equipment is strongly discouraged. To define the required envelope, the following information must be provided:

- The location of the entrance cavern of the underground infrastructure.
- The dimensions of the largest components to be transported.
- The location of where the component must be transported to.

Although the location and orientation of the entrance shaft or tunnel is site dependent, an entrance cavern is expected close to where the noisy room for the cryogenic infrastructure and the payload assembly cleanroom for LFI are located. For the analysis, this location is considered to be the starting point of the logistical routes.

The largest components to transported are assumed to be:

- Conical base design: 4.0x4.0x3.0 m
- Largest segment of the vacuum vessel of the baseline LF-TM tower: Ø4.5x3.1 m
- Pre-assembled IP legs: 7.0x3.0x3.0 m
- Beampipe segment of the arm cavity: Ø1.3x20.0 m

The dimensions given are excluding packaging materials and a lateral clearance must be taken into account as well, thus 2x a 0.5 m offset is assumed. For a path from the entrance cavern to the LF-TM towers, a path on the main cavern floor with a minimum span of 5.5 m is reserved where possible. For a path of a tower base vessel for HFI, a path on the main cavern floor with a minimum span of 5.0 m is reserved where possible. For

transportation of a beampipe segment into the main arm cavity tunnel, the last cavern before the tunnel is extended by 22 m to maneuver the beampipe segments in between the arm cavity beampipes.

It is important to note that the envelopes for the components with their offset also apply to the required envelope for the access tunnel or access shaft from the surface infrastructure to the subsurface infrastructure.

5.1.7 Impact of Optical Layout flexibility demand on Detector Layout

The Optical layout describes in Section 3.5 the importance of the flexibility demand, which has a direct interface with the detector layout envelope to be reserved in the subsurface civil infrastructure. The list of flexibility demands is provided in [TAB3D] where the rationale for these flexibilities are given. Moreover, these flexibilities are reviewed on the following topics:

- Position changes of optics within the initial provided detector layout envelope, e.g. repositioning the optic on a suspended bench or the shift of a tower vessel by a few centimeters.
- Position changes of optics that would necessitate insignificant additional excavation, thus implemented in the current baseline detector layout envelope.
- Position changes of optics that would necessitate significant additional excavation, thus not implemented in the current baseline detector layout envelope and therefore requires excavating years after construction.
- Traffic-light system for impact on the detector layout envelopes following the options mentioned in the previous points (small impact, medium impact, large impact).

The flexibility demands that necessitate insignificant additional excavation, meaning increasing the span of the caverns up to a meter in a few locations providing symmetry between caverns while either mitigating optical design risk or providing volumes for future upgrades, are mainly located in the HFI corner station. However, most of the flexibility demands not requiring additional excavation can be met by utilizing the space reserved for logistics, necessitating alternative logistical routes to be determined.

5.2 Baseline Triangle layout (i.e. our choice), main features and comparison with 2024 reference

Over the duration of the ETO Task Force, various solutions for the detector layout have been discussed, of which the baseline solutions are explained in this section. The alternatives are explained in the supporting document.

As mentioned in the beginning of Section 5, the main constraints for the detector layout derive from the optical layout and integrated tower categorization, along with the common features explained. This section summarizes the differences with the 2024 reference Triangle detector layout [14] and the features driving the main volume claims. The minimum functional volumes will be explained in Section 6.

5.2.1 Comparison with 2024 reference

Section 3.1 outlines differences between the 2024 reference and the updated optical layout by repositioning and co-locating core optical components mostly in HFI (5) and LFI (1) resulting in fewer tower nodes, which reduces the overall volume for HFI and LFI central area and the co-location HF IMCs into one tunnel. The squeezed light system has be re-designed with the effort of integrating the filter cavities into the main arm cavity tunnel, which implies the change from a three-mirror to a two-mirror cavity and the addition of a few tower nodes for a 4.0 m periscope and a steering bench for LF-FC and a 2.0 m periscope for HF-FC plus one extra node for an additional LF-FC squeezing bench, however reducing the number of tunnels. Other differences are the LF-IMC length reduced from 300 m to 120 m, the LF BHD-beam runs internally from INJ to OMC instead of via a diagonal vacuum beampipe and the SQZ-beam enters the LF corner station in the SEM tower node and runs then internally parallel to the main- and BHD-beam to SQI in an enlarged vacuum beampipe.

By comparing the tower categorization for the 2024 reference layout [7] and the categorization described in Section 4, the main differences can be summarized by stating the following:

- An additional category is added for the core optics (LFI IOO).
- Two added categories for the two filter cavity periscopes.
- The baseline solution for vertical isolation systems for all categories except *CAT6* considers a bench-loaded suspension system (lowering the total suspension height); bottom-loaded for *CAT5* and top-loaded for *CAT4* down to *CAT1*.
- The height of the baseline solution for the vertical isolation system for *CAT6* is reduced from 17 m to 12 m.
- Standardization in bench-footprints; 1.5x1.5 m (*small*) and 1.8x1.8 m (*medium*), where the 2.5x2.5 m (*grand*) version has been removed from the classification.

The result of these changes are smaller volumes for all tower nodes, reducing suspension heights and reducing bench footprints for auxiliary nodes:

Susp. RM. Cat.	**2024 Ref Susp. height**	**2025 Baseline Susp. height**
CAT 6 (was CAT 5 in 2024 ref)	17m	12m
CAT 5 (was CAT 4 in 2024 ref)	12m	8m
CAT 4 (not present in 2024 ref)	-	8m
CAT 3	9.5m	5.5m
CAT 2	6.5m	3.5m
CAT 1	3.5m	3.5m

Table 6: Suspension height comparison between 2024 reference and new 2025 baseline

Although the largest impact changes are mostly coming from optical layout and integrated tower categorization updates, the additional tower envelopes updates have impact on the overall detector envelope as well. The volume envelopes directly connected to the tower vessels, e.g. scaffolding and cleanrooms, slightly differentiate from the 2024 reference detector layout.

The tower scaffolding was considered to be parametric to the tower footprint, however an offset of 0.5 m for 3 sides was considered plus a 1.5 m offset for the access side, resulting in a 5.0x8.0 m rectangular footprint for a single 4.0x4.0 m footprint tower node, compared to a 5.4x5.4 m footprint in the new baseline detector layout. The main driver for the 2024 reference scaffolding footprint was to facilitate space for electronic racks for the suspension and vacuum systems near the tower vessel. It is assumed that there is sufficient allocated space on the 5.4x5.4 m scaffolding for electronic racks, especially there where scaffolding of multiple tower nodes are combined.

The lateral access ISO 5 cleanrooms increased in footprint from 2.5x3.0 m to 2.5x4.0 m, to accommodate more space for opening the tower base, regardless of the final design for the vessel doors. Since the orientation of these lateral access cleanrooms is with the long side parallel to the vacuum beampipes, this does not have an impact on the overall footprint of the large ISO 7 cleanrooms of the LFI and HFI corner stations. The LZM1-nodes have lateral access, as opposed to the 2024 reference layout, to ensure as much flexibility as possible. Therefore, the LZM1-node, along its adjacent auxiliary vessels and the LF ITM are placed inside a common ISO 7 cleanroom. The bottom access cleanroom for LF-TMs decreased in volume compared to the 2024 reference, while maintaining a similar approach for the maintenance operations. The ISO 7 cleanroom housing the HF ITM and HZM5 nodes with the adjacent auxiliary vessel reduced insignificantly in footprint compared to the 2024 reference. A final difference for cleanrooms compared to the 2024 reference is the locations and quantity of payload assembly cleanrooms, which previously were located at every large ISO 7 cleanroom alternatively to the strategy explained in Section 5.1.3.

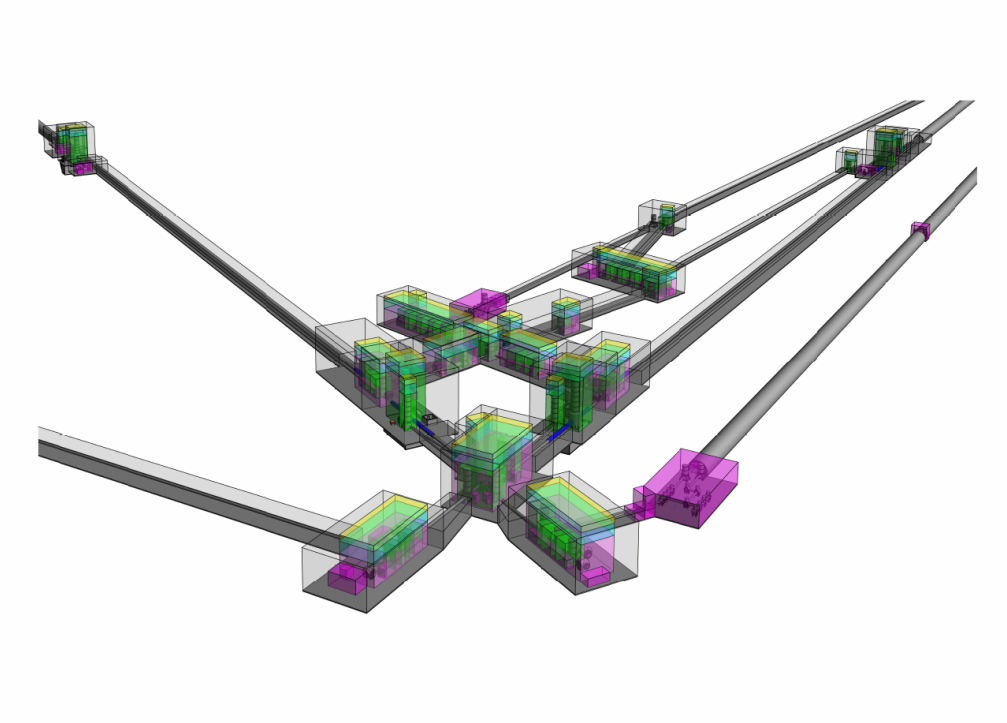

(a) Corner station of Triangle 2024 reference detector layout

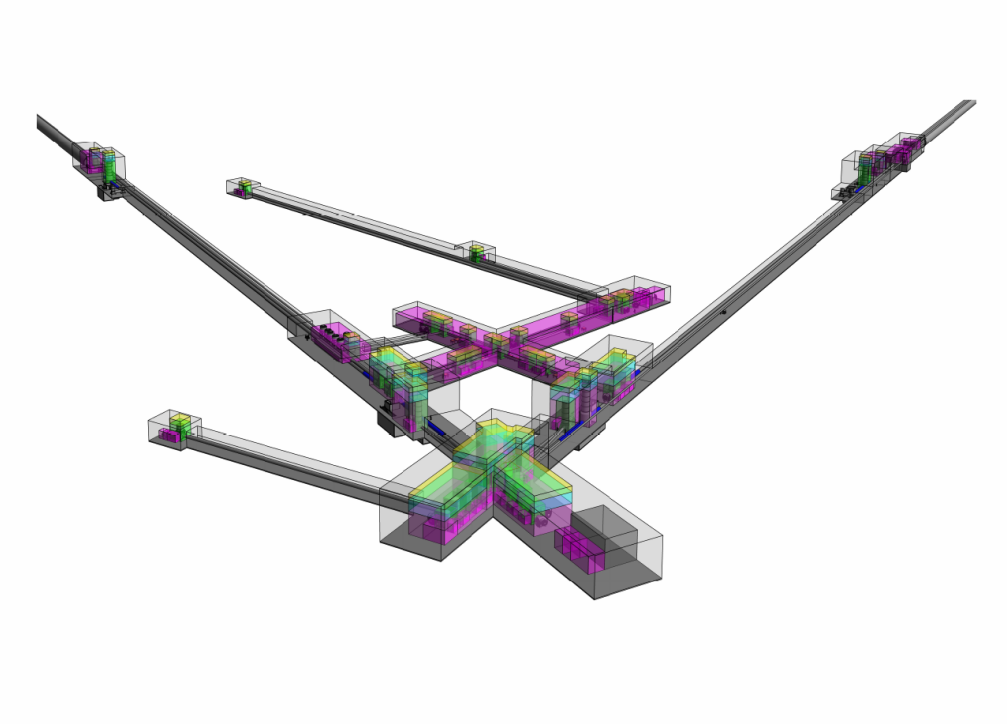

(b) Corner station of Triangle baseline detector layout

Figure 14: Comparison of the 2024 reference detector layout (14a) the ETO Task Force baseline detector layout (14b) [Triangle configuration]

With the re-design of both SQZ-labs, the footprints of the cleanrooms for the squeezing systems changed accordingly, resulting in an increase in overall footprints for the SQZ-labs in the caverns, but a decrease in overall volume in the tunnels. Where the vacuum beampipe for the LF SQZ-injection beam widens the LITM_X-cavern insignificantly, the HF SQZ-injection beam necessitates a relatively small tunnel to be excavated from the HFI corner station towards the Y-arm.

The volumes of the vacuum beampipes compared to the 2024 reference are undifferentiated with the exception of the LFI corner station, since the spotsizes of the updated optical layout are similar to the 2024 optical layout update [4]. The vacuum beampipes in the LFI corner station are enlarged as a result of having multiple beams propagating parallel to each other in the same vacuum envelope. The impact of these larger vacuum beampipes on the overall detector footprint are insignificant. A major difference for the vacuum beampipes with a large impact on the detector layout is the addition of a vacuum beampipe for the LF and HF SQZ-injection beams and the diameter of the LF-FC and HF-FC arm vacuum beampipes, since this impacts the cavern-span of the LITM_X-cavern and the diameter of the arm cavity tunnels.

The logistics envelopes considered are depending on the dimensions of the largest components to be transported, where the foreseen logistics scenario defining the strategy is unchanged from the 2024 reference detector layout. The dimensions provided earlier differentiate only for the LF-TM tower components, where in the 2024 reference layout it was assumed that the assembled tower base would be the largest component, however new assumptions state that this component can be partly assembled underground. As a result, the footprint of the largest component changed from 5.0x5.0 m to 4.5x4.5 m, decreasing the largest logistics envelope span by 0.5m for the underground infrastructure.

Noisy rooms are a crucial part of the infrastructure in gravitational wave detectors, as they isolate the noise from equipment to the detector. It was mentioned in the 2024 Detector Layout document [7], however no mature information was available at the time of writing, opposed to the current status of information for noisy rooms described in Section 5.1.5 to be foreseen in the baseline detector layouts. The addition of these inputs results in more volume claims for noisy rooms, thus requiring more volume in the subsurface civil infrastructure.

The differences between the baseline and the 2024 reference are visualized in Figure 14.

5.2.2 Flexibility envelope of the Triangle Detector Layout

Similarly to the optical layout, the detector layout provides a flexibility envelope for the local host teams to exploit for the site dependent civil infrastructure design studies. Where the optical layout flexibility envelope mostly regards the position of optics and therefore constraining the position of the vessels, the detector layout provides flexibility for the following features:

- Integrated Tower Categorization flexibility envelope regarding seismic isolation concepts, impacting height of the tower vessel. The integrated tower categorization output tables provides the default baseline option and provides alternative options if applicable.
- Integrated Tower Categorization flexibility envelope regarding tower access (bottom or lateral), impacting the footprint and height of the cavern. The integrated tower categorization output tables provides the default baseline option and provides alternative options if applicable.
- Lateral tower access orientation (north or south side of the vessel) in combination with optical layout flexibility envelope regarding auxiliary vessels, which should not impact the cavern footprint but could improve cavern symmetry or logistical routes.
- The scaffolding footprint is allowed to be increased along the beam-axis direction, as this does not increases the cavern span. Perpendicular to the beam-axis is allowed as long as it does not impact the cavern span or logistics envelopes.
- The noisy rooms can be relocated within the specified requirements provided in **TAB.4** and **TAB.10**.

- Electronic racks, primarily for the tower vessels, can be relocated within the specified requirements provided in **TAB.4** and **TAB.10**.
- The position of the LF-FC periscope vessel. For the baseline detector layout, the periscope is positioned in the LFI corner station, raising the beam-plane from 1.5 m to 5.5 m with respect to the cavern floor for the injection beam from the Squeezing Lab to the LFI corner station. The argument for the position of the periscope is the logistics envelope that can be foreseen underneath the vacuum beampipe. If this however complicates the LFI corner station, the periscope can be moved along the LF-FC injection beam axis up to the LSQ-ZM tower node.
- The length of the LF filter cavities, so the relative position of LFC-EMs to LFC-IMs. Technical details of this are outlined in the Supporting Document [6], section 3.3.2, where it is highlighted that shifting the position of the LFC-EMs has an effect on the sensitivity performance of ET. Shorting the LF-FC length reduces sensitivity, thus the maximum allowable flexibility for shortening the LF-FC length is 10% of the total length, so -500 m. Increasing the length of LF-FC has no technical upper limit, but is geometrically limited by the position of the HFC-EM vessel from the other vertex, positioned 4 km away from the initial baseline position of the LFC-EMs. The maximum allowable flexibility envelope of increasing the LF-FC length is thus up to 4 km. However, increasing the length of the cavity increases the beam size, necessitating larger mirrors and subsequently larger vacuum beampipes, resulting in a larger tunnel envelope required since the horizontal center-to-center distance between the LF filter cavities is fixed.
- The length of HF filter cavity, similarly to the previous item and described in section 3.3.2 of the Supporting Document [6], the maximum allowable flexibility for length of the HF-FC is up to 10% of the total length, so $\pm$100 m.
- The relative position of one detector to the other detector - the horizontal separation between the ETM of the far vertex to the ITM of the close vertex - as reducing the separation will reduce excavation volume. In output table **TAB.4**, a requirement on minimum horizontal separation has been provided; 300 m distance means up to about 0.1 s time offsets of seismic Newtonian noise transients in the two affected ET-LF interferometers. This is a good fraction of a 3 Hz oscillation, which means that the time offset should have an important impact on background rejection. Environmental monitoring and NN cancellation will also help. The flexibility envelope is to shift the independent detectors as long as the ETM-ITM horizontal separation is at minimum 300 m, and the beampipe-to-beampipe horizontal separation is minimum 3800 mm center-to-center.

The logistics envelopes cannot be altered as flexibility envelope, as this has large impact on assembling and manufacturing processes, although not currently taken into account.

Modifying the baseline detector layout within the flexibility envelopes must be done in consultation with the ETO Engineering Department.

5.3 Baseline 2L layout (i.e. our choice), main features and comparison with 2024 reference

Similarly for the Triangle configuration, several solutions for triangular configuration detector layout have been discussed. The Triangle and 2L configuration share a majority of common features with minor differences driven by the optical layout.

5.3.1 Comparison with 2024 reference

Similarly for the Triangle, the largest impact changes are coming from optical layout and integrated tower categorization. For the optical layout update, comparable changes for the Triangle as for the 2L configuration are implemented, thus the differences between the 2024 reference and the new baseline are similar as described in the beginning of Section 5.2.1. A difference to highlight is the position of the LF-FC periscope, as the preferred

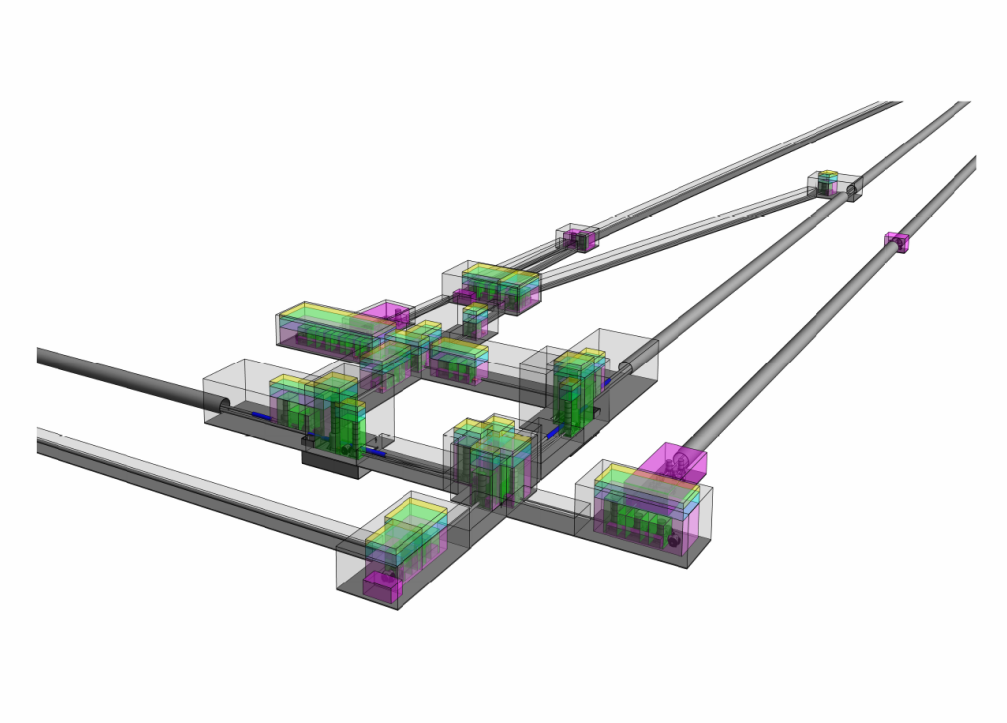

(a) Corner station of 2L 2024 reference detector layout

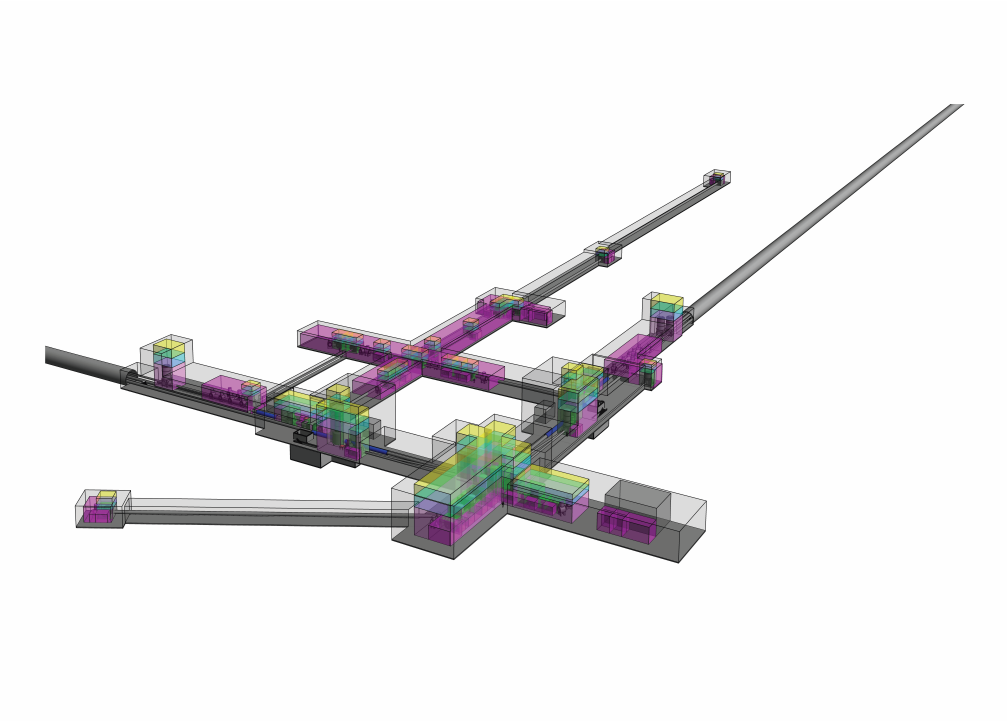

(b) Corner station of 2L baseline detector layout

Figure 15: Comparison of the 2024 reference detector layout (15a) the ETO Task Force baseline detector layout (15b) [2L configuration]

location is at the LF SQZ-lab, therefore the additional steering node added in the Triangle configuration is not required for the 2L configuration.

Tower categorization for the baseline 2L can for the majority be copied from the Triangle layout, with the exception of tower access for a few nodes as result of the position of HFI relative to LFI, which is unchanged from the 2024 2L reference [7].

Tower scaffolding assumed for the new baseline altered from the 2024 reference similarly as for Triangle, described in Section 5.2.1.

The cleanroom volumes and orientations changed equally from 2024 reference for Triangle baseline as for the 2L baseline, although the access cleanrooms remain tailored to the orientation and type of access per tower node.

Volumes for vacuum beampipes changed proportional to the changes in the optical layout compared to the 2024 reference, however the changes in spotsizes are minimal. There are several sections where multiple beams are propagating through a single vacuum beampipe segment, of which the approach for calculating the required aperture will be similar as for the Triangle configuration.

The logistics envelopes considered for the Triangle configuration are equal for the 2L configuration, thus the changes between the Triangle 2024 reference and the baseline are similar as done for the 2L configuration, explained in Section 5.2.1.

With more mature information available for the noisy rooms, the changes in the detector layout are equal for both configurations compared to the 2024 references.

The differences between the baseline and the 2024 reference are visualized in Figure 15.

5.3.2 Flexibility envelope of the 2L Detector Layout

The flexibility envelopes for the 2L Detector Layout are similar to the flexibility envelopes for the Triangle configuration, with the following changes:

- Exception: The position of the LF-FC periscope, as this is required to be located at the SQZ-lab.
- Exception: The ETM-ITM separation, as the L configuration only host one interferometer-pair instead of three in case of the Triangle.
- Amendment: The length of the LF filter cavities, which for the 2L configuration is not geometrically limited by the HF filter cavity, allowing the maximum length of the LF-FCs to be 15 km instead 9 km for the Triangle. This impacts, similarly to the Triangle, the tunnel envelope since the increasing of the length necessitates larger vacuum beampipes (see the Supporting Document [6], section 3.3.2). Reducing the length is, similarly to the Triangle, allowed to maximum 10% of the total length. For HF-FC, the flexibility envelope is maximum 10% of the total length in both directions (reducing and increasing).
- Addition: The beamplane heights between LFI and HFI. Although modifying the beamplane heights independently of the interferometers is a benefit of the L configuration, the two interferometers together drive the envelope for the 15 km long tunnels, combined with the filter cavities. HFI and LFI share a physical dependency in the baseline design through the shared bottom access cleanroom for LITM and HZM5 nodes. It is assumed that the kinematics of the HZM5-payload does not necessitate a 6 m tall cleanroom, thus a quantitative flexibility of 1 m for vertical beamplane separation between HFI and LFI is provided. The employment of this flexibility envelope must be analyzed on its impact on the tunnel envelope.

Equal to the Triangle configuration flexibility envelopes, modifying the baseline detector layout within the flexibility envelopes must be done in consultation with the ETO Engineering Department.

5.4 The Detector Layout Technical Annexes

5.4.1 Output Tables

TAB.4 and **TAB.10** provides the information used for the design of the detector layout and highlights certain dependencies, collecting;

- broader requirements and specifications regarding the technical infrastructure.
- inputs for cleanrooms regarding their ISO class, dimensions and function.
- inputs for noisy rooms regarding their dimensions, locations and function.
- inputs for beampipe segments (those mentioned in the system decomposition **TAB.1** and **TAB.7**) regarding the dimensions and function.
- inputs for the cryogenic infrastructure regarding their function, dimensions and locations

5.4.2 Drawings

As part of the technical annexes for the detector layout, 2D drawings **TD.2** have been produced as intermediate step towards the 3D models on Trimble **TD.3**.

Two drawing types are provided:

- **2D**: a full scale drawing of each configuration showing the HFI and LFI detectors with the footprints for vacuum vessels, vacuum beampipe segments, cryogenic pumping sections, scaffolding, cleanrooms, noisy rooms and logistics envelopes.
- **3D**: An extension of the 2D drawing depicting the footprints, heights and individual vertical positioning of the aforementioned elements, providing a first insight on volume envelope claims for the subsurface civil infrastructure hosting the Einstein Telescope detector layouts.

6 Interface with infrastructure

This section provides a description of the criteria used to determine alternative detector designs of the underground civil infrastructure of the Einstein Telescope (Triangle and 2L configurations).

It explains the rationale and guiding principles for assessing and defining the Triangle and 2L configurations as potential detector arrangement schemes, emphasizing their geometric designs within the underground civil infrastructure.

Civil infrastructure specifics are not included here, as further engineering development and site location details are required. However, the impact of detector requirements on infrastructure planning is outlined to guide local teams in advancing the next design stages.

6.1 Functional Volumes and Geometrical Criteria

A system of caverns and tunnels is designed to accommodate the instrument envelopes described in Section 5. The design follows fundamental civil engineering principles to ensure structural stability and long-term functionality.

These elements, considered as the estimated minimal excavated volumes, for two baseline configurations of the Einstein Telescope underground infrastructure: the Triangle and the 2L configuration can be broken down into three main excavation components:

- Caverns – large underground rooms housing experimental or technical infrastructure.
- Tunnels – typically short access or connection tunnels.
- TBM Tunnels – long, straight tunnels bored using a Tunnel Boring Machine (TBM), generally corresponding to the main arm cavity tunnels.

The estimation of excavated volumes for caverns and tunnels in this study is subject to several limitations. The considered civil engineering criteria emphasize key factors influencing infrastructure costs, deliberately omitting site-specific features, conditions, or construction details that could significantly impact initial estimates. It does not take into account construction planning aspects such as excavation sequencing, logistical constraints, or contractor-specific methodologies. The cavern and tunnel shapes are assumed to be general and are not optimized for structural stability or excavation feasibility. Access considerations, including shafts, entry tunnels, and depth-related factors, are excluded, as are additional service tunnels that may be required during construction. Surface works such as site preparation, spoil management, and supporting infrastructure are also not considered. Finally, the study does not include safety-related elements such as emergency access routes, ventilation systems, or other provisions for personnel during excavation.

Key considerations for the final design, including cable drainage and lining types, air quality management and monitoring, relative humidity control, access and personnel safety logistics, background noise reduction, and extreme event handling (e.g., fire, implosion, seismic loads), as well as consequence classes and maintenance logistics, are excluded from the current ET design task Force scope.

The cost analysis represents a comparative evaluation of potential savings, relying on simplified assumptions, such as reducing the overall envelope (e.g., tunnel DNmin, cavern volumes, detector layout optimization).

The applied approach enables initial comparison of design alternatives; however, subsequent phases will need to incorporate local data and stakeholder input to refine cost projections and technical solutions.

6.1.1 Caverns

The structural design of the cavern, whether a conventional horseshoe-shaped vertical cavern or an elliptical one, remains still undefined. Local site studies will guide the modeling process to optimize cavern geometry, balancing shape, stability conditions, minimum volume, and performance requirements. It is also envisaged that the caverns—especially those within proximity to the test masses—will have cast in-situ concrete secondary lining. Additionally, a waterproofing and drainage membrane will be placed between the primary and secondary linings. This will help keep the cavern dry and prevent excessive water pressure caused by any existing groundwater.

Site-specific geotechnical investigations and numerical models (e.g., finite element analysis, Q-system, or RMR-based evaluations) will support the more advanced construction solutions. However, within the scope

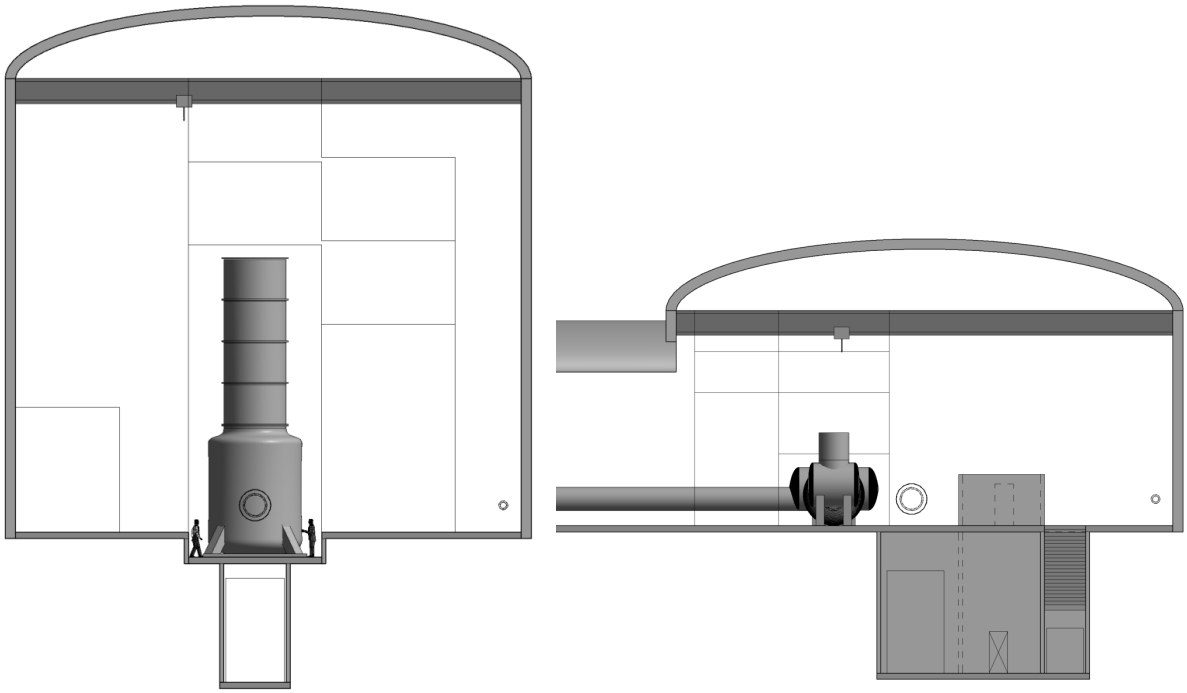

(a) Cross section of a Cavern A4-1 - L layout

(b) Cross section of a Cavern A4-2 - L layout

Figure 16: Conceptual cross-section of 2L baseline caverns (retrieved from **TD.3**). Not equally scaled.

of this document and for the purposes of the task force activity, the following assumptions were adopted and represent a first reference:

- The aspect ratio adopted the define the size of the caverns do not exceed 1:2 or 2:1, with a preference of taller vs wider caverns whenever possible due to stress distribution considerations [19].
- An arbitrary maximum cavern width of 25m for cavern stability (construction excavation not considered over excavation) is considered based on historical literature data [20]. This limit may be conservative for strong, massive rocks, but overly optimistic for weak or heavily fractured formations.
- An arched ceiling of the caverns is taken into consideration only for the calculation of excavation volumes. The ceiling shape is not shown in the detector layout 3D model, as that represents the minimum volume needed for the instruments and omits the actual structural geometry.
- The spacing between caverns should be determined based on the strength and stiffness of the rock mass, ensuring that each cavern remains structurally independent. Various studies have attempted to empirically formulate the relationship[19][21][22].The general principle used for the task force design iteration was a separation of 1.0xH(H=height of the tallest cavity). The local site specific layout should take the relationship that best works for the local rock conditions, as the top level requirement for any of these criteria/principles used in the initial layout design is the allowable deformation (instrument related) and structural integrity/stress optimization of the infrastructure.

These additional elements added on top of the detector layout minimal envelopes resulting in a concept of a cross section of a cavern and used for calculation of the estimated minimal excavated volumes are shown in Figure 16.

For subsequent phases, if the feasibility studies conducted by local host sites determine that variations in boundary conditions are justifiable, adjustments to the optical and/or detector layouts can be implemented. These modifications should align with the flexibility parameters outlined in Section 5.

6.1.2 Mechanized/TBM Tunnels

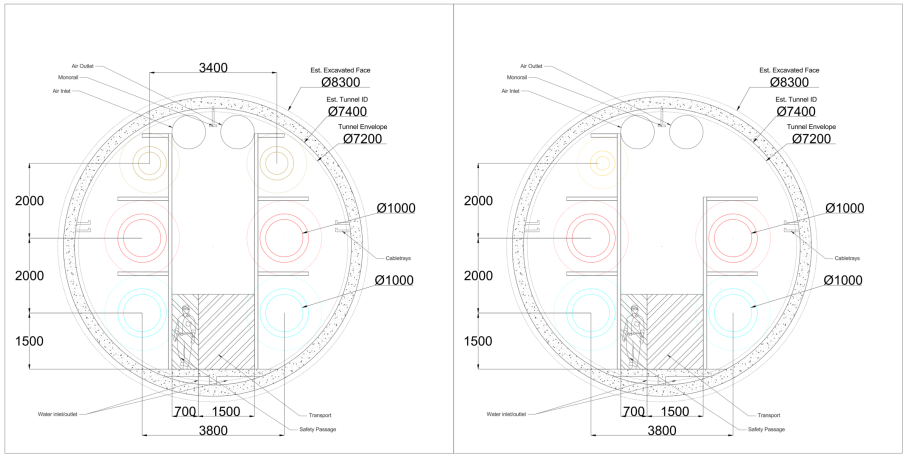

Figure 17: Conceptual cross section of the Triangle baseline configuration main arm cavity tunnel

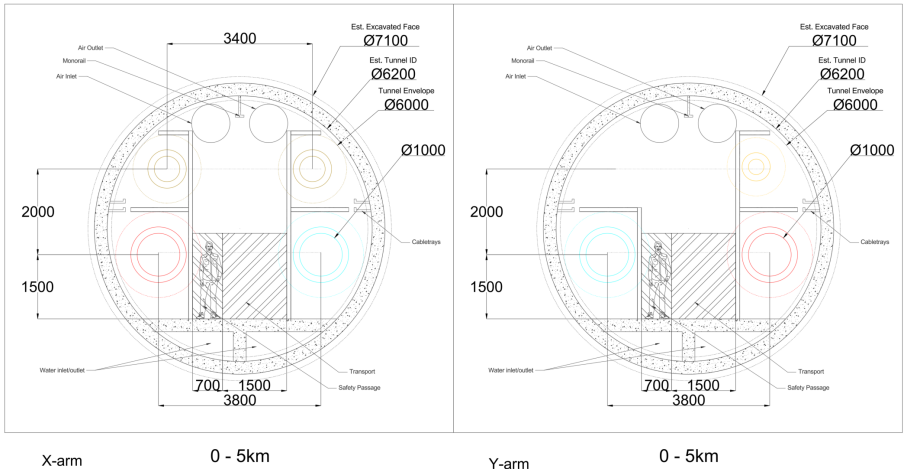

Figure 18: Conceptual cross section of the 2L baseline configuration main arm cavity tunnel

The main arm cavity tunnels of 10 km (Triangle) or 15 km (2L) in length mainly house the vacuum cavity envelopes containing the beampipes, along with any service infrastructure and a transportation corridor which allows for appropriate safety corridors as specified in [23]. These tunnels are envisaged to be TBM-driven excavations, regardless of the machine type, necessitates a perfectly straight envelope. This is driven by the requirement of the laser, which consequently determines the positioning of beampipes inside the main arm cavity tunnel. The requirements of these main arm cavity tunnels are described further in [23], 5, **TAB.4**+**TAB.5** for the Triangle configuration, and **TAB.10**+**TAB.11** for the L configuration.

Tunnel excavation will employ TBM-driven methods, which may cause slight alignment deviations due to varying geological conditions along the route. This deviation could be as much as 0.5m on all sides of the tunnel (shielded TBM) or 0.1m (open/gripper-type TBM) [24]. To avoid conflicts between the tunnel clearance profile and the required envelope for the beampipes, additional over-excavation or construction tolerance must be planned. This consideration depends on the type of TBM utilized. Proper planning ensures alignment and prevents structural issues.

In addition, it is assumed that the main arm cavity tunnels will be supported by precast reinforced concrete segmental lining.

Further advancements in excavation methodologies will be explored to define local site construction solutions. Within the scope of this document and the task force activities, the following assumptions are adopted alongside the specified tunnel envelope as illustrated in Figure 17 for the Triangle configuration and Figure 18 for the L configuration:

- Radius enlargement of 0.1m to account for TBM deviation/construction tolerance.
- Radius enlargement of 0.1m–0.3m for tunnel lining.
- Radius enlargement of 0.1m–0.15m for the annulus gap.

6.1.3 Volumetric Breakdown of the Layout(s)

Considering the factors above, a summary of the estimated minimal excavated volumes and proportions of each of the elements (caverns, conventionally excavated tunnels, and TBM tunnels) for the Triangle and L layouts can be summarized in Table 7. The volumes are for a single instance of the L configuration and thus the numbers should be multiplied if constructed in 2 locations. But the proportions of the volumes would remain the same.

Est. Exc. Vol. (m3)	Triangle (Baseline)		L (Baseline) - Single instance	
Total	2.794 mil. m^3	100.0%	1.497 mil. m^3	100.0%
Caverns	1.023 mil. m^3	36.6%	0.331 mil. m^3	22.1%
Tunnels	0.250 mil. m^3	9.0%	0.029 mil. m^3	2.0%
TBM Tunnels	1.521 mil. m^3	54.4%	1.137 mil. m^3	75.9%

Table 7: Estimated minimal excavated volumes - breakdown summary of the baseline triangle and L layout(s)

Key observations on estimated minimal excavated volume breakdown:

1. **Triangle Configuration**
   - The **TBM tunnels** represent the largest component of the excavated volume, accounting for approximately **54.4%** of the total. While this is a substantial portion, it is relatively smaller when compared to the L configuration.
   - The **caverns** constitute a significant share of the excavation at **36.6%**. When comparing the estimated minimal excavated volumes for the caverns in the Triangle layout, it is nearly triple the estimated volume in the L layout (for a single site; ∼1.5x when compared to a 2L total). This difference is due to having 6 interferometers instead of 2 as in the L configuration.
   - **Non-TBM tunnels** (e.g. connecting tunnels) account for **9.0%**, a moderate share that reflects the additional complexity of connecting infrastructure within the triangular arrangement.
2. **L Configuration (Single instance; totals should be doubled for 2L)**
   - The **TBM tunnels** make up a dominant share of the excavation, comprising **75.9%** of the total volume. This indicates a highly tunnel-efficient layout focused primarily on the 15km arms.
   - **Caverns** represent only **22.1%** of the total, substantially less than in the Triangle configuration. This suggests a simpler or more compact central infrastructure. But 3 geologically feasible sites still need to be located for the 3 vertexes of the facility.
   - The proportion of **non-TBM tunnels** is minimal at **2.0%**, consistent with a less complex layout that requires fewer auxiliary connections.
3. **Comparative Summary**
   - In **absolute terms**, the Triangle layout requires a larger excavation volume in all categories. But when considering the L configuration is to be built in 2 locations, the total volume (not yet accounting for the access, any additional infrastructure needed on the surface, and additional surface-to-subsurface connections needed) is roughly similar.
   - In **relative terms**, the Triangle layout emphasizes **cavern space**, while the L configuration emphasizes **tunnel length**, particularly TBM-driven tunnels.
   - It is important to note that although the Triangle configuration has a higher total volume of TBM tunnels, their **proportional share** of the total excavation is **lower** than in the L configuration.

6.2 Cost Estimation Methodology

In the scope of the Task Force activity, a simplified approach has been proposed to estimate the relative cost changes among various underground laboratory layouts based solely on estimated minimal excavated volumes. This method operates under the assumption that excavation costs are directly proportional to the volume of rock/soil removed, while intentionally ignoring potential optimizations related to technology or work plan strategies that could significantly impact final costs. The results shown in this section are not not an ETO costing for ET. The cost estimate exercise purpose was to highlight the optimization of the Task Force baseline layout(s) compared to the reference 2024 layout(s). No other conclusion should be drawn from this theoretical exercise, as ETO does not stand behind any further interpretation of this chapter. The detailed cost analysis, which will include the impact of the specific geological conditions of each site, will be conducted in a later and more advanced phase of the project by the local teams, once the baseline layout has been defined and more in-depth geotechnical studies are available.

By applying a unit cost (cost per cubic meter of excavated material), the Task Force aims to provide an initial comparative analysis that can guide decision-making and future discussions regarding the feasibility and financial implications of each potential layout on a broad scale. However, these values carry a possible estimated uncertainty range [25], depending on local conditions, excavation methods, technical requirements, etc. As such, all comparative figures should be interpreted within this uncertainty margin.

The approach based solely on the estimated excavation volume is intended as a preliminary, parametric, and indicative rough estimate of the **relative variation in costs**, and **not as an absolute forecast of costs**. Some inherent limitations of this approach include neglecting the geological variability, the impact of different excavation techniques, the worksites settings, the different regulatory constraints related to environmental impact and safety and, market fluctuations in labour and material prices over time.

If one configuration requires a significantly larger excavation volume than another, it can be hypothesized (with caution) that the excavation costs will also be relatively higher, ceteris paribus (all other factors being equal, which we know is not realistic). It can help identify orders of magnitude in the potential cost differences related to excavation among the various options. A volumetric difference of 50% would suggest (again, with due caution) a potentially significant variation in excavation costs.

In an initial phase of exploring different configurations, this preliminary estimate can help discard options that appear clearly more "onerous" in terms of excavation volume, providing a basis for focusing attention on those potentially more efficient from this point of view.

The volumetric estimate can serve as a starting point for more in-depth discussions, highlighting the need to consider the more complex factors that influence real costs. However, it is crucial to emphasize and remind all stakeholders of the inherent limitations of this approach.

- It does not represent an accurate estimate of the final costs. Which will be done by the local teams.
- The real cost variations could deviate significantly from the volume variations due to the neglected factors.
- It is essential to proceed with more detailed and methodologically advanced analyses to obtain reliable estimates.

In summary, if used with full awareness of its limitations and with the objective of providing a very first relative indication of the potential cost variations related to excavation volume, this preliminary parametric approach can have its usefulness in the initial evaluation phase of the different configurations. The key is not to interpret the results as definitive cost estimates, but as a rough indication to be further investigated with more comprehensive subsequent analyses.

6.2.1 Unit cost of mechanized tunnels

The specific construction methodology for the main arm cavity tunnels aren't yet known, but assumed to utilize a type of mechanized tunneling (presumably TBMs). This method contrasts with traditional methods like drill-and-blast or hand mining. Mechanized tunneling is a broader term that includes TBM tunneling but also encompasses other methods that use mechanical excavation equipment. This can include roadheaders, microtunneling machines, and shield tunneling, which use mechanical cutters but are not necessarily full TBMs.

Unit costs for these mechanized tunnels are based on data collected by Infrastructure UK of various rail, highway, water and power sectors projects in the UK and EU [26].

A linear correlation between tunnel outer diameter/OD (m) and costs (m€/km) and adjusted for inflation can be drawn. In which a TBM-driven tunnel with a tunnel envelope of 6.2m (estimated excavated diameter of at least 7.3m), would cost approximately m€33.66/km, and a tunnel envelope of 7.2m (estimated excavated diameter of at least 8.3m), would cost approximately m€37.72/km.

6.2.2 Unit cost of caverns and tunnels constructed using traditional methods

Unit costs for caverns and traditionally excavated tunnels are typically expressed per cubic meter of excavated volume. This approach allows for a straightforward comparison of excavation costs between different layouts, as it directly relates to the amount of material removed. Since excavation costs depend on factors such as geological conditions, support requirements, and construction methods, the unit cost serves as a simplified estimate that provides a baseline for assessing the financial impact of various design choices.

For caverns and conventionally excavated (non-mechanized/TBM driven) tunnels, a unit cost of €700/m3 is taken, from a possible considered range of €450-800/m3. This number is based on similar projects that are currently undergoing feasibility studies of their own [27]. While this approach does not capture the full variability of construction factors, its purpose is not to provide precise cost figures but to give a proportional comparison of excavation volumes across layout options. As a preliminary tool, it helps identify and eliminate configurations that are clearly less favorable in terms of excavation volume, allowing focus to shift toward more potentially efficient alternatives.

It should be noted that the excavation methods that are assumed here do not dictate the construction method/approach. The local teams are free to choose the appropriate construction method/approach based on the local conditions, as long as all of the scientific and functional requirements are met.

6.2.3 Key Cost Drivers

Summary of the comparison of the differences between the baseline Triangle layout (the result of this study) compared to the 2024 reference layout is shown in the Table 8. The breakdown per element (i.e. each cavern and tunnel) is shown in Section 7.4 of [6]. As previously stated, the estimated costs carry a range of uncertainty.

Triangle		**Baseline**		**2024**		**Relative Difference**		**v.s. total**
Est. Vol. (m3)	Total	2.794 mil. m^3	100.0%	3.723 mil. m^3	100.0%	-0.929 mil. m^3	-24.9%	
	Caverns	1.023 mil. m^3	36.6%	1.132 mil. m^3	30.4%	-0.110 mil. m^3	-9.7%	-2.9%
	Tunnels	0.250 mil. m^3	9.0%	0.668 mil. m^3	18.0%	-0.418 mil. m^3	-62.5%	-11.2%
	TBM Tun.	1.521 mil. m^3	54.4%	1.922 mil. m^3	51.6%	-0.401 mil. m^3	-20.9%	-10.8%
Est. Cost	Total		100%		100%		-29%	
	Caverns	m€ 716	37%	m€ 793	29%	m€ (77)	-10%	-3%
	Tunnels	m€ 175	9%	m€ 468	17%	m€ (293)	-63%	-11%
	TBM Tun.	m€ 1,060	54%	m€ 1,493	54%	m€ (432)	-29%	-16%

Table 8: Relative Differences - Triangle - Baseline vs Reference 2024 Layout

Summary of the comparison of the differences between the baseline L layout (the result of this study) compared to the 2024 reference layout is shown in the Table 9. The volumes and costs are shown for a single L, numbers are to be multiplied if constructed in 2 locations. The breakdown per element (i.e. each cavern and tunnel) is shown in Section 7.4 of [6]. As previously stated, the estimated costs carry a range of uncertainty.

L (single instance)		**Baseline**		**2024**		**Relative Difference**		**v.s. total**
Est. Vol. (m3)	Total	1.499 mil. m^3	100.0%	2.068 mil. m^3	100.0%	-0.569 mil. m^3	-27.5%	
	Caverns	0.333 mil. m^3	22.2%	0.468 mil. m^3	22.7%	-0.136 mil. m^3	-28.9%	-6.6%
	Tunnels	0.029 mil. m^3	2.0%	0.103 mil. m^3	5.0%	-0.073 mil. m^3	-71.4%	-3.5%
	TBM Tun.	1.136 mil. m^3	75.8%	1.497 mil. m^3	72.4%	-0.360 mil. m^3	-24.1%	-17.4%
Est. Cost	Total		100%		100%		-23%	
	Caverns	m€ 233	19%	m€ 328	21%	m€ (95)	-29%	-6%
	Tunnels	m€ 21	2%	m€ 72	5%	m€ (51)	-71%	-3%
	TBM Tun.	m€ 961	79%	m€ 1,184	75%	m€ (224)	-19%	-14%

Table 9: Relative Differences - 2L (Single instance; totals should be doubled for 2L) - Baseline vs Reference 2024 Layout

Key observations on cost and volume comparison vs. 2024 reference layout:

1. **General Observations**
   - Both the Triangle and L baseline configurations demonstrate substantial reductions in estimated excavation volume and cost when compared to the 2024 reference layouts.
2. **Triangle Layout**
   - Total excavation volume is reduced by **24.9%**, while total cost is reduced by ∼**29%** compared to the 2024 reference layout.
   - **TBM tunnels** show a significant volume reduction of **20.9%** compared to the 2024 layout (this contributes 10.8% to the total volume reduction and ∼16% to the total cost reduction), mainly due to the combination of the previously separate tunnels for the LF and HF filter cavities with the main arm cavity tunnels. In our estimation, TBM tunnels represent the major component of the excavation cost.
   - **Caverns** are only slightly reduced by **9.7%** compared to the 2024 layout (this contributes 2.9% to the total volume reduction and ∼3% to the total cost reduction). Although the reduction of tower sizing in certain areas (i.e. HFI) results in significantly smaller cavern volumes needed for those caverns, due to the configuration reshuffling and further mature tower concepts as discussed in Section 4 and Section 5 leads to more cavern space needed in certain areas, the total reduction in cavern volumes is not as apparent.
   - The largest relative saving comes from the **tunnel component** (non-TBM), which sees a **62.5%** reduction (this contributes 11.2% to the total volume reduction and ∼11% to the total cost reduction) in both volume and cost.
3. **2L Layout (Single Instance; totals should be doubled for 2L)**
   - Total excavation volume is reduced by **27.5%**, and total cost by ∼**23%**.
   - The **TBM tunnels** see a **24.1%** volume reduction and ∼**19%** cost reduction (this contributes 17.4% to the total volume reduction and ∼14% to the total cost reduction). As with the case of the Triangle configuration, this reduction is mainly due to the combination of the previously separate tunnels for the LF and HF filter cavities with the main arm cavity tunnels.
   - **Cavern volume and cost** both are reduced by around **29%** (this contributes 6.6% to the total volume reduction and ∼6% to the total cost reduction), indicating major improvements in the central infrastructure due to a more mature design that has been described in the Sections 4 and Section 5.
   - **Tunnels (non-TBM)** again show large reductions of over **71%** (this contributes 3.5% to the total volume reduction and ∼3% to the total cost reduction), similar to the Triangle case.

To better understand which design modifications contribute most significantly to the differences in volume and cost compared to the 2024 reference layout(s), a series of isolated change analyses was performed. In each iteration, a single design change was applied to the 2025 baseline layout(s), and the resulting estimated excavation volume and costs were recalculated using the parametric tool as described in Section 7.1 of [6]. This method allows for the rough quantification of the impact of individual decisions.

A couple of high impact decisions were tested:

1. LF Filter cavities in X arm with periscope
   Although the utilization of a periscope as described in Section 3.2 is seen as a high risk technology, as explained in Section 8, the analysis shows that it is a high contributor to the volume and cost reduction, as when considering the length of tunneling along, it was a reduction of 5km (for each LF system). Using the baseline layout and only removing the use of a periscope for the LF squeezed light system results in a configuration similar to the 2024 reference layout where the LF filter cavity beampipes were in a separate tunnel from the main arm cavity tunnel. This is illustrated as "T-TBM_LF-FC_A" in Figure 19a (Triangle configuration) or "T-TBM_LF-FC" in Figure 19b (L configuration).
   The changes compared to the baseline layout(s) are summarized in Table 10.
   - For the Triangle layout, this means in adding ∼454 mil. m^3 in excavation, even after the main arm cavity tunnels' envelope was reduced, which overall results in 16.2% of volume and ∼23% potential costs compared to the 2025 baseline Triangle layout.

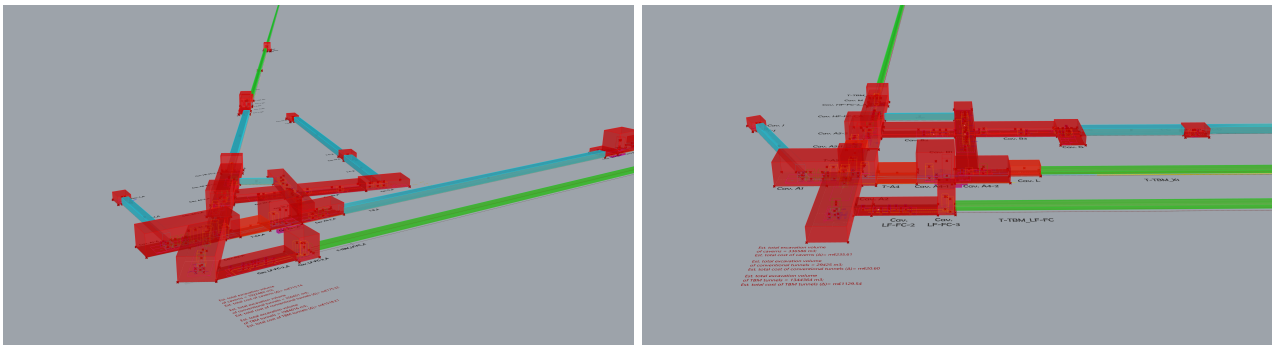

(a) Triangle (b) 2L

Figure 19: Low level of detail concept of LF squeezed light system without periscope

- For the L layout, this means in adding ∼209 mil. m^3 in excavation (for a single L; totals should be doubled for 2L), even after the main arm cavity tunnels' envelope was reduced, which overall results in 14% additional volume and potential costs compared to the 2025 baseline L layout.

2. Reduced tower footprint for residual motion CAT 1 and 2 HFI towers, and
3. Reduced tower footprint for all tower categories compared to the 2024 design.
   Table 10 shows a modest increase in volume and subsequently costs when reverting the tower footprints back to the 2024 concepts While volumetric estimations and unit cost estimations based on the excavation volume provide a useful tool for comparing layouts, they do not fully capture the construction feasibility advantages of these smaller caverns. Smaller caverns are generally easier and safer to excavate, posing lower stability risks and allowing for more flexible sequencing and access during construction. These practical benefits may not be directly reflected in volumetric cost comparisons—especially when comparing a large single cavern to a longer series of smaller caverns with a similar total volume. However, from an execution perspective, smaller caverns often offer greater manageability and reduced construction risk, which can ultimately contribute to improved overall project feasibility. It also does not reflect the effort done in Section 3.1 and Section 4 and the changes made to simplify the layout to the current state.

Table 10: Comparison of certain changes compared to the 2025 baseline layout(s)

Comparison vs 2025 basline layout(s)	**Total Est. Min. Exc. Vol. (m^3)**	**Vol. diff. vs baseline (m^3)**	**Vol. diff. vs baseline (%)**	**Cost diff. vs baseline (m€)**	**Cost diff. vs baseline (%)**
2025 Baseline Triangle	**2.794 mil. m^3**	-	-	-	-
Reverted HF tower height	2.895 mil. m^3	0.101 mil. m^3	3.6%	m€ 71	4%
Reverted tower concepts (all)	3.051 mil. m^3	0.256 mil. m^3	9.2%	m€ 180	9%
2024 LF FC concept (without periscope)	3.248 mil. m^3	0.454 mil. m^3	16.2%	m€ 451	23%
2025 Baseline L (totals for a single L)	**1.497 mil. m^3**	-	-	-	-
Reverted HF tower height	1.535 mil. m^3	0.038 mil. m^3	2.5%	m€ 27	2%
Reverted tower concepts (all)	1.579 mil. m^3	0.082 mil. m^3	5.5%	m€ 57	5%
2024 LF FC concept (without periscope)	1.707 mil. m^3	0.210 mil. m^3	14.0%	m€ 170	14%

6.3 Technical requirements

In addition to geometrical criteria as explained in Section 6, underground infrastructure projects—especially those involving high-precision equipment—must account for a broad set of engineering requirements that critically impact cost, feasibility, and long-term performance. Such examples of non inherently geometrically related technical requirements that would have an impact on overall costs include requirements on cavern/tunnel water tightness, allowable water flow, allowable inclination, cavern/tunnel cleanliness, environmental constraints, electrical needs, safety requirements, and future proofing needs.

Although not yet concluded as of this study, those requirements would be an important input for the feasibility study conducted by the local host sites. This could necessitate certain design choices which are more costly than what was initially conceptualized. Further explanation of these technical requirements are described in **TAB.5**, **TAB.11**, and in section 7 of the supporting document [6].

7 Risk and flexibility analysis

7.1 Simplified risk analysis on baseline detector layout in comparison with 2024 reference

7.1.1 Introduction

The Einstein Telescope (ET) performance can, in principle, be achieved through several possible instrumental configurations. These configurations may differ either in the optical layout or in the design of specific subsystems such as seismic isolation, the vacuum system, and cryogenic payloads, or in both. Each configuration imposes different requirements on the supporting infrastructure, which can lead to significantly different civil engineering costs. Conversely, more cost-effective configurations may introduce additional technical challenges or risks compared to more conservative approaches.

7.1.2 Simplified Risk Analysis

To assist in selecting the most suitable detector layout, a simplified risk analysis was conducted to compare these different instrumental configurations. Although this study does not represent a comprehensive risk evaluation of the full detector design, it serves to highlight relative technical risks among options. The findings from this analysis were then combined with a simplified cost assessment of the civil infrastructure implications (see Section 6.2), enabling a balanced decision that weighs both cost and technical risk.

The task force began by identifying a set of technically viable configurations that could simplify the detector layout compared to the 2024 reference configuration, while also aiming to reduce civil infrastructure expenses. For each alternative configuration, specific risk items were identified where the design diverged from the 2024 reference, focusing on differences in design complexity, feasibility of installation, long-term maintainability, and expected scientific performance.

A standard risk assessment methodology was applied to these items, comparing the potential impact of each configuration against the 2024 baseline. This included a study of the Technology Readiness Level (TRL) of a subset of critical design elements. The TRL assessment followed ISO standards and aimed to determine the maturity of these subsystems and their anticipated readiness level before 2029, thus informing their associated technological risks.

A more comprehensive analysis of alternative configurations is presented in the extended supporting document, which also outlines the rationale behind the applied risk and flexibility analysis methodologies.

(For a full detailed Risk Register, please check this table **TAB.14**)

7.1.3 Technology Readiness Levels (TRL)

The TRL assessment used in this study provides a standardized metric for evaluating the maturity of technologies. The scale ranges from TRL 1, which represents basic theoretical research and observation, to TRL 9, which reflects real-world deployment and operational performance.

TRL 2 covers the initial conceptualization and modeling stages. At TRL 3, early-stage laboratory experiments serve to demonstrate proof-of-concept. TRL 4 involves testing individual components in controlled lab settings to verify functionality. By TRL 5, these components are integrated and tested in simulated environments to assess their collective performance. TRL 6 introduces prototype demonstrations under relevant, though still controlled, conditions. TRL 7 escalates this testing to actual operational environments. TRL 8 confirms readiness for full-scale deployment following extensive validation. Finally, TRL 9 confirms full operational maturity, including successful performance in live, real-world settings.

For the Einstein Telescope, TRLs are used to assess readiness across numerous subsystems such as seismic isolation, cryogenics, optical elements, vacuum pipelines, and squeezing technologies. A detailed TRL table is available for further reference. (see Table **TAB.13**)

7.1.4 2025 Baseline Configuration Changes

In developing the 2025 baseline configuration, the task force implemented several key modifications to both the Triangle and 2L layouts relative to the 2024 reference.

The low frequency LF squeezing filter cavities in the X arm are now routed through the LSEM tower to the LSQI tower using a 2 meter high , for the 2L, and 4 meter high , for the Triangle. Meanwhile, the high-frequency (HF) squeezing filter cavity in the Y arm is routed directly to the HSQI tower via a similar periscope mechanism. The two-mirror filter cavity design has been adopted, featuring a reduction in beampipe diameter from one meter to 650 millimeters. The length of the LF input mode cleaner (IMC) has been shortened from 300 meters to 120 meters. The high-frequency IMCs have been consolidated within the same tunnel. The balanced homodyne detection (BHD) signal is now routed through the beam splitter (BS) in the LF interferometer. Additional spatial reorganization of the central area was carried out to accommodate these architectural changes. The suspension height of the LF test masses has been reduced from 17 meters to a range between 12 and 13 meters, and the tower height for other high-frequency interferometer optics has also been decreased. Furthermore, the footprint of Category 1 benches has been minimized. The task force also considered several alternative options, including the use of a double cavern structure, removing the periscope for the LF filter cavity, exploring alternative routing options for the squeezing beam, implementing a bow-tie configuration for the input mode cleaner, and reducing tower heights for both high-frequency test masses and low-frequency interferometer optics. Additionally, a reduction in cryostat size was examined as a potential design improvement.

7.1.5 Outcome on common Risks for both Triangle and 2L Geometries

For a full detailed Risk Register please check this table **TAB.14**
The Risk Study in the first stage is mainly a comparative risk assessment between the 2024 Baseline and the 2025 Task Force Baseline configurations for the 2L and the Triangle Geometries of Einstein Telescope (ET).
A rigorous risk assessment methodology was used. Risks were identified through interdisciplinary workshops that included experts in optics, vacuum systems, cryogenics, suspensions and engineering. Each risk was rated in terms of severity and likelihood on a qualitative five-point scale, with risk criticality calculated as the product of these two factors.
This enabled a structured cross-comparison between both configurations. The analysis spans multiple subsystems, including squeezed light injection (SQZ), optical layout, suspension, vacuum infrastructure, beam injection, and beam routing, and aims to give a complete and narrative-based understanding of how design evolution has affected the risk landscape of the project.

Squeezed Light Injection (SQZ) One of the most significant changes in the 2025 Task Force Baseline relates to the geometry and routing of squeezed light optics. A critical risk involves beam clipping within the filter cavity beampipes. In the 2024 design, a safe beam-to-pipe diameter ratio of 5:1 was maintained. However, in the 2025 configuration, this ratio has been reduced to 3.5:1. This change results in a much narrower clearance, increasing the likelihood of beam clipping especially in the presence of point absorbers or beam misalignments. Such clipping can cause a rise in residual transmission loss (RTL), undermining the quantum noise reduction intended by the squeezed light injection. The absence of a clear mitigation strategy in the 2025 design further compounds the concern.
Another risk associated with the SQZ subsystem in the new baseline arises from the routing of the squeezed beam through SEM/BS locations. This path increases the likelihood of stray light coupling into the main interferometer, thereby introducing additional optical noise. The suggested mitigation for this scenario is the implementation of a baffling system, which aims to limit backscatter and confine stray light. While this mitigation is technically sound, it adds design complexity and must be validated through simulations and physical testing.
The 2025 Task Force design also exhibits a risk due to possible filter cavity finesse mismatches. Unlike the 2024 configuration, where parameters were closely aligned, the updated design anticipates discrepancies between the actual interferometer parameters and the pre-designed filter cavity characteristics. This mismatch can lead to suboptimal squeezing performance. The proposed mitigation involves fabricating multiple mirrors with different reflectivities and possibly employing etalon-based tuning of the mirror reflectivity. However, this requires additional spatial provisions to replace components during commissioning, a consideration that must be integrated early into infrastructure planning.
A novel risk introduced by the 2025 design concerns the use of an oversized periscope to elevate the beamline

by 2 meters in the 2L configuration and 4 meters in the Triangle configuration. This configuration involves periscopes significantly larger than any previously employed and remains unvalidated at the precision levels required for optimal performance. The principal concern is that such a tall periscope introduces phase noise into the squeezed light path, degrading the squeezing injected into the interferometer. This degradation is especially critical at low frequencies, where the Einstein Telescope Low Frequency (ET-LF) configuration is designed to be most sensitive. The mechanical characteristics of the periscope, including its susceptibility to vibration and flexing, can lead to misalignment of optical components. This misalignment introduces fluctuations in the phase of the squeezed beam, which in turn results in decoherence and a loss of squeezing fidelity. The impact of this degradation is an increase in quantum noise, which directly lowers the sensitivity of the interferometer. The effect is particularly severe at frequencies below 30 Hz, which are crucial for detecting massive black hole mergers, one of the primary scientific targets of the ET-LF. The most straightforward mitigation strategy is architectural: eliminate the need for the periscope by placing the ET-LF interferometer and its squeezing and filter cavity systems on the same horizontal plane. This approach, while less risky, may involve varying levels of cost depending on the extent of infrastructure modifications required. Alternatively, a more experimental mitigation strategy involves prototype testing of the periscope in an existing gravitational-wave detector. Such a test would evaluate its mechanical stability and its impact on squeezing, providing data on whether stability can be achieved using specialized materials or advanced isolation systems. Although this option introduces additional cost and potential delays, it could help assess the feasibility of incorporating periscopes in future designs. The risk associated with the periscope is important for the 2L configuration but is even more critical for the Triangle configuration, given the greater beamline elevation and increased precision requirements. The full implications of this risk remain uncertain due to the lack of experimental validation, making it a priority area for further investigation and mitigation.

Suspension Systems The 2025 Task Force Baseline also presents several new challenges related to the suspension systems, particularly in the ET-LF configuration.
A key suspension-related risk emerges from the limited cavern height available for the low-frequency test mass (LF TM) suspensions, which are approximately 13 meters tall. If the cavern height does not accommodate the required pendulum length, the system's seismic isolation will be compromised. In response, the Task Force suggests adding a five-meter safety margin or incorporating active seismic platforms. While technically feasible, both options involve substantial infrastructure modification, which must be reconciled with cost and construction constraints.
Additionally, the risk of glass fiber explosion persists in the ET-HF design. This risk is elevated by the high integration level and limited access for cleaning and inspection. A break in a glass fiber could contaminate nearby optics with particles, potentially necessitating complete detector shutdown and cleaning. Although this risk was recognized in the 2024 baseline, no significant new mitigations have been introduced in 2025. Proposed responses include isolating test masses and maintaining clean integration practices, but the likelihood remains a concern.
An alternative option of multi-cavern layout to reduce interference between many subsystems including the suspension and cryostat, would cause a risk that involves the bounce frequencies of the inter-cavern suspension wires. Due to the geometry imposed by the updated multi-cavern layout, these frequencies are too low, thereby reducing the isolation performance of the system. This is a significant issue because the suspension must provide effective isolation at very low frequencies. The proposed mitigation involves adding vertical filter stages or increasing the separation between caverns to raise the system's natural frequency. However, this may conflict with architectural and geological constraints.

Optical Layout The optical layout in the 2025 configuration has undergone substantial changes, leading to several critical new risks. In both high-frequency (HF) and low-frequency (LF) paths, the Task Force plan proposes merging towers into one tower or increasing the number of optics in one tower instead of the more stable, complex suspensions used in 2024. This decision is largely driven by space constraints and integration complexity. Mitigation entails reverting to the 2024 layout with a larger footprint and additional vessels, though this would conflict with goals of compactness and cost efficiency.
Another risk arises in the HF recycling cavities, where short optical paths and high beam curvatures are introduced due to co-location constraints. These changes drastically reduce phase and spatial mode tolerances,

complicating control systems and increasing the risk of performance degradation. The Task Force recommends redesigning the beam geometry to allow more gradual transitions in beam size and phase accumulation, but this would likely require significant redesign and additional space.

Infrastructure and Vacuum Risks tied to infrastructure and vacuum systems have also grown in the 2025 Task Force configuration. One notable risk concerns safety margins within the tunnel system. The 2025 baseline introduces four vacuum beampipes for the 2L Geometry and 6 vacuum beampipes for the Triangle Geometry within a single tunnel, reducing the available space for alignment activities and future upgrades. This creates a higher probability of accidental damage to critical components and complicates logistics during upgrades. The suggested mitigation is to construct a prototype tunnel section at the surface to test practical maintenance procedures. This prototype would help validate the Task Force's assumptions and allow adjustments before full-scale implementation. This Risk would be higher for the Triangle than the 2L.
Another infrastructure-related risk stems from the reduced tunnel diameter, which complicates cleaning procedures and may lead to increased scattered light due to contamination. The impact is a potential rise in absorption losses and reduced optical performance. Mitigation strategies include implementing dedicated cleanrooms around vacuum vessels and clearly defined handling protocols. Although these are sound engineering practices, their effectiveness depends heavily on available space, which is already constrained in the 2025 design.

Injection Optics The injection optics system presents two high-risk items in the 2025 configuration. Both concern the length of the Intermediate Mode Cleaner (LIMC), which is reduced from 300 meters in the 2024 baseline to 120 meters. This shortening significantly affects the IMC's ability to filter high-frequency noise and to maintain stable injection of the laser beam. The resulting impact is a rise in amplitude and frequency noise at the input of the interferometer. Proposed mitigations include adopting a high-finesse IMC design, albeit with more complex control, or constructing a longer tunnel during an upgrade phase. Both strategies require careful evaluation due to their engineering implications and costs.
The removal of one vacuum tower in the HF injection path is another risk. This change reduces the distance between IMC2 and PRM, limiting the flexibility for beam steering and mode-matching. The constraint may reduce the performance of the telescope's input optics. Mitigation involves refining the optical design and thoroughly simulating the mode-matching telescope under the new constraints.

Beam Control and Routing Several risks in the 2025 Task Force Baseline relate to the routing of critical optical beams, including the BHD (Balanced Homodyne Detection) and SQZ (squeezed) beams. These beams are now co-located in key towers such as LSEM, LSQI, and BS. The overlapping of multiple critical beam paths in confined volumes creates a lack of flexibility in positioning steering mirrors and diagnostic elements. The main impact is a potential increase in alignment errors, reduced tuning capability, and higher probability of interference between beams. Task Force recommendations include using advanced ray-tracing and layout simulations to confirm the feasibility of the design. While these simulations are essential, they must be validated with hardware prototypes or scaled-down physical models to ensure they accurately reflect real-world constraints.

7.1.6 Conclusion

The transition from the 2024 Baseline to the 2025 Task Force Baseline for the Einstein Telescope introduces a wide range of new and elevated risks.

While these changes align with objectives for feasibility and cost control, they introduce complexity and demand more advanced mitigation. Configurations relying on periscopes or compact geometries would require some additional developments to mitigate technical risk.

It is important to validate mirror positions, benches, beam paths through optical simulations before deciding on the type, footprint and height of chosen suspension design, and also deciding on the Tower Integration carefully following those steps. This study identifies and assesses the main technical risks that correspond to design solutions to make the ET civil infrastructure cost effective.

7.2 Flexibility analysis on baseline detector layout

7.2.1 Introduction

The flexibility study in complex projects like the Einstein Telescope (ET) is essential to evaluate how robust the design is against foreseeable changes. Flexibility involves the system's ability to adapt to new constraints, updated requirements, or uncertainties; without significant loss of performance or prohibitive redesign costs. This study involves two complementary approaches:

- Design Structure Matrix (DSM) Interdependency Analysis
- Penalty of Change and Risk-Based and DSM-based Evaluation

Together, they support system architects and engineers in identifying where flexibility matters most, and which design choices carry the greatest penalty if changes are needed later. As for technical risks, the present flexibility evaluation is based on a simplified analysis focused on configuration elements which concern differences between the baseline detector layout and the 2024 reference.

7.2.2 Design Structure Matrix (DSM) Interdependency Study

Purpose of DSM The Design Structure Matrix (DSM) (see table **TAB.15**) is a compact visual representation of the interdependencies between components or subsystems in a complex design. It reflects the rigidity of a configuration. It is used to:

- Understand how changes in one element affect others
- Identify highly coupled components that may be design bottlenecks
- Aid in modularization to improve change adaptability and reduce risk

Interdependencies in the ET Configuration In the case of the Einstein Telescope's dual configuration (LF and HF interferometers), the DSM maps interdependencies in:

- Physical layout (arm lengths, beam paths, etc.)
- Performance effects (squeezing quality, noises, etc.)
- Mechanical interfaces (towers, benches, etc.)

This is particularly relevant when considering optics, noises, and mechanical constraints that span both the low- and high-frequency (LF/HF) systems.

7.2.3 Penalty of Change and Risk Integration :

Methodology This study overlays the DSM with risk assessments (probability and severity) to simulate the impact of potential design modifications. By selecting a new alternative configuration as the baseline, we assess:

- What changes might become necessary
- What penalties those changes would entail What cost implications (both increase and potential savings) arise

Key Assumptions

- The chosen alternative configuration is treated as a baseline for evaluation.
- Change penalties may affect performance, sensitivity, or structural complexity.
- Costs include direct civil engineering costs and indirect operational complexity.

7.2.4 Identified Change scenarios and evaluations from the 2025 2L and Triangle Task Force Configuration

In this Section, some defined scenarios (see Table **TAB.16**) of possible future changes in the configuration are described.
Those scenarios were studied within the Penalty of Change study included in the flexibility study. The final change in the Configuration is well defined before it's delivered to the Engineering Department to calculate the cost of the new configuration.
In the following you can find differential costs that were computed with the parametric tool used for section 6 (see Section 6.2) and described in supporting document
The changes are applied directly to the 2025 Task Force Configurations for both 2L and Triangle, and the percentage increase or decrease is calculated in relation to the 2025 configuration cost.

1) Arm Length Reduction and Optics Change

- Change: ET LF Arm cavity reduced from 15 km to 10 km due to LF TM diameter constraint (if the ET LF TM diameter is reduced from 450 mm to 350 mm, if reduced more the arm cavity length will be also reduced).
- Penalty: Reduced sensitivity at low frequencies due to the shorter ET LF Arm cavity; sensitivity in interferometers improves with arm length.
- Cost: we suggest taking into consideration the differential cost estimate between 10 km to 15 km ET LF Arm length. Also we suggest taking into consideration some strategies regarding the civil engineering infrastructure taking a decision on which option to go for regarding the length of ET arm cavities Length in general and ET LF configuration (with respect to future upgrades).

  The cost of the 2025 2L configuration (10 km) shows a 26,41% reduction with respect to cost for 2025 2L configuration (15 km).

  The trade off should take into account the impact of the length reduction on the scientific scope.

  The Triangle cost remains unchanged. (as it already has 10 km arm length)

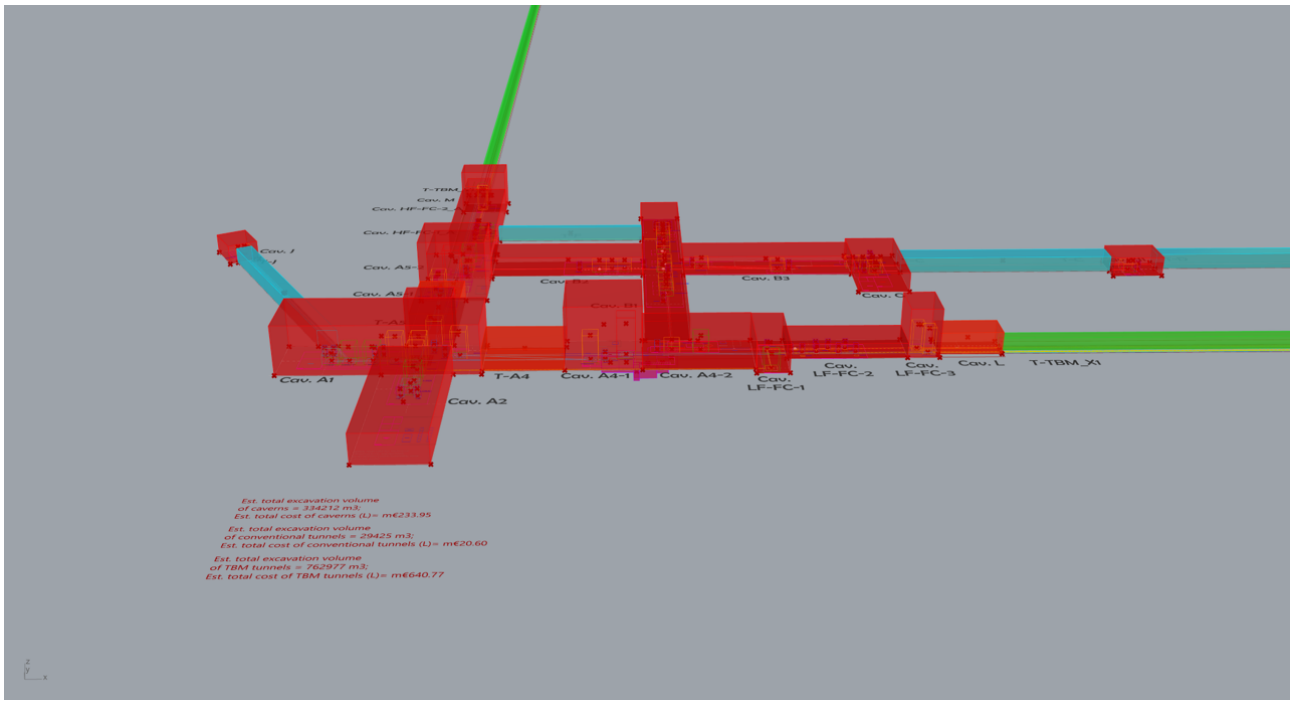

Figure 20: Baseline 2025 Task Force 2L with a 10 Km Arm length (see the table **TAB.16**)

2) Periscope Use and Squeezing Quality

- Periscopes may introduce vibrations, especially critical at Low Frequencies (LF) where quantum noise dominates.
- Penalty: Degraded squeezing level and thus quantum noise suppression essential at LF. Quantum noise suppression via squeezing is highly sensitive to mechanical stability.

Option A: Periscope for HF Only, Return to Baseline for LF

- Impact: Simplifies the LF path, reducing vibration risks, but adds complexity in having two different setups.
- Penalty: Operational complexity and potential alignment issues.
- Cost: Additional cost for ET LF Squeezing FC (same as baseline 2024).

The Cost of the 2025 2L configuration but considering the 2024 configuration for the LF Filter Cavity (No periscope for LF FC - no change in HF FC) shows a 14, 01 per cent increase with respect to Cost for 2025 2L Configuration.

The Cost of the 2025 Triangle configuration but considering the 2024 configuration for the LF Filter Cavity (No periscope for LF FC - no change in HF FC) shows a 23,13 per cent increase with respect to Cost for 2025 Triangle Configuration.

The Trade off should be analysed between a cost increase and the risk minimization for the performances of the squeezing cavity.

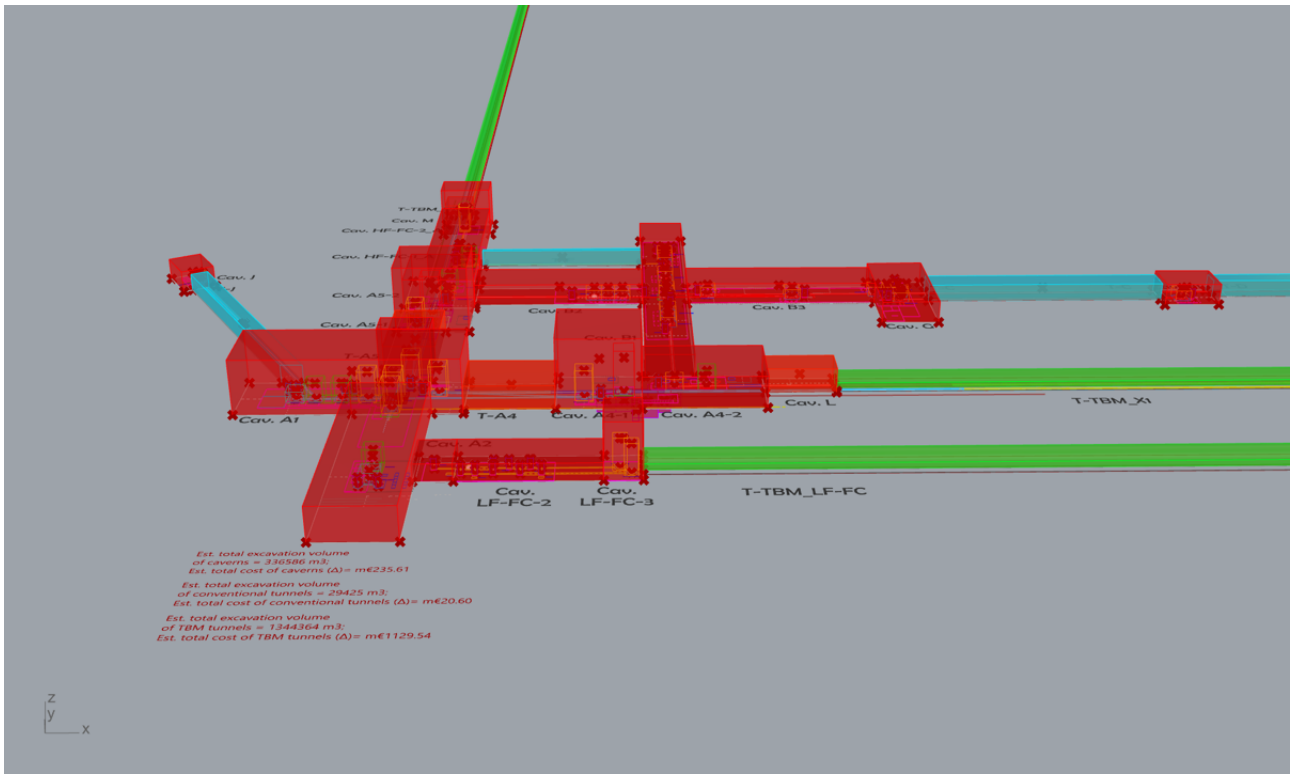

Figure 21: Baseline 2025 Task Force 2L with Squeezing LF FC from the 2024 configuration (see the table **TAB.16**)

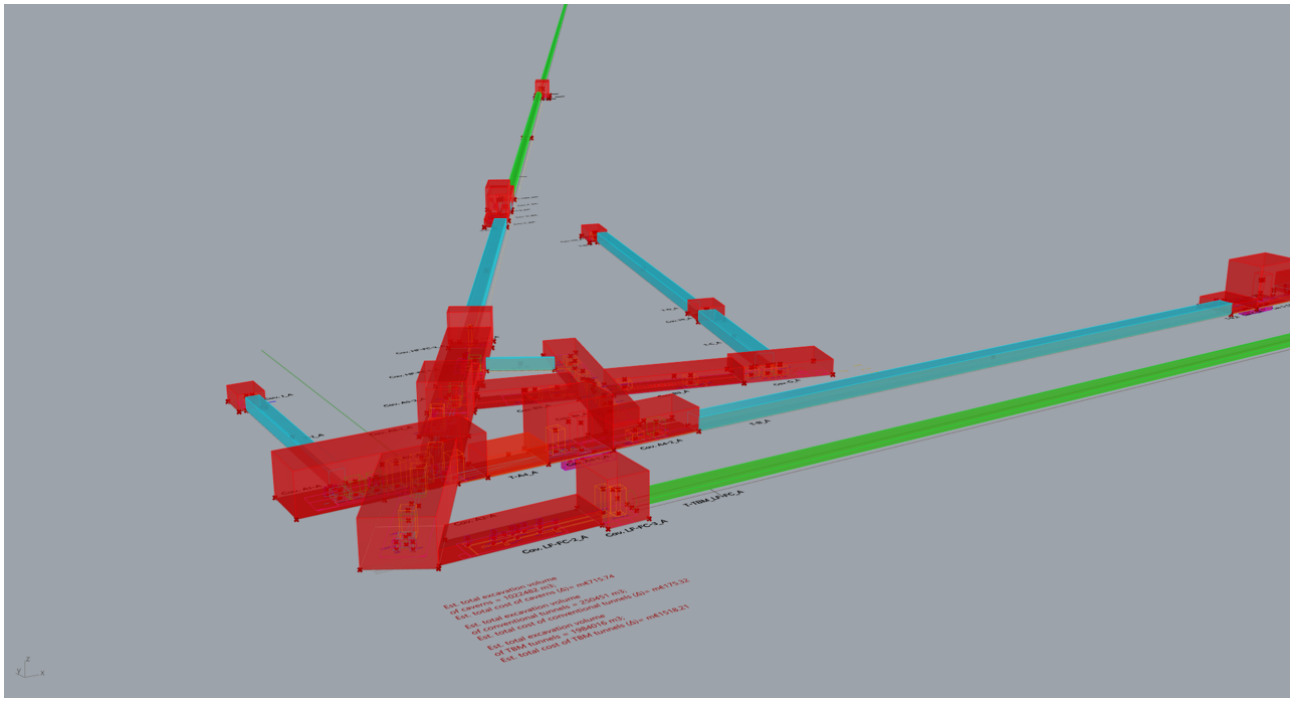

Figure 22: Baseline 2025 Task Force Triangle with Squeezing LF FC from the 2024 configuration (see the table **TAB.16**)

Option B-1 : Reroute Squeezing Through BS, Folded telescopes Length Increase This scenario was not applied to the Triangle Geometry. It was only applied to the 2L Geometry.

In order not to have astigmatism in the folded telescopes, we decided to create a scenario where we can increase the length between LBS and LZM1-X and LZM1-Y respectively. the distance will be increased of 10 meters allowing the squeezing LF-FC to route from the LBS allowing a safety margin to access towers (LZM2-X and LZM2- Y).

- Impact: Increases length of the signal recycling cavities (folded telescopes near the LBS) by 10 m on both LF recycling cavities and HF recycling cavities. LBS – LZM1Y : +10m ; LBS – LZM1X : +10m ; HBS – HZM5Y : +10 m ; HBS – HZM5X : +10m
- Penalty: Longer ET HF SRC may degrade sensitivity.
- Cost: adding 10m on both ET LF and HF recycling cavities

The cost shows a 0,48 per cent increase with respect to Cost for 2025 2L Configuration.

This scenario was not applied to the Triangle Geometry.

Option B - 2 : Reroute and Shift LZM2$_X$ $and LZM2_Y by 10m, Increased Astigmatism$ In this scenario (similar to B-1) we're not increasing the distance of 10 m between LBS and LZM1-X and LZM1-Y respectively. Instead we're just shiftting both towers (LZM2- X and LZM2- Y) to allow accessibility. This will shorten the folded telescopes on both X and Y arms (LZM1-X; LZM2-X and LZM1-Y; LZM2-Y).

- Impact: Increased angles (or just shorten the length) in folded telescopes lead to astigmatic beams.
- Penalty: increases astigmatism in the LF recycling cavities.
- Cost : remains the same for both 2L and Triangle.

Option C: LBS Tower and Optical Bench Space

- Common Impact in both Options A and B (B-1 and B-2): More optics in LBS.
- Penalty: Structural redesign and cost, as well as alignment risk with more optics.
- Cost of the infrastructure : remains the same.

3) Increasing LIMC Length: from 120m to 300m

- Risk : Insufficient filtering capability due to shortened IMC length (300m to 120m).
- Mitigation: Use a high-finesse cavity to enhance filtering despite the reduced length.
- Trade-off: A high-finesse IMC is harder to control and lock (more sensitive to small fluctuations), so it requires better feedback control systems. Increased sensitivity to control noise and complexity in locking systems.

Or
Revert to Configuration 2024 only with respect to LIMC.

- Cost: Increasing LIMC Length from 120m to 300m

The Cost shows a 0,7 per cent increase with respect to Cost for 2025 2L Configuration.
The Cost shows a 1,31 per cent increase with respect to Cost for 2025 Triangle Configuration.
Trade off to be analysed between the cost increase and the IMC performance (to be evaluated)

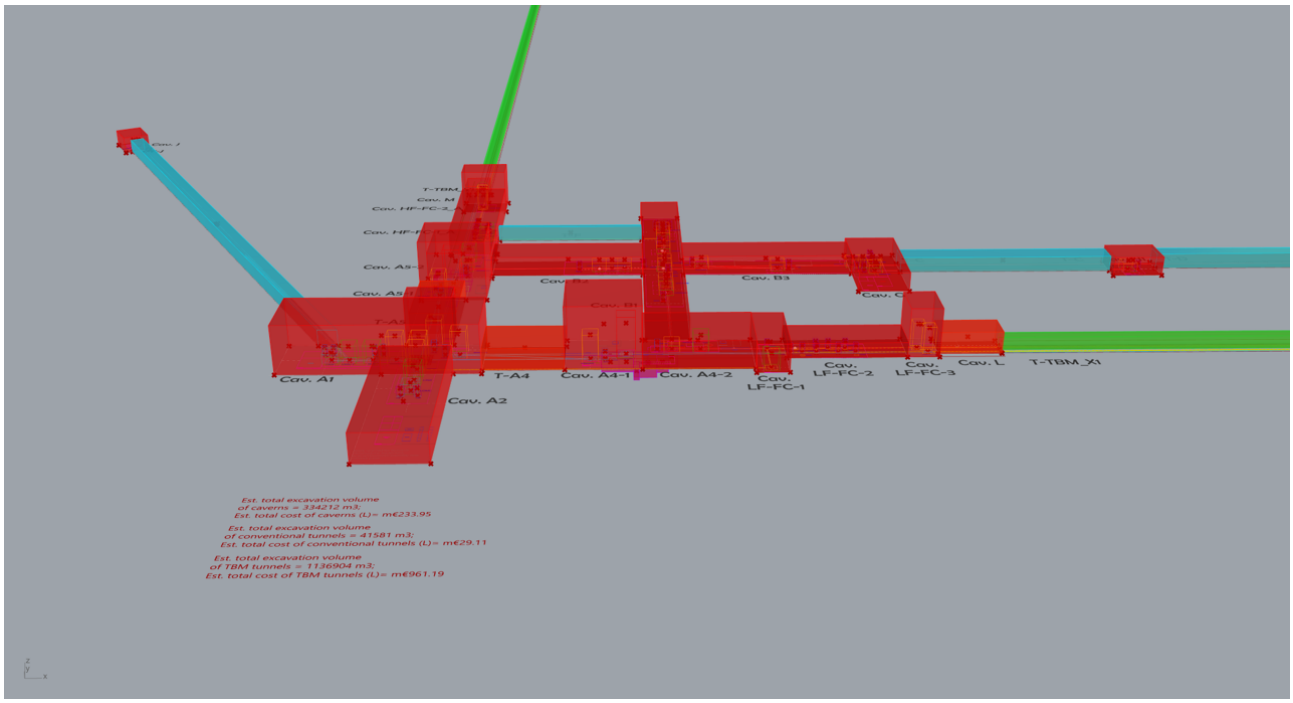

Figure 23: Baseline 2025 2L Task Force with LIMC length of 300m(see the table **TAB.16**)

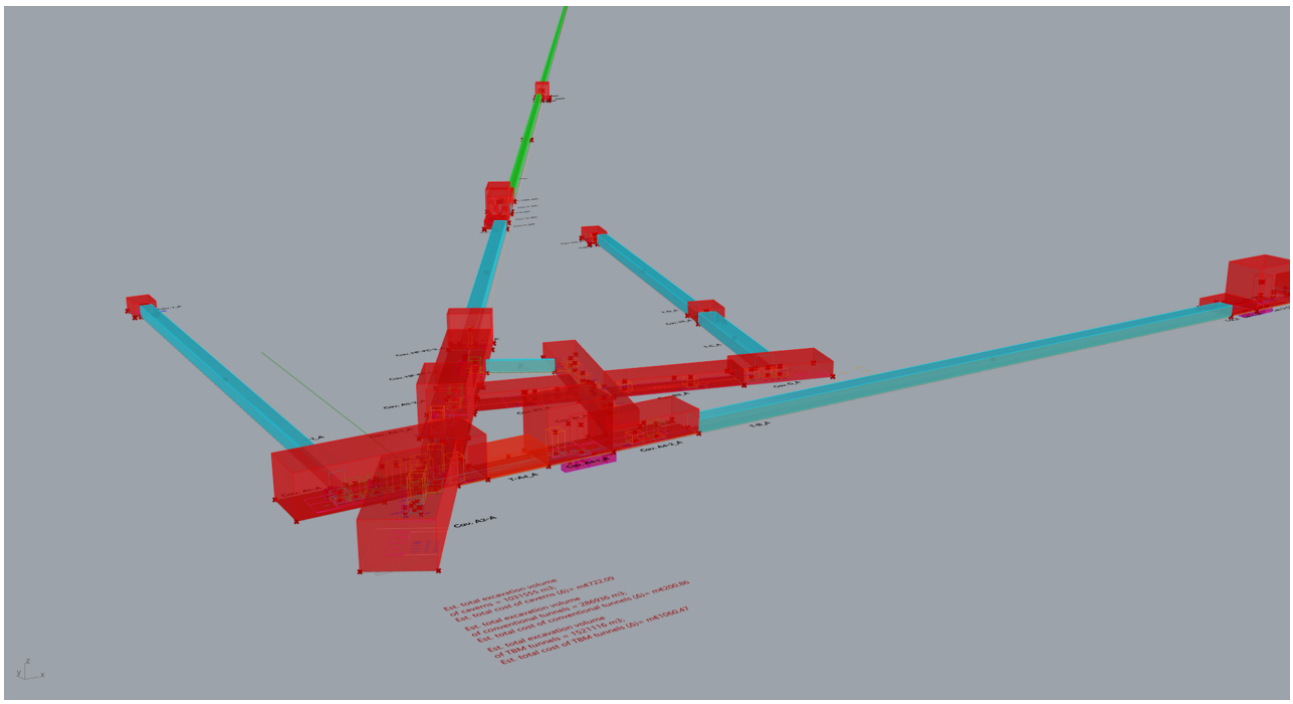

Figure 24: Baseline 2025 2L Task Force with LIMC length of 300m(see the table **TAB.16**)

4) Increasing LIMC Length : from 120m to 500m

- Risk : Insufficient filtering capability width=12L 300 m.pnggth (300 m to 120 m).

- Mitigation: Use a high-finesse cavity to enhance filtering despite the reduced length.
- Trade-off: A high-finesse IMC is harder to control and lock (more sensitive to small fluctuations), so requires better feedback control systems. Increased sensitivity to control noise and complexity in locking systems.

Or
Plan for tunnel extension (up to 500 m) from the outset to ensure long-term compatibility with future upgrades.

- Cost : Increasing LIMC length from 120m to 500m

5) LF TM Cavern : additional 3 m safety margin/ height

- Risk: Not enough cavern height available (12 m tall LF TM suspension). The actual performance of the suspension is not compliant with the design one (i.e.: not enough pendulum length to observe from 2Hz)
- Mitigation: Keep an adequate safety margin (can be going to 5m) on the caverns height / Update the design adding some active seismic filtering (platform)
- Cost: Adding 3m to the height of Caverns hosting ET LF TM Towers

The Cost shows a 0,37 per cent increase with respect to Cost for 2025 2L Configuration.
The Cost shows a 0,78 per cent increase with respect to Cost for 2025 Triangle Configuration.
The Trade off is between cost increase and minimization of the risk associated to the suspensions system technical design

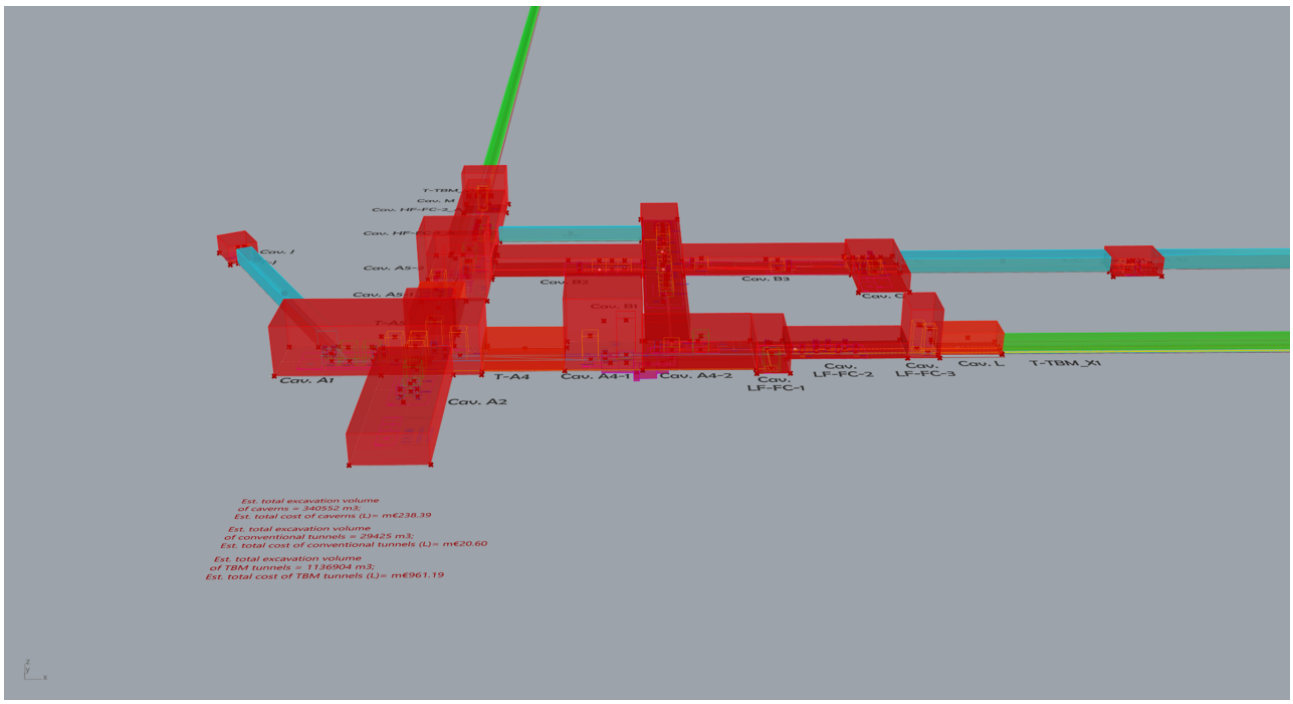

Figure 25: Baseline 2025 2L Task Force with additional 3m height to Caverns hosting LF TM (see the table **TAB.16**)

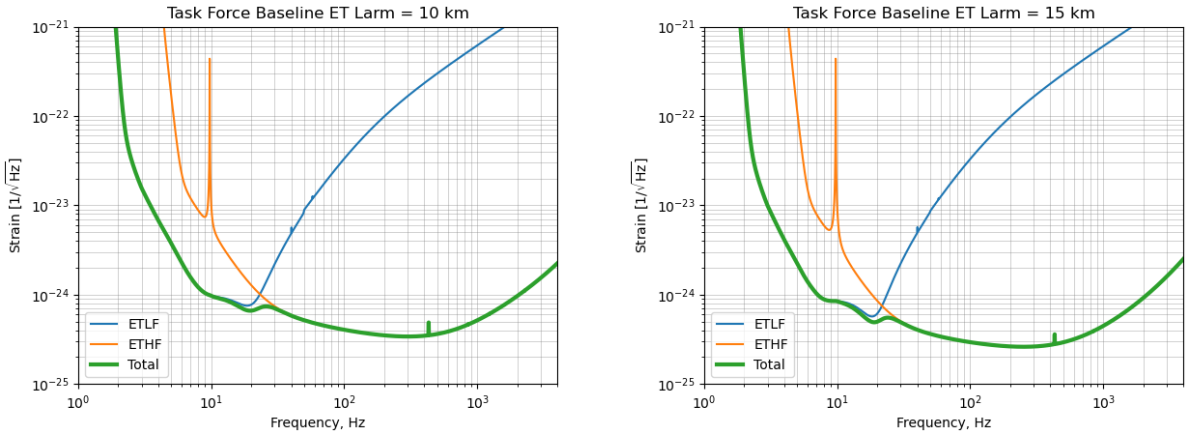

Figure 26: Sensitivity curves based on the Task Force design for both the 10 km and the 15 km detectors.

8 Performance

8.1 Noise budget for baseline configuration, comparison with 2024 reference

The stationary performance of the detector is defined by the noises that limit the ability to resolve signals. The sensitivity curve represents, for each frequency, the minimum GW strain the detector can measure, expressed in terms of amplitude spectral density. Current sensitivity is computed using the pyGWINC [28] software, developed independently in the context of LIGO design, and modified with ET-specific scripts. The models within the software use a limited set of parameters, which capture main features of the detector design, but lack many specific details that have been optimized in the process of this task force. Despite this, they provide sufficient detail to serve as the benchmark for judging the impact of the changes on the scientific case.

The reference sensitivity, provided by the ISB, results from the optical layout design work carried out in 2024. We used as the reference to evaluate the impact of any changes, quantified by the scientific case, as described in the next section. Figure 26 shows the sensitivity curves of ET-LF and ET-HF and the corresponding total sensitivity for both the triangular (10 km) and the 2L (15 km) configuration. Presented noise budget assumes 90 deg opening angle for both 10 km and 15 km detector, although in the 10 km Triangle the angle is in fact 60 deg. This is accounted for in the science case calculations.

Figure 28 shows the individual contributions of different noise sources to the ET-LF and ET-HF sensitivities, for both the 2L and the triangular configuration. These sources are described in detail in [28]. The main limiting noises for ET-LF are seismic noise, Newtonian noise, suspension thermal noise and quantum noise. For ET-HF, the dominant noises are quantum noise and coating thermal noise.

Figure 27 shows the comparison between the reference design based on the 2024 configuration and the updated design proposed by the Task Force. For ET-LF the main impact on the sensitivity comes from the quantum noise, seismic noise and suspension thermal noise. Only the seismic noise coupling has changed due to the change in the suspension tower design. Modifications to the optical layout had no effect on the parameters within the models, with the exception of the HF SEC length.

8.2 Summary of science case for baseline configuration, comparison with reference

Thanks to their technological advancements and the bigger facility, ET has the potential to trigger fundamental discoveries and deepen our understanding of several topics in Astrophysics, Fundamental Physics, and Cosmology. We refer the interested reader to [29, 30, 31] and references therein for broader discussions of specific aspects of ET's science case. In particular, ET alone will be able to detect tens to hundreds of thousands of compact binary coalescences (CBCs) per year formed through different channels, as compared to the ~ 100 observations per year at current instruments in the ongoing O4 run. Apart from the sheer number of sources observed, several of the detections will feature a very high signal-to-noise ratio (SNR), allowing for an exquisite

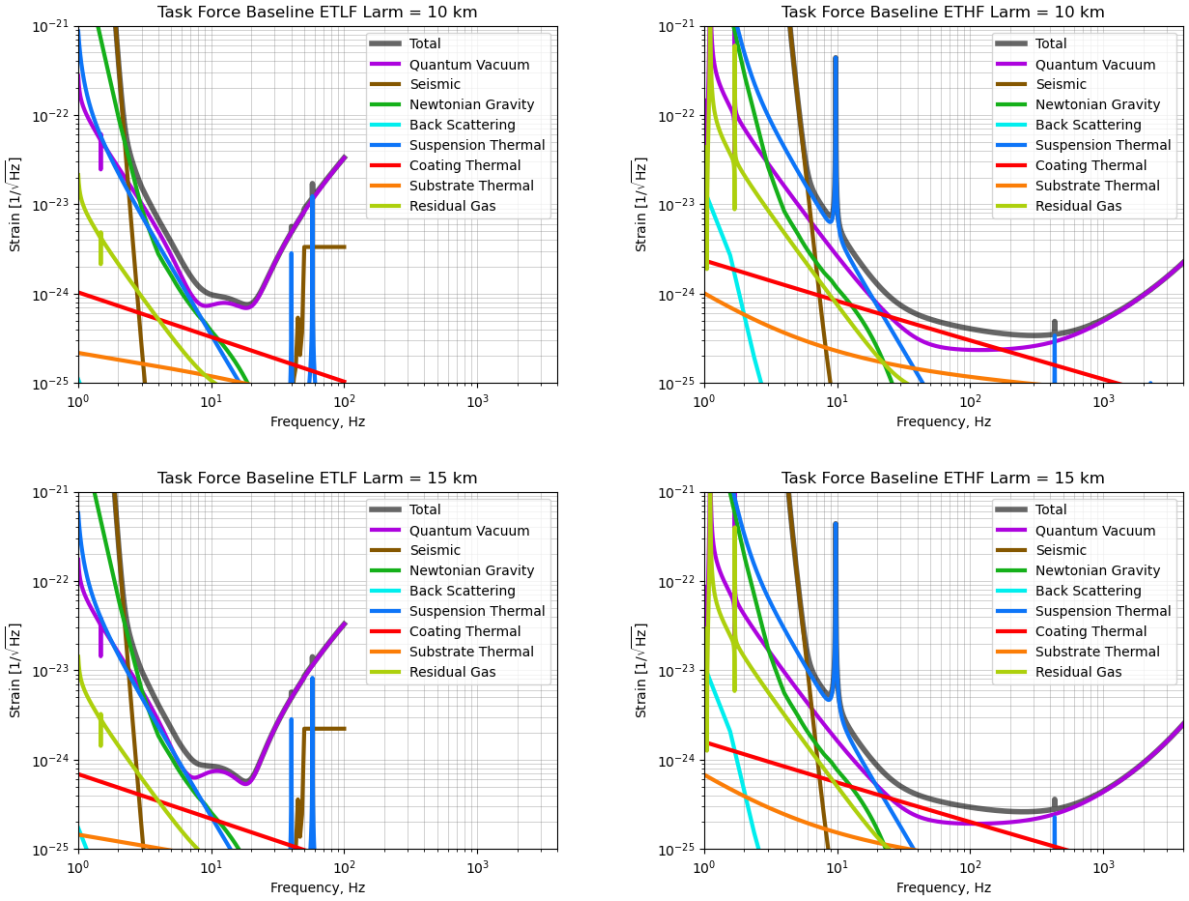

Figure 27: Noise contributions for ETLF (left) and ETHF (right), for 10km (top) and 15km (bottom) designs. Note: the flat region for the seismic noise around 50+ Hz is the artifact of the computation, and is not a real contribution. It has no effect on the overall sensitivity. The angle between the arms is not taken into account for the sensitivities.

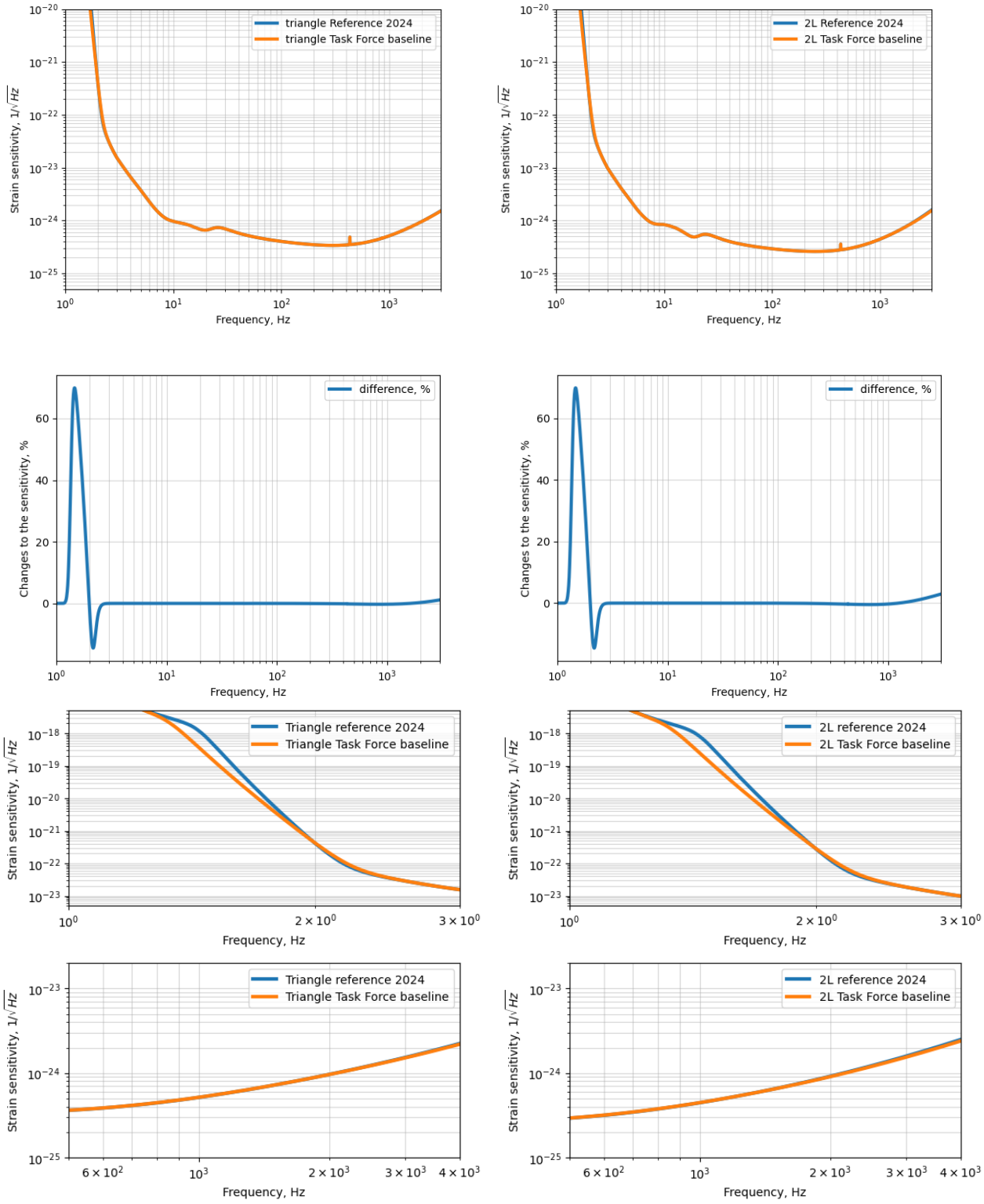

Figure 28: Top: comparison between the baseline sensitivity and the task force result for the triangle (left column) and the 2L (right column). Middle: difference between the old and new sensitivities for the triangle, expressed in %. Positive represents better sensitivity in the task force design. Two bottom plots show the zoomed-in difference for the low-frequency (first) and high-frequency (second) components. The difference at very low frequency comes from the new suspension design, and the difference at the very high frequency from slightly reduced HF signal extraction cavity length.

reconstruction of the source parameters, which will be fundamental to infer their distribution, nature, composition, and formation pathways, as well as test GR and probe the expansion history of the Universe. Moreover, the improved sensitivity and enlarged bandwidth of ET could allow us to observe GW sources which are yet elusive at current instruments, including continuous waves emitted e.g. by non axi-symmetric rapidly rotating neutron stars, bursts emitted by Core Collapse Supernovæ, which are also ideal multimessenger candidates, and stochastic GW backgrounds of both astrophysical and cosmological origin.

Given the broadness of its scope, evaluating the scientific output of ET and reducing it to simple numbers is not an easy task. For example, forecasts on CBC populations would inevitably depend on our still limited astrophysical knowledge about them, and would thus come with significant uncertainties. More importantly, all science cases are extremely valuable, and prioritizing one over the other should be avoided. Also, present-day forecasts rely on our current knowledge about possible GW sources, but one should keep in mind that ET has the potential to be a discovery machine, and unexpected revolutionary events might be found. Given these caveats, we will evaluate the scientific performance of different sensitivities for the experiment on a broad, quick and yet meaningful set of metrics, in particular:

Number of detections of binary black holes (BBHs) and binary neutron stars (BNSs)
This is a fundamental metric to assess the overall performance of the instrument across the full frequency band. For the BBHs, we include events produced by Population I and II stars (the most likely progenitors of binaries observed at current instruments), high-redshift Population III stars, and primordial BHs. For the last two kinds of sources, the LF sensitivity is particularly relevant, hence the importance of considering them in the analysis, even if the population is highly uncertain. We always consider 1 yr of observation.

Parameter estimation uncertainties for BBHs and BNSs
Along with the sheer number of CBC detections, we provide forecasts for the statistical uncertainties on the parameters for the observed sources. We include only systems generated by Population I and II progenitors. This is again a measure of the performance of the instrument over the entire frequency spectrum. We adopt a Fisher matrix approach for this metric, which, despite its well-known limitation, can provide meaningful results in a reasonable time for the large sets of sensitivities and configurations studied here.

BNS premerger alert and localization
The ability to give early warnings for systems that might emit an electromagnetic signal is of pivotal importance for multimessenger astrophysics, allowing telescopes to point before the merger. We thus provide the numbers of detections at different times before the merger, as well as the forecasted sky localizations at that time. For this metric, the low-frequency sensitivity plays a crucial role.

SNR in the post-merger phase of BNS systems
One of the most interesting prospects at ET will be to constrain the internal structure of NSs and learn their Equation of State (EoS). A particularly tantalizing way of achieving this endeavor is analyzing the post-merger phase of BNS mergers, for which an extremely good sensitivity in the high-frequency band is fundamental. We thus compute the SNR in the post-merger phase of 6 selected BNS numerical relativity simulations from the CoRe database [32] with varying masses and EoS.

Detection horizons
A typical metric to assess a GW instrument performance is the detection horizon, which gives the maximum redshift out to which it is possible to observe a given CBC source with optimal sky position and orientation. We will focus on equal-mass non-spinning binaries.

Power-law integrated sensitivity to SGWB
To assess the performance in searching for a stochastic GW background, we will compute the Power-law integrated sensitivity (PLS). Every signal at least tangent to it will be detectable in the specified observation time with a chosen SNR.

Number of detections of continuous waves from pulsars and minimum detectable ellipticity
We produce two different metrics for the prospects of detecting continuous waves from pulsars. Fol-

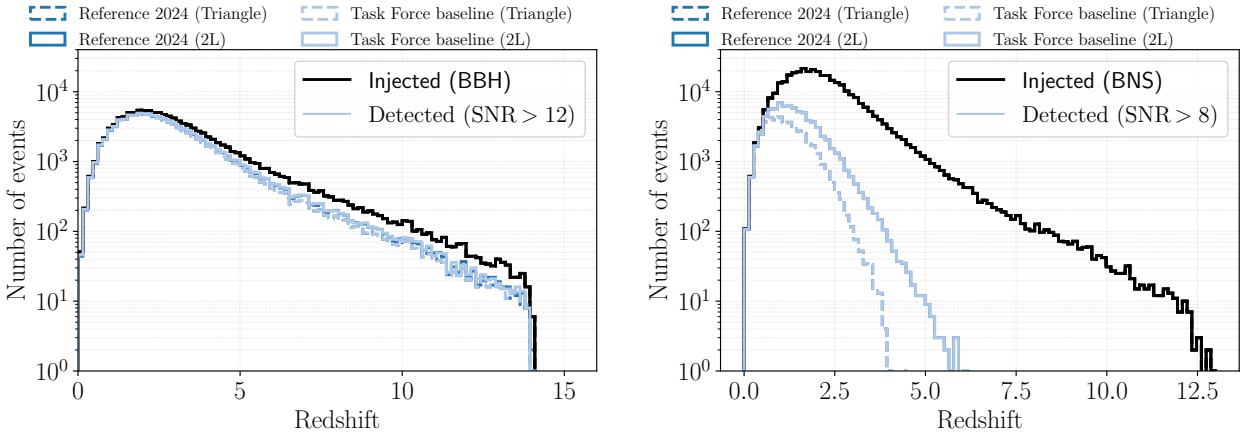

Figure 29: Detection of BBH (BNS) sources as a function of redshift on the left (right). The solid black line represents the starting population: 118119 for BBH and 351205 events for BNS binaries. The colored lines show the detections in dependence on the sensitivity curve. The detection threshold is set at SNR $\geq$ 12 (SNR $\geq$ 8) for BBHs (BNSs). The dashed lines refer to the triangular configuration, while the solid ones to the 2L one. There is no appreciable difference between the reference 2024 curve and the Task Force baseline.

lowing [31], we use the ATNF Pulsar Catalogue[1] and compute the number of events with detectable amplitude. For broad-band all-sky searches, we instead compute the minimum detectable ellipticity for the `FrequencyHough` pipeline [33].

SNR of CCSNæ

To assess the capability of observing bursts from CCNæ, we compute the optimal SNR with perfect template for signals from state-of-the-art simulations [34] placed at a distance of 100 kpc. For such systems, high frequency sensitivity is particularly relevant.

All computations are performed using the publicly available tools `gwfast` [35] and `gwfish` [36]. The considered detector geometries are a single-site triangle consisting of 3 nested instruments and two widely separated L-shaped instruments with misaligned arms with respect to local East, as in Ref. [30]. Only for the PLS evaluation we consider the more optimistic scenario for this metric in which the two L-shaped instruments are parallel with respect to local East.

We here present the results for the comparison of the sensitivities defined during the optical layout study in 2024 (Reference 2024 in the following) for the triangular and 2L designs, and the ones obtained with the changes to the optical design developed during the task force operation (Task Force baseline in the following). *In general, given the small difference between the two PSDs, we find almost no change in the metrics chosen to evaluate the scientific output of the instrument.*

Concerning the CBC-based metrics, in Figure 29 we report the redshift distribution of the full population used for BBHs ($\sim 1.2 \times 10^5$ sources) and BNSs ($\sim 3.5 \times 10^5$ sources) and of the detected ones with a significant SNR (> 12 for BBHs and > 8 for BNSs, as they can be accompanied by an electromagnetic emission, increasing the significance of detection). As it is apparent from this plot, no difference is found between the two sensitivities, both for the triangular and 2L geometries. We observe that almost all BBH sources are detected. On the BNS side, the detected sources go up to redshift 6 with respect to the injected population that extends beyond redshift 12.

The findings regarding the negligible differences among sensitivities are further supported by looking at the statistical uncertainties attainable on the reconstruction of both intrinsic and extrinsic parameters. Indeed, as it is apparent from Figure 30, where we report the relative statistical uncertainties on the detector-frame chirp mass and luminosity distance for both BBHs (top row) and BNSs (bottom row), the curves corresponding to

[1] `https://www.atnf.csiro.au/research/pulsar/psrcat/`.

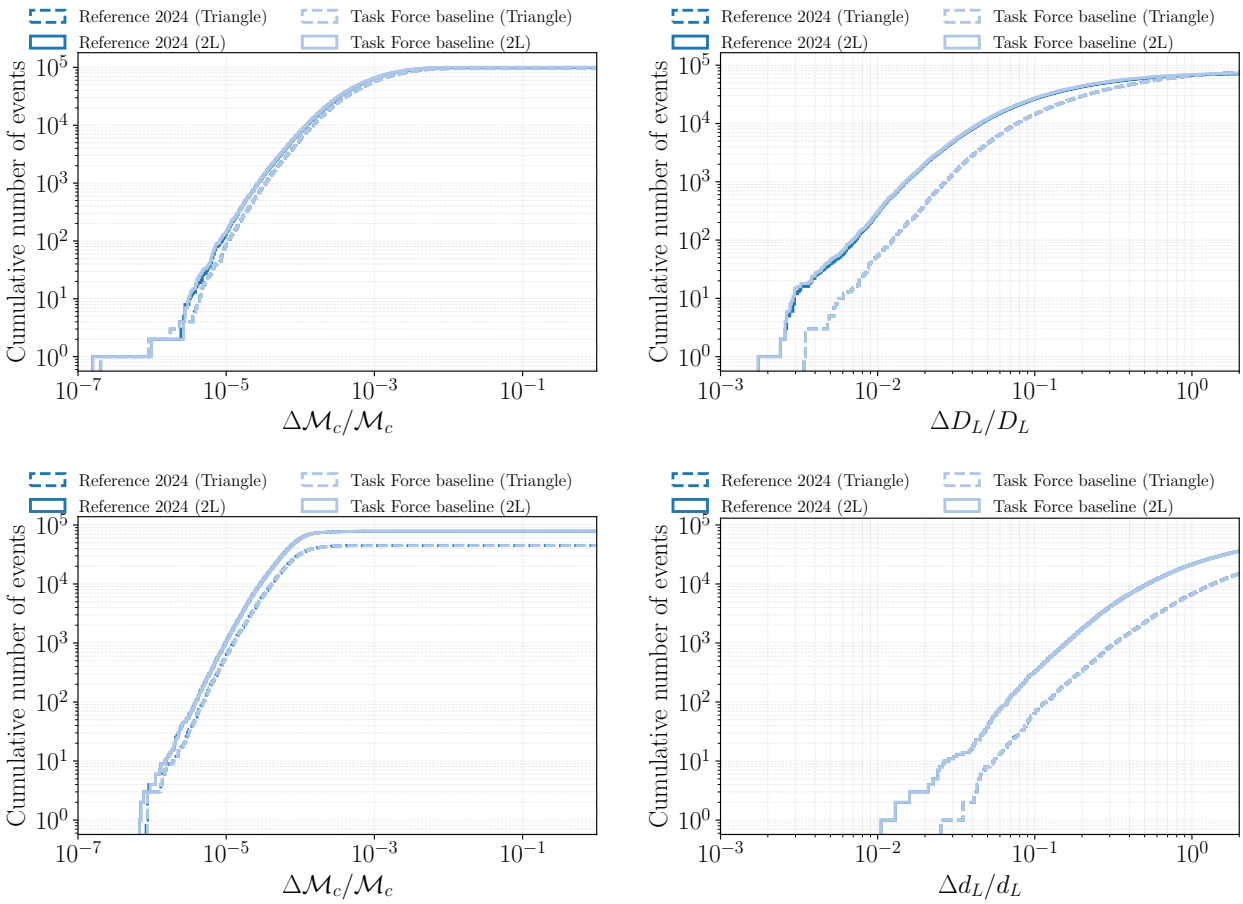

Figure 30: Comparison of relative errors on chirp mass and luminosity distance for BBHs (upper panels) and BNSs (lower panels) for the triangular and 2L geometries. The two sensitivity curves, Reference 2024 and Task Force design, do not show any significant difference.

the Reference 2024 and the Task Force baseline are almost indistinguishable for both the triangular and 2L geometries. Similar results are also found for other intrinsic and extrinsic parameters, see [6] for more plots and tables.

Focusing on BNS systems, we also find no difference in the number of detections at different times before mergers, with 262 (26), 613 (66), and 1417 (156) detections 30 minutes, 10 minutes and 1 minute before merger with localized below $1000\,\mathrm{deg}^2$ ($100\,\mathrm{deg}^2$), respectively, for both configurations at the 2L geometry. As for the post-merger analysis instead, we find slightly improved results by about 1%, for the Task Force baseline sensitivity, which is indeed slightly more performant at high frequencies.

Finally, as a general metric for CBSs independent of any Astrophysical population, in the left panel of Figure 31 we report the detection horizon for equal-mass non-spinning systems using an SNR threshold for detection of 8 and the `IMRPhenomHM` approximant. Again, we notice no appreciable difference between the two PSDs considered for both the Triangle and the 2L geometries.

Moving to other sources, in the right panel of Figure 31 we show the PLS of the two geometries with the different PSDs to stochastic GW backgrounds. A very minor difference can be seen in the curves for frequencies below 3 Hz, but the results are otherwise indistinguishable, also in this case. Configuration-wise, we see that the 2L setup is more sensitive at lower frequencies, while the after $\sim 90\,\mathrm{Hz}$ the Delta one gives a better return.

As for the detection of continuous waves from pulsars, we find again no appreciable difference in the two considered PSDs in terms of the number of individually detectable sources (~ 800 and ~ 900 for the triangular

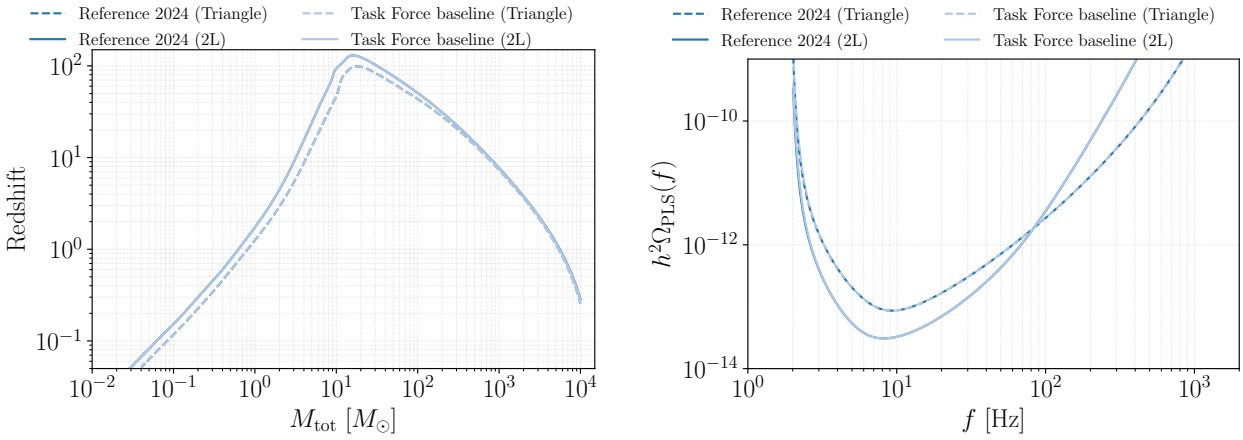

Figure 31: Horizon plot at SNR = 8 for the triangular and 2L geometries, comparing the Reference 2024 and the Task Force baseline sensitivities. PLS for 1 yr of observation and an SNR of 1 for both network geometries, comparing the 2024 Reference and Task Force baseline. There is no appreciable difference between the reference 2024 curve and the Task Force baseline.

and 2L geometries with both the PSDs), and the minimum detectable ellipticity as a function of frequency (with values never being ore different than $\mathcal{O}(1\%)$ across all the frequency band), see [6].

Finally, concerning the detectability of CCSNæ, we find again negligible difference among the Reference 2024 and the Task Force baseline noise curves.We find the maximum SNR in our analysis to be SNR=12.63 (12.21) in the triangular configuration (2L) for the best case scenario waveform, and SNR=1.88 (1.96) for the triangular geometry (2L) in the worst case scenario.

To summarize, *no appreciable difference is found when comparing the Reference 2024 and the Task Force baseline noise curves, both for the triangular and 2L geometries, for the broad set of metrics considered in this work.* This indicates that the scientific performance of the detector will remain consistent with the one forecasted in recent years [30, 31].

In addition to comparing the Reference 2024 and Task Force baseline configurations – both in the triangular and 2L geometries – we investigate a series of scenarios where individual parameters are varied one at a time. These variations include:

- **Filter cavity length**, with a worst-case scenario set to 1 km and an intermediate case at 3 km,
- **Signal extraction cavity length**, set to 200 m in the worst-case scenario
- **Beampipe and chamber pressures** for both the HF and LF instruments,
- **Suspension length**, reduced to 9 m in the worst-case scenario,
- **Suspension and coating temperatures**, including a worst-case of 70 K and an intermediate case at 20 K.
- **Tilting and size of the beam**, spanning from an intermediate case where the tilt angle is of 1.5 mrad and the size of the laser beam on the ITM/ETM is reduced to 80%, to the worst case scenario where the angle is increased to 3.0 mrad, and the beam size reduced to 60% of the current.

Additionally, we consider a combined worst-case sensitivity curve, where all parameters[2] are set to their least favorable values. To complement this, we perform a binned analysis that begins with the Reference 2024 curve and applies a 1.5 degradation factor to the sensitivity, either across all the frequency band or one frequency bin at a time. The frequency bins are: < 7 Hz, 7–10 Hz, 10–30 Hz, 30–450 Hz, and > 450 Hz. These two sets

[2]except for the tilting and beam size ones, which are not included in the overall worst case scenario.

of analyses are designed to identify the most relevant technologies and to pinpoint the frequency ranges that have the greatest impact on the scientific performance. The results are reported in [6], with the main findings being: *(i)* the low-frequency region of the sensitivity, below $\sim 30\,\mathrm{Hz}$, is the one affecting more the results for the various metrics; *(ii)* the most impactful individual design parameters in the worst-case scenario, for the LF instrument, are the Filter cavity length, the suspension and coating temperatures, and the tilting of the beam, and for the HF instrument the beam size, with their combination considerably impacting the scientific performance; *(iii)* the intermediate variations provide a good level of sensitivity across our set of metrics *(iv)* the results are consistent for both geometries.

9 List of External Documents

This section contains a list of drawings, output tables and risk analysis tables. This list will refer to documents that will be attached to the two output documents of the ETO Design Task Force.

9.1 Technical drawings

TD.1 2D models of the baseline optical layouts:

- Triangle - scale drawing: `2025-05-21 ET Triangle Optical Layout (scale version).pdf`
- Triangle - vector drawing (with beam lines): `2025-05-21 ET Triangle Optical Layout (vector version).pdf`
- L - scale drawing: `2025-05-21 ET L Optical Layout (scale version).pdf`
- L - vector drawing (with beam lines): `2025-05-21 ET L Optical Layout (vector version).pdf`

TD.2 2D models of the baseline detector layouts

- Triangle - Detector layout drawing (2D): `2025-06-27 ET Triangle Detector Layout`
- L - Detector layout drawing (2D): `2025-06-27 ET L Detector Layout`

TD.3 3D models of the baseline detector layouts

- Trimble Connect Detector Layout: Triangle Configuration: `https://app21.connect.trimble.com/tc/api/2.0/s/FzrrAFZw088AKW5uuVLQ_G7fZhN78-3_z2rt5_e2LkaLb8lmGndsjFTWhM3PpeEp`
- Triangle - Detector layout drawing (3D): `2025-06-27 ET Triangle Detector Layout.rvt`
- Triangle - Detector layout drawing (3D): `2025-06-27 ET Triangle Detector Layout.ifc`

- Trimble Connect Detector Layout: L Configuration: `https://app21.connect.trimble.com/tc/api/2.0/s/1gfKqNXiyuyC9d_ELgxFpOw7SHLq8QumOOdEE2XYScwLo40IQTizFFQFTfa3cnP3`
- L - Detector layout drawing (3D): `2025-06-27 ET L Detector Layout.rvt`
- L - Detector layout drawing (3D): `2025-06-27 ET L Detector Layout.ifc`

TD.4 2D models of the Tower Categorization mapping:

- ET Triangle Tower CAT mapping: `2025-05-23 ET Triangle Tower CAT mapping.pdf`
- ET 2L Tower CAT mapping: `2025-05-23 ET 2L Tower CAT mapping.pdf`

9.2 Tables

Output tables TAB.1-6 capture the technical details of the Triangle configuration, tables TAB.7-12 capture the technical configuration of the 2L layout. Tab.13-16 are risk related tables.

TAB.1 ET-Triangle System Decomposition Output Table: `TAB1_ ET-Triangle System Decomposition output table - FINAL.pdf`

TAB.2 ET-Triangle Integrated Towers Output Table: `TAB1_ ET-Triangle System Decomposition output table - FINAL.pdf`

TAB.3 ET-Triangle Optical Layout Output Table (`TAB3_ ET-Triangle Optical Layout output table - FINAL.pdf`), consisting of sub-tables:

TAB.3A High-level optical requirements and assumptions;

TAB.3B Layout specifications, i.e. positions, footprints and orientations of optical elements and optical sub-assemblies;

TAB.3C Optical element specifications - additional derived parameters for each optical element or optical sub-assembly;

TAB.3D Optical flexibility demands.

TAB.4 ET-Triangle Technical Infrastructure Output Table: `TAB4_ ET-Triangle Detector Layout output table - FINAL.pdf`

TAB.5 ET-Triangle Infrastructure Layout Output Table: `TAB5_ ET-Triangle Infrastructure Layout output table - FINAL.pdf`

TAB.6 ET-Triangle Sensitivity and Noise Budget Output Table: `TAB6_ ET-Triangle Sensitivity and Noise Budget output table - FINAL.pdf`

TAB.7 ET-2L System Decomposition Output Table: `TAB7_ ET-2L System Decomposition output table - FINAL.pdf`

TAB.8 ET-2L Integrated Towers Output Table: `TAB8_ ET-2L Integrated Towers output table - FINAL.pdf`

TAB.9 ET-2L Optical Layout Output Table (`TAB9_ ET-2L Optical Layout output table - FINAL.pdf`), consisting of sub-tables:

TAB.9A High-level optical requirements and assumptions;

TAB.9B Layout specifications, i.e. positions, footprints and orientations of optical elements and optical sub-assemblies;

TAB.9C Optical element specifications - additional derived parameters for each optical element or optical sub-assembly;

TAB.9D Optical flexibility demands.

TAB.10 ET-2L Technical Infrastructure Output Table: `TAB10_ ET-2L Detector Layout output table - FINAL.pdf`

TAB.11 ET-2L Infrastructure Layout Output Table: `TAB11_ ET-2L Infrastructure Layout output table - FINAL.pdf`

TAB.12 ET-2L Sensitivity and Noise Budget Output Table: `TAB12_ ET-2L Sensitivity and Noise Budget output table - FINAL.pdf`

TAB.13 Technology Readiness Level TRL Study
This document records the development status and readiness level of various technologies, mapping each one to a specific Technology Readiness Level (TRL)

TAB.14 Full Risk Study
This document is a Risk Register that identifies, assesses and tracks potential risks of different configurations (2024 and 2025 configurations of 2L Geometry and Triangle Geometry) detailing their likelihood, impact and mitigation strategies.

TAB.15 DSM - Rigidity Matrix
This is a tool that maps and analyzes dependencies between subsystems, technical decisions, and requirements in a complex project to optimize design planning, identify interdependencies, and manage change impacts. It shows the rigidity of a configuration.

TAB.16 Volume and Cost Calculations - Penalty of Change
Calculation of the cost of different alternative scenarios for both 2L and Triangle Geometries

9.3 Other external documents

DOC.1 Electrical Engineering requirements - TETI List of requirements for electrical load, electrical continuity, and simultaneity of vacuum pumps. The list was produced by TETI and is validated by the Task Force.

DOC.2 Guideline on how to read the background documentation for the External Review Committee

DOC.3 Draft version of ET Naming Conventions for the ETO Design Task Force update, explaining the uniquely identifying naming conventions used in the layout drawings and system decompositions.

References

[1] ISO Technical Committee ISO/IEC JTC 1/SC 7. Systems and software engineering — system life cycle processes. techreport ISO/IEC/IEEE 15288:2023, 01 2023.

[2] Sellers Thomas Verma Larson, Kirkpatrick. *Applied Space Systems Engineering*. McGraw-Hill Professional, 2009.

[3] International Council on Systems Engineering. *Systems Engineering Handbook - Fifth Edition*. Wiley, 2023.

[4] D. Bersanetti, D. D. Brown, J. Casanueva, S. Danilishin, J. Degallaix, A. C. Green, S. Hild, M. Korobko, M. Majoor, M. Mantovani, S. Melo, A. Perreca, C. De Rossi, and S. Steinlechner. ET optical layout update 2024: main document. techreport ET-0443A-24, Einstein Telescope Collaboration, 06 2024. issue v1.0.1-240624-dirty.

[5] D. D. Brown, J. Casanueva, A. Chiummo, J. Degallaix, A. C. Green, M. Korobko, M. Majoor, and A. Perreca. ET-15km-l optical layout update 2024: main document. techreport ET-0695A-24, Einstein Telescope Collaboration, 12 2025.

[6] ETO Design Task Force. Supporting Document for The ET Baseline Detector Layout, 2025.

[7] M.B. Majoor, M.Y. Barel, A. Bertolini, J. Bratanata, J. Gargiulo, N.A. Holland, G. Iaquaniello, R. Meijer, A. Pasqualetti, P. Rosier, and P. Werneke. Preliminary detector layout - 10km triangle. techreport ET-0676A-24, Einstein Telescope Organization, 11 2024. issue v2.0.0-241218-print.

[8] G. Ciani, M. De Laurentis, A. Lartaux-Vollard, V. Sequino, S. Steinlechner, M. Vardaro, and J.-P. Zendri. Flexibility analysis of et-lf squeezing filter cavities. techreport ET-0098A-25, Einstein Telescope Collaboration, 02 2025.

[9] F Bondu, A Brillet, F Cleva, H Heitmann, M Loupias, C N Man, H Trinquet, and the VIRGO Collaboration. The virgo injection system. *Classical and Quantum Gravity*, 19(7):1829, mar 2002.

[10] P. Kwee, C. Bogan, K. Danzmann, M. Frede, H. Kim, P. King, J. Pöld, O. Puncken, R. L. Savage, F. Seifert, P. Wessels, L. Winkelmann, and B. Willke. Stabilized high-power laser system for the gravitational wave detector advanced ligo. *Opt. Express*, 20(10):10617–10634, May 2012.

[11] Craig Cahillane, Georgia L. Mansell, and Daniel Sigg. Laser frequency noise in next generation gravitational-wave detectors. *Opt. Express*, 29(25):42144–42161, Dec 2021.

[12] Teng Zhang. Response of laser frequency and intensity noise of et. Technical Report ET-0139A-22, 2022.

[13] Peter Fritschel, Matthew Evans, and Valery Frolov. Balanced homodyne readout for quantum limited gravitational wave detectors. *Opt. Express*, 22(4):4224–4234, Feb 2014.

[14] M.B. Majoor, J. Bratanata, and P. Werneke. Preliminary detector layout - 15km l. techreport 3207058, Einstein Telescope Organization, 12 2024. issue v1.1.0-241212-print.

[15] N.A. Holland, A. Spencer and R. Meijer on behalf of ETC-Suspension division and ETO-Project Office. Memo: Et preliminary suspension system classification. Technical Report ET-0577A-24, Einstein Telescope Collaboration, Instrument Science Board, Suspension Division and Einstein Telescope Organization, Project Office, 11 2024.

[16] J.Gargiulo, A. Pasqualetti, P. Rapagnani with contribution from G. Ciani, L. Conti and A. Moscatello. Cleanroom design concepts for the et detector layout. Technical report, 2025. ET-0150A-25.

[17] A. Grado, M.Y. Barel, T. Bulik, M. Andres-Carcasona, G. Ciani, L. Conti, J. Gargiulo, S. Hanke, H. Lück, M. Martinez, A. Moscatello, N. van Remortel, C. Scarcia, E. Tofani, and P. Werneke. Einstein telescope beampipe requirements. techreport ET-0385A-24, 06 2024.

[18] L. Busch and S. Grohmann. Conceptual layout of a helium cooling system for et-lf. techreport ET-0376A-21, KIT and ITTK, 07 2021.

[19] Evert Hoek. *Practical Rock Engineering*. Hoek Notes by Evert Hoek, 2013.

[20] François Laigle. Réflexions générales sur le comportement et la conception des grandes cavernes souterraines. *Tunnels et Espace Souterrain*, (251), 10 2015.

[21] Guidelines for the design of large underground openings. 2015.

[22] Q. et al. Zhang. Stability analysis of twin tunnels in weak rock masses. *Rock mechanics and rock engineering*, 2019.

[23] M.B. Majoor, J. Bratanata, and P. Werneke. Tunnel diameter requirements for the triangular and 2l configuration. techreport 3254468, Einstein Telescope Organization, 4 2025.

[24] Einstein Telescope Steering Committee. Design Report Update 2020: for the Einstein Telescope. Technical Report ET-0007C-20, Einstein Telescope Collaboration, 11 2020.

[25] AACE International. Aace international recommended practice no. 17r-97: Cost estimate classification system. 2020.

[26] Infrastructure UK HM Treasury. Infrastructure cost review: Technical report. 2010.

[27] E. MacTavish, L. Bromiley, J. Osborne, and T. Watson. Clic – fcc civil engineering cost comparison. Internal CERN document available to CERN members as 3297658 v.1.

[28] Mikhail Korobko for the ET Instrument Science Board Teng Zhang, Stefan Danilishin. Conceptual design and noise budget of einstein telescope. techreport ET-0007C-23, Einstein Telescope Collaboration, 02 2025.

[29] Michele Maggiore et al. Science Case for the Einstein Telescope. *JCAP*, 03:050, 2020.

[30] Marica Branchesi et al. Science with the Einstein Telescope: a comparison of different designs. *JCAP*, 07:068, 2023.

[31] Adrian Abac et al. The Science of the Einstein Telescope. 3 2025.

[32] Alejandra Gonzalez et al. Second release of the CoRe database of binary neutron star merger waveforms. *Class. Quant. Grav.*, 40(8):085011, 2023.

[33] Pia Astone, Alberto Colla, Sabrina D'Antonio, Sergio Frasca, and Cristiano Palomba. Method for all-sky searches of continuous gravitational wave signals using the frequency-Hough transform. *Phys. Rev. D*, 90(4):042002, August 2014.

[34] David Vartanyan, Adam Burrows, Tianshu Wang, Matthew S. B. Coleman, and Christopher J. White. Gravitational-wave signature of core-collapse supernovae. *Phys. Rev. D*, 107(10):103015, 2023.

[35] Francesco Iacovelli, Michele Mancarella, Stefano Foffa, and Michele Maggiore. GWFAST: A Fisher Information Matrix Python Code for Third-generation Gravitational-wave Detectors. *Astrophys. J. Supp.*, 263(1):2, 2022.

[36] Ulyana Dupletsa, Jan Harms, Biswajit Banerjee, Marica Branchesi, Boris Goncharov, Andrea Maselli, Ana Carolina Silva Oliveira, Samuele Ronchini, and Jacopo Tissino. gwfish: A simulation software to evaluate parameter-estimation capabilities of gravitational-wave detector networks. *Astron. Comput.*, 42:100671, 2023.

Glossary

beam-plane Two dimensional plane, typically horizontal, in which the main science beam propagates. Alternative beam/s must be specified on a case-by-case basis when no science beam is available. If appropriate more than one beam plane may be defined – for example in the case of a periscope which propagates between at least two, typically parallel, planes.. 39, 75, 76

bench stage Single stage of a suspension system possessing a large surface area, usually for mounting multiple modular payload and/or many compact optics.. , 75, 76

bottom-loaded bench Suspension system designed to position and partially separately isolate multiple optics, exceeding three, in the beam-plane. Unlike multi-optic suspension systems larger, partially separately isolated, individual optics may be replaced by many compact optics. These smaller optics are, typically, one and two inches in diameter, rigidly mounted to a bench stage, and also located in the beam-plane - this beam-plane is located below the bench stage of the suspension system. Similar to the MO architecture the larger, partially separately isolated, individual optics qualify as modular payloads..

distributed system A collection of subsystems that perform a similar function across many different physical locations of the larger system, satisfying a higher-level system function when considered together. Sometimes conventionally referred to as 'bus-systems'.

extreme high vacuum Extreme high vacuum is defined as the pressure range below 10^{-9} Pa. Such pressures can be achieved using sophisticated materials (e.g., vacuum-fired low-carbon stainless steel, aluminum, copper-beryllium, titanium), metal sealing, specific surface preparation and cleaning, bake-out procedures, and additional getter pumps; gas flow occurs in the molecular flow regime.

integrated system A collection of multiple components or subsystems that when put together form a larger functional system that meets a specific set of requirements. Typically, integrated systems can also be clearly physically defined. 6, 75

modular payload Suspension subsystem, typically hosting one substantial optic, which provides additional residual motion isolation only to that optic. In addition it provides independent control authority over the position of this optic. . , 75, 76

multi-optic Suspension system designed to position and partially separately isolate multiple optics, typically three or four, in the beam plane. Unlike for single optic suspension systems the geometric placement of these optics is not restricted by the kinematics of the suspension system. The separate subsystems, each isolating a single optic, qualifies as a modular payload.. , 75, 76

node a unique identification of an integrated system at level 3 of the system decomposition. Examples include (vacuum) vessels containing either a single optic or optical subassembly, cryopump systems, noisy rooms, cryogenic infrastructure, cleanrooms, underground caverns and tunnels. 2, 6

single optic Suspension system designed to position and isolate at most two optics in the beam-plane. If a second optic is present geometric restrictions on its positions arise due to the kinematics of the suspension system.. , 75

suspension system Entire mechatronic system which provides residual motion attenuation and control of one or more discrete optics.. , 75, 76

top-loaded bench Suspension system designed to position and partially separately isolate multiple optics, exceeding three, in the beam-plane. Unlike multi-optic suspension systems larger, partially separately isolated, individual optics may be replaced by many compact optics. These smaller optics are, typically, one and two inches in diameter, rigidly mounted to a bench stage, and also located in the beam-plane - this beam-plane is located above the bench stage of the suspension system. Similar to the MO architecture the larger, partially separately isolated, individual optics qualify as modular payloads..

ultra-high vacuum Ultra-high vacuum is defined as the pressure range between 10^{-6} Pa and 10^{-9} Pa. Such pressures can be achieved using specialized materials, metal sealing, dedicated surface preparation and cleaning, bake-out procedures, and high vacuum pumps; in this regime, gas flow is in the molecular flow domain..

vacuum beampipe Vacuum beampipe is a round shape pipe in which the light beam is propagating in partial vacuum conditions, meaning lower air-pressure than atmospheric pressure.

Acronyms

aLIGO advanced Laser Interferometer Gravitational wave Observatory.

AdV advanced Virgo.

ALS auxiliary laser system.

ASD amplitude spectral density.

BB bottom-loaded bench. *Glossary:* bottom-loaded bench,

BHD balanced homodyne detection.

BS beamsplitter.

CSU cryogenic supply unit. 33,

ET Einstein Telescope. , 76

ETC Einstein Telescope Collaboration.

ETM end test-mass.

ETO Einstein Telescope Organization.

FC squeezing filter cavity. 33,

GW gravitational wave. , 76, 77

HFI high frequency interferometer. 30, 31,

HWS Hartmann wavefront sensor.

IMC input mode cleaner. 35,

INJ injection.

IOO input, output optics. 36,

IP inverted pendulum. 34,

ISB Instrument Science Board.

ITF interferometer. , 76, 77

ITM input test-mass.

laser light amplification by stimulated emmission of radiation. , 76, 77

LFI low frequency interferometer. 31, 32, 33,

LIGO Laser Interferometer Gravitational wave Observatory. , 76

MC mode cleaner. , 76, 77

MO multi-optic. *Glossary:* multi-optic, , 75, 76

OMC output mode cleaner.

OSB Observational Science Board.

PAY payload.

PB periscope bench.

PRC power recycling cavity.

PRM power recycling mirror.

RMS root mean square.

SEC signal extraction cavity.

SEM signal extraction mirror.

SO single optic. *Glossary:* single optic,

SPI seismic platform interferometer.

SQZ squeezing. 32,

TB top-loaded bench. *Glossary:* top-loaded bench,

TCS thermal compensation system.

TM test-mass. 33, , 76, 77

UHV ultra-high vacuum. *Glossary:* ultra-high vacuum,

XHV extreme high vacuum. *Glossary:* extreme high vacuum,